NASA TECHNICAL NOTE

NASA TN D-3165

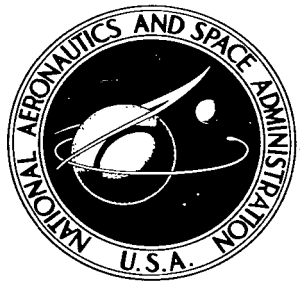

NASA TN D-3165

LIQUID BEHAVIOR IN THE RESERVOIR OF THE SOUND SUPPRESSOR SYSTEM

by Helmut F. Bauer

George C. Marshall Space Flight Center
Huntsville, Ala.

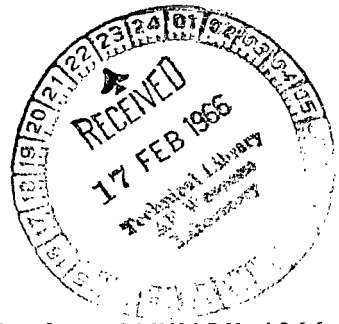

NATIONAL AERONAUTICS AND SPACE ADMINISTRATION - WASHINGTON, D. C. - JANUARY 1966

LIQUID BEHAVIOR IN THE RESERVOIR OF THE SOUND SUPPRESSOR SYSTEM

By Helmut F. Bauer*

George C. Marshall Space Flight Center
Huntsville, Ala.

*Consultant, Georgia Institute of Technology

NATIONAL AERONAUTICS AND SPACE ADMINISTRATION

For sale by the Clearinghouse for Federal Scientific and Technical Information
Springfield, Virginia 22151 – Price $4.00

TABLE OF CONTENTS

LIST OF ILLUSTRATIONS

LIST OF ILLUSTRATIONS (Cont'd)

LIST OF ILLUSTRATIONS (Cont'd)

LIST OF ILLUSTRATIONS (Concluded)

LIST OF TABLES

(NOTE: The information contained at the bottom of each equation in Figures 12 through 55 is for file reference only.)

DEFINITION OF SYMBOLS

Symbol	Definition
a	length of container
g	gravity constant
h	height of liquid
m	total mass of liquid
n	number of liquid vibration mode
p	pressure in liquid
$p_{y=o}$	pressure at container wall y = 0
$p_{y=a}$	pressure at container wall y = a
p_{bottom}	pressure at container bottom x = -h
t_o, t_1	duration of excitation pulse
u, v	fluid velocities in x and y direction
$v_o(t), v_1(t)$	excitation velocity
x, y, z	cartesian coordinates
y_o	translational excitation amplitude
$\bar{x}$	elevation of free fluid surface
F_y	fluid force
M_z	moment of liquid about axis through undisturbed center of gravity
$\phi(y, x, t)$	velocity potential function of fluid due to harmonic excitation
$\phi(y, x, \Omega)$	"admittance" of liquid
$\Phi(y, x, t)$	velocity potential of fluid due to pulse excitation

DEFINITION OF SYMBOLS (Concluded)

Symbol	Definition
Ω	forcing frequency
ω_n	natural frequency of liquid
ρ	mass density of liquid
$\eta_n = \frac{\Omega}{\omega_n}$	frequency ratio of forcing frequency to n^{th} natural frequency
t, τ	time

LIQUID BEHAVIOR IN THE RESERVOIR OF THE SOUND SUPPRESSOR SYSTEM

SUMMARY

A large water reservoir of rectangular plan form is part of a sound suppression system projected for use in the static firings of the booster stage of the Saturn V launch vehicle. Upon ignition of the rocket engines, a surge wave is created in the water mass at the discharge side of this reservoir. The surge wave will travel across the water surface and be reflected on the opposite wall, and thus travel back and forth until it is eventually damped out by wall and internal friction.

The characteristics of the surge wave are investigated by treating first the response of the liquid to harmonic excitation of one side wall of the reservoir; "admittance" is thus determined, with which the response of the liquid to any arbitrary motion of the container wall can be obtained. Motion is investigated for a rectangular and a sinusoidal velocity respectively of one container wall. The liquid is considered incompressible, nonviscous, and irrotational.

The velocity potential, free liquid surface displacement, velocity and pressure distribution, fluid force and moment have been obtained for various pulse durations; these results serve as design values for the reservoir structure. The wave form was computed electronically for a time coordinate with one-sixteenth second increments. These increments yield the wave motion in true time by assembling them in a film which shows quite lucidly the behavior of the liquid surface.

SECTION I. INTRODUCTION

A reservoir of five-million gallon capacity is part of the projected sound suppression system of the Saturn V Static Test Facility. By injecting large quantities of water into the exhaust jets near the engine nozzle exit, the sound power generated by the exhaust jets will be reduced considerably (Fig. 1). The high velocity of the exhaust creates a suction which causes the water to flow, but also creates a surge wave in the container when the rocket engines

are ignited. The water system reacts as if one wall were suddenly moved. However, the water level is kept constant during the operation; the surge wave is of two-dimensional form. For this reason the motion of the liquid in the rectangular container can be treated as that in a rectangular container of infinite width.

The container is considered to be of length a and filled with incompressible liquid to a height h. To describe the real physical effect of the suction created by the firing of the rocket engines, one wall of the container is assumed suddenly to move for a finite duration. The displacement y_o of the wall caused by this motion is considered small compared to the length of the container; the level of the undisturbed liquid thus remains in the average at its location x = 0 (Fig. 2).

The problem posed is to determine the characteristics of the surge wave. To resolve this problem, the characteristics of the liquid motion are investigated by treating first the response of the liquid to harmonic excitation of one side wall of the basin. By determining the "admittance," the response of the fluid to an arbitrary motion of the container wall can be obtained. This is performed for a rectangular and a sinusoidal velocity respectively of one container side wall. The velocity potential of the liquid is determined both for the time interval of the pulse and for the time after completion of the pulse. The free fluid surface displacement, velocity and pressure distribution, fluid force and moment can then be determined and serve as design values for the reservoir structure.

The motion of an ideal incompressible liquid in a rectangular container of infinite length filled to a height h is then considered. A cartesian coordinate system Oxyz is introduced such that the yz plane is located in the quiescent surface of the liquid perpendicular to the gravity vector. The x-axis is pointing vertically upward. The height of the free liquid surface above the plane x = 0 is called $\overline{x} = \overline{x}(y,t)$; and is caused by some disturbance of the container or one of its parts, such as a side wall.

The velocity of the ideal, incompressible liquid in the container can be represented as a gradient of a velocity potential ϕ, which, due to the continuity equation has to satisfy the Laplace equation. The normal velocity of the liquid at the container walls is equal to that of the container wall. The free fluid surface boundary condition is described by the kinematic and dynamic condition, of which the first expresses that the normal velocity of the fluid particles at the free surface is equal to the normal velocity of the free fluid surface. The latter condition is obtained from the unsteady Bernoulli equation for the pres-

sure p equal to the ambient gas pressure p_o. It is the first integral of the Euler equation.

The problem is then to find those solutions from the class of harmonic functions satisfying the container wall boundary conditions which also satisfy the kinematic and dynamic condition. By proper transformation, the wall boundary conditions can be made homogeneous, and the problem is then to solve the Poisson equation with these boundary conditions.

The problem of free fluid oscillations in a rectangular container has been treated by Rayleigh [1], in 1876. In recent years, the problem of forced fluid oscillations has grown in importance [2, 3, 4]. Lorell [5] gave the linearized flow of a liquid in a rectangular container of infinite length for translatory harmonic excitation of the complete container. The purpose of the present investigation is to determine the liquid response (such as free fluid surface amplitude, pressure and velocity distribution, fluid force and moment) caused by pulse excitation of one container side wall.

SECTION II. RESPONSE OF LIQUID IN A RECTANGULAR CONTAINER OF INFINITE WIDTH DUE TO HARMONIC EXCITATION OF ONE SIDE WALL

Before proceeding to arbitrary wall excitation the solution for harmonic excitation must be known. Treating the liquid as incompressible, irrotational and inviscid results in a presentation of the velocity as a gradient of a velocity potential ϕ that satisfies the Laplace equation

$$\nabla^2 \phi = 0 . \tag{2.1}$$

This equation has to be solved together with the boundary conditions of the problem. At the tank walls the normal velocity of the liquid and the container are equal to each other; after linearization it is obtained

$$\frac{\partial \phi}{\partial y} = 0 \qquad \text{at the side wall } y = 0 \tag{2.2}$$

$$\frac{\partial \phi}{\partial y} = y_o i\Omega e^{i\Omega t} \qquad \text{at the side wall } y = a \tag{2.3}$$

$$\frac{\partial \phi}{\partial x} = 0 \qquad \text{at the container bottom } x = -h . \tag{2.4}$$

The free fluid surface condition is obtained from the linearized kinematic condition $\partial\phi/\partial x = \partial\bar{x}/\partial t$ and from the dynamic condition for $p = 0$ obtained by eliminating the free fluid surface displacement $\bar{x}$ from the linearized instationary Bernoulli equation $\partial\phi/\partial t + g\bar{x} + p/\rho = 0$. Thus,

$$\frac{\partial^2\phi}{\partial t^2} + g\,\frac{\partial\phi}{\partial x} = 0 \qquad \text{at the free fluid surface } x = 0. \tag{2.5}$$

Here, g is the gravity constant. The displacement y_o is considered small in order to maintain the undisturbed free fluid surface in the average at $x = 0$ (i.e., $a.h = (a \pm y_o) \cdot h^*$ which yields $h^* \approx h(1 \mp \frac{y_o}{a})$; therefore, it should be $y_o/a \ll 1$).

The transformation

$$\phi(y,x,t) = \left[\Psi(y,x) + i\Omega y_o \frac{y^2}{2a}\right] e^{i\Omega t} \tag{2.6}$$

makes the boundary conditions (2.2) and (2.3) homogeneous. Instead of the Laplace equation (2.1), one has to solve the Poisson equation

$$\nabla^2\Psi = -\frac{i\Omega y_o}{a} \tag{2.7}$$

with the transformed boundary conditions

$$\frac{\partial\psi}{\partial y} = 0 \qquad \text{at } y = 0,\ a \tag{2.8}$$

$$\frac{\partial\psi}{\partial x} = 0 \qquad \text{at } x = -h \tag{2.9}$$

$$g\,\frac{\partial\psi}{\partial x} - \Omega^2\psi = i\Omega^3 y_o \frac{y^2}{2a} \qquad \text{at } x = 0 \tag{2.10}$$

A solution satisfying the boundary conditions (2.8) is given by

$$\Psi(y,x) = \sum_{n=0}^{\infty} A_n(x)\,\cos\left(\frac{n\pi}{a}\,y\right). \tag{2.11}$$

Introducing this expression into Poisson's Equation (2.7) yields

$$A_n''(x) - \frac{n^2\pi^2}{a^2} A_n(x) = 0 \quad \text{for } n = 0 \tag{2.12}$$

and

$$A_o''(x) = -i\Omega \frac{y_o}{a} \quad . \tag{2.13}$$

This infinite set of ordinary differential equations in x has to be solved with the boundary conditions (2.9) and (2.10) which with (2.11) yield

$$A_n'(-h) = 0 \qquad \text{for } n = 0,\ 1,\ 2,\ \ldots\ldots \tag{2.14}$$

and

$$gA_n'(o) - \Omega^2 A_n(o) = 2(-1)^n \frac{i\Omega^3 a y_o}{n^2\pi^2} \qquad \text{for } n = 1,\ 2,\ \ldots\ldots \tag{2.15}$$

$$gA_o'(o) - \Omega^2 A_o(o) = \frac{i\Omega^3 y_o a}{6} \quad . \tag{2.16}$$

Here, the right-hand side of equation (2.10) has been expanded into a Cosine-Fourier-series and terms of the left-hand side of equation (2.10) have been set equal to those of the right-hand side. These become

$$i\Omega^3 y_o \frac{y^2}{2a} = \frac{\alpha_o}{2} + \sum_{n=1}^{\infty} \alpha_n \cos\left(\frac{n\pi}{a} y\right) \tag{2.17}$$

where

$$\alpha_o = \frac{i\Omega^3 a y_o}{3} \quad \text{and} \quad \alpha_n = \frac{2a(-1)^n i\Omega^3 y_o}{\pi^2 n^2} \quad . \tag{2.18}$$

The solution of equation (2.12) with the boundary conditions (2.14) and (2.15) together with $\eta_n = \Omega/\omega_n$ as the ratio of the exciting frequency to the natural frequency of the liquid and $\omega_n^2 = \frac{gn\pi}{a} \tanh\left(n\pi \frac{h}{a}\right)$ (see Table 1.) is

$$A_n(x) = 2(-1)^n \frac{i\Omega a y_o \eta_n^2 \cosh\left[\frac{n\pi}{a}(x+h)\right]}{\pi^2 n^2 (1 - \eta_n^2) \cosh\left(\frac{n\pi h}{a}\right)} \tag{2.19}$$

while that of equation (2.13) with the boundary conditions (2.14) and (2.16) is

$$A_o(x) = -i\Omega \frac{y_o}{2a}(x^2 + 2xh) - \frac{iy_o}{\Omega} g \frac{h}{a} - \frac{i\Omega a y_o}{6} \quad . \tag{2.20}$$

The velocity potential ϕ (y, x, t) caused by the harmonic excitation $y_o e^{i\Omega t}$ of one tank wall (y = a) is, therefore, with (2.6) given by

$$\phi(y,x,t) = y_o e^{i\Omega t} i\Omega \left\{ \frac{y^2}{2a} - \frac{a}{6} - \frac{gh}{a\Omega^2} - \frac{1}{2a}(x^2 + 2hx) + \frac{2a}{\pi^2} \sum_{n=1}^{\infty} (-1)^n \frac{\eta_n^2}{(1-\eta_n^2)} \frac{\cosh\left[\frac{n\pi}{a}(x+h)\right]}{n^2 \cosh(n\pi \frac{h}{a})} \cos\left(\frac{n\pi}{a} y\right) \right\} \tag{2.21}$$

The free surface displacement, pressure distribution and velocity distribution, as well as fluid force and moment can be determined from the potential by differentiations and integrations with respect to the time and spatial coordinates.

The surface displacement of the liquid which is measured from the undisturbed position of the fluid is (Figs. 3, 4, 5 and 6)

$$\bar{x}(y,t) = -\frac{1}{g}\left(\frac{\partial\phi}{\partial t}\right)_{x=0} = \frac{\Omega^2}{g} y_o e^{i\Omega t} \left[\frac{y^2}{2a} - \frac{a}{6} - \frac{gh}{a\Omega^2} + \frac{2a}{\pi^2} \sum_{n=1}^{\infty} \frac{(-1)^n \eta_n^2}{(1-\eta_n^2)} \frac{\cos\left(\frac{n\pi}{a} y\right)}{n^2} \right] \quad . \tag{2.22}$$

For very small $\Omega << 1$ and very large $\Omega >> 1$, the liquid surface regresses like $-\frac{h}{a} y_o e^{i\Omega t}$. The pressure distribution at a depth (-x) is given by

$$p = -\rho \frac{\partial\phi}{\partial t} - \rho g x = -\rho g x + \rho y_o \Omega^2 e^{i\Omega t} \left[\frac{y^2}{2a} - \frac{a}{6} - \frac{gh}{\Omega^2 a} - \frac{1}{2a}(x^2 + 2hx) + \frac{2a}{\pi^2} \sum_{n=1}^{\infty} (-1)^n \frac{\eta_n^2}{(1-\eta_n^2)} \cdot \frac{\cosh\left[\frac{n\pi}{a}(x+h)\right]}{n^2 \cosh\left(\frac{n\pi h}{a}\right)} \cos\left(\frac{n\pi}{a} y\right) \right] \quad . \tag{2.23}$$

The pressure distribution at the wall y = a is, therefore,

$$p_{y=a} = -\rho g x + \rho y_o \Omega^2 e^{i\Omega t}\left[\frac{a}{3} - \frac{gh}{\Omega^2 a} - \frac{1}{2a}(x^2 + 2hx) + \frac{2a}{\pi^2}\sum_{n=1}^{\infty}\frac{\eta_n^2}{(1-\eta_n^2)}\cdot\frac{\cosh\left[\frac{n\pi}{a}(x+h)\right]}{n^2\cosh\left(\frac{n\pi h}{a}\right)}\right] \tag{2.24}$$

and at the wall y = 0, it is (Figs. 7, 8 and 9)

$$p_{y=0} = -\rho g x + \rho_o y_o \Omega^2 e^{i\Omega t}\left[-\frac{a}{6} - \frac{gh}{\Omega^2 a} - \frac{1}{2a}(x^2 + 2hx) + \frac{2a}{\pi^2}\sum_{n=1}^{\infty}\frac{(-1)^n\eta_n^2}{(1-\eta_n^2)}\cdot\frac{\cosh\left[\frac{n\pi}{a}(x+h)\right]}{n^2\cosh\left(\frac{n\pi h}{a}\right)}\right] . \tag{2.25}$$

At the container bottom (x = -h) the pressure distribution is

$$p_{bottom} = \rho g h + \rho y_o \Omega^2 e^{i\Omega t}\left[\frac{y^2}{2a} - \frac{a}{6} - \frac{gh}{\Omega^2 a} + \frac{h^2}{2a} + \frac{2a}{\pi^2}\sum_{n=1}^{\infty}\frac{(-1)^n\eta_n^2\cos\left(\frac{n\pi}{a}y\right)}{(1-\eta_n^2)\,n^2\cosh\left(\frac{n\pi h}{a}\right)}\right] . \tag{2.26}$$

The fluid force is obtained from integration of the pressure along the sidewalls

$$F_y = \int_{-h}^{o}\left(p_{y=a} - p_{y=o}\right)dx \tag{2.27}$$

which with the fluid mass m = ρ ah yields the expression (Fig. 10)

$$F_y = m y_o \Omega^2 e^{i\Omega t}\left[\frac{1}{2} + \frac{4}{\pi^2}\sum_{n=1}^{\infty}\frac{\tanh\left[(2n-1)\pi\frac{h}{a}\right]\eta_{2n-1}^2}{(2n-1)^3\pi\frac{h}{a}\left(1-\eta_{2n-1}^2\right)}\right] . \tag{2.28}$$

The moment of the liquid about the center of gravity of the undisturbed fluid is given by

$$M_z = \int_{-h}^{o} \left(p_{y=a} - p_{y=o}\right) \left(\frac{h}{2} + x\right) dx - \int_{o}^{a} p_{bottom} \left(y - \frac{a}{2}\right) dy$$

and yields the expression

$$M_z = ma\Omega^2 y_o e^{i\Omega t} \left[\frac{1}{24h/a} + \frac{2}{\pi^3} \sum_{n=1}^{\infty} \frac{\eta_{2n-1}^2}{\left(1 - \eta_{2n-1}^2\right)}\right] \cdot \left[\frac{\tanh\left[(2n-1)\frac{\pi h}{a}\right]}{(2n-1)^3} + \frac{2\left(\frac{2}{\cosh\left((2n-1)\frac{\pi h}{a}\right)} - 1\right)}{\frac{\pi h}{a}(2n-1)^4}\right]. \quad (2.29)$$

The velocity distribution is given by

$$v = \frac{\partial \phi}{\partial y} = y_o i\Omega e^{i\Omega t} \left[\frac{y}{a} - \frac{2}{\pi} \sum_{n=1}^{\infty} (-1)^n \frac{\cosh\left[\frac{n\pi}{a}(x+h)\right]\eta_n^2}{n \cosh\left(\frac{n\pi h}{a}\right)\left(1-\eta_n^2\right)} \sin\left(\frac{n\pi y}{a}\right)\right]. \quad (2.30)$$

At the left container wall (y = o) the velocity v is zero and at the right container wall (y = a) it is $y_o i\Omega e^{i\Omega t}$, which agree with the given boundary conditions. The vertical velocity distribution is

$$u = \frac{\partial \phi}{\partial x} = y_o i\Omega e^{i\Omega t} \left[-\frac{x+h}{a} + \frac{2}{\pi} \sum_{n=1}^{\infty} (-1)^n \frac{\sinh\left[\frac{n\pi}{a}(x+h)\right]\eta_n^2}{n \cosh\left(\frac{n\pi h}{a}\right)\left(1 - \eta_n^2\right)} \cos\left(\frac{n\pi y}{a}\right)\right]. \quad (2.31)$$

At the container bottom (x = -h) the velocity is u = 0, which agrees with the boundary condition.

SECTION III. RESPONSE OF LIQUID DUE TO ARBITRARY EXCITATION

To determine the response of a liquid with a free fluid surface in a rectangular container of infinite length with one moving side wall caused by an arbitrary nonperiodic excitation $\dot{y}(t)$, the function $\dot{y}$ is written into its simple harmonic components by means of the Fourier integral

$$\dot{y}(t) = \frac{1}{\pi} \int_0^{\infty} \int_{-\infty}^{\infty} \dot{y}(\tau) \cos \Omega (t - \tau) \, d\tau \, d\Omega \quad .$$

The solution to the steady state problem yields the "admittance" of the fluid system, which is combined with the components of the response of the liquid to obtain the response of the system to the original nonperiodic excitation functions. Then

$$\Phi(y, x, t) = \frac{1}{\pi} \int_0^{\infty} \int_{-\infty}^{\infty} \phi (y, x; \Omega) \, \dot{y}(\tau) \cos \Omega (\tau - t) \, d\tau d\Omega$$

is the velocity potential of the liquid due to the nonperiodic excitation $\dot{y}(t)$.

Therefore, by rewriting the potential (2.21) as

$$\phi (y, x, t) = \dot{y}_o \cos \Omega t \left[\frac{y^2}{2a} - \frac{a}{6} - \frac{1}{2a} (x^2 + 2hx) - \frac{gh}{\Omega^2 a} \right.$$

$$\left. + \frac{2a}{\pi^2} \sum_{n=1}^{\infty} \frac{(-1)^n \eta_n^2}{(1 - \eta_n^2)} \frac{\cosh \left[\frac{n\pi}{a} (x + h) \right]}{n^2 \cosh \left(\frac{n\pi h}{a} \right)} \cos \left(\frac{n\pi}{a} y \right) \right]$$

the "admittance" ϕ is given by

$$\phi (y, x; \Omega) = \frac{y^2}{2a} - \frac{a}{6} - \frac{1}{2a} (x^2 + 2hx) - \frac{gh}{\Omega^2 a}$$

$$+ \frac{2a}{\pi^2} \sum_{n=1}^{\infty} (-1)^n \frac{\Omega^2}{(\omega_n^2 - \Omega^2)} \frac{\cosh \left[\frac{n\pi}{a} (x + h) \right]}{n^2 \cosh \left(\frac{n\pi h}{a} \right)} \cos \left(\frac{n\pi}{a} y \right)$$

and the velocity potential for an arbitrary nonperiodic excitation $\dot{y}(t)$ yields

$$\Phi (y, x, t) = \frac{1}{\pi} \int_0^{\infty} \int_{-\infty}^{+\infty} \left[\frac{y^2}{2a} - \frac{a}{6} - \frac{1}{2a} (x^2 + 2hx) - \frac{gh}{\Omega^2 a} \right.$$

$$\left. + \frac{2a}{\pi^2} \sum_{n=1}^{\infty} (-1)^n \frac{\Omega^2}{\left(\omega_n^2 - \Omega^2 \right)} \cdot \frac{\cosh \left[\frac{n\pi}{a} (x+h) \right]}{n^2 \cosh \left(\frac{n\pi h}{a} \right)} \cos \left(\frac{n\pi y}{a} \right) \right] \dot{y}(\tau) \cos \Omega (\tau - t) \, d\tau d\Omega .$$

A. RESPONSE OF LIQUID DUE TO SINGLE RECTANGULAR PULSE

A single rectangular pulse of magnitude v_o and duration t_o starting at $t = o$ (Fig. 11) can be described by the Fourier-Integral

$$\dot{y}(t) = v(t) = \frac{1}{\pi} \int_o^\infty \int_{-\infty}^\infty v(\tau) \cos \Omega (t - \tau) \, d\tau \, d\Omega \quad .$$

With

$$v(t) = \left\{ \begin{array}{lll} v_o & \text{for} & o < t < t_o \\ o & \text{for} & t > t_o \end{array} \right\}$$

the expression obtained is

$$v(t) = \frac{v_o}{\pi} \int_o^\infty \frac{\cos \Omega t \sin \Omega t_o}{\Omega} \, d\Omega + \frac{v_o}{\pi} \int_o^\infty \frac{\sin \Omega t (1 - \cos \Omega t_o)}{\Omega} \, d\Omega \quad .$$

The velocity potential for rectangular pulse excitation is, therefore,

$$\begin{aligned} \Phi(y, x, t) = {} & \frac{v_o}{\pi} \int_o^\infty \left[\frac{y^2}{2a} - \frac{a}{6} - \frac{1}{2a} (x^2 + 2hx) \right] \frac{\cos \Omega t \sin \Omega t_o}{\Omega} \, d\Omega \\ & - \frac{v_o}{\pi} \int_o^\infty g \frac{h}{a} \frac{\sin \Omega t_o \cos \Omega t}{\Omega^3} \, d\Omega \\ & + \frac{2a v_o}{\pi^3} \sum_{n=1}^\infty (-1)^n \frac{\cosh\left[\frac{n\pi}{a} (x + h)\right] \cos\left(\frac{n\pi}{a} y\right)}{n^2 \cosh\left(\frac{n\pi h}{a}\right)} \int_o^\infty \frac{\Omega \cos \Omega t \sin \Omega t_o}{(\omega_n^2 - \Omega^2)} \, d\Omega \\ & + \frac{v_o}{\pi} \int_o^\infty \left[\frac{y^2}{2a} - \frac{a}{6} - \frac{1}{2a} (x^2 + 2hx) \right] \frac{\sin \Omega t \left[1 - \cos \Omega t_o \right]}{\Omega} \, d\Omega \\ & - \frac{v}{\pi} \int_o^\infty \frac{gh}{a} \frac{\sin \Omega t \left[1 - \cos \Omega t_o \right]}{\Omega^3} \, d\Omega \qquad (3.1) \\ & + \frac{2a v_o}{\pi^3} \sum (-1)^n \frac{\cosh\left[\frac{n\pi}{a} (x + h)\right] \cos\left(\frac{n\pi}{a} y\right)}{n^2 \cosh\left[\frac{n\pi h}{a}\right]} \int_o^\infty \frac{\Omega \sin \Omega t \left[1 - \cos \Omega t_o\right]}{(\omega_n^2 - \Omega^2)} d\Omega \, . \end{aligned}$$

The occurring integrals can be solved with complex integration methods (see Appendix).

The solutions are:

$$\int_0^\infty \frac{\cos \Omega t \sin \Omega t_o}{\Omega} \, d\Omega \qquad \begin{cases} \frac{\pi}{2} & \text{for} \quad t < t_o \\ o & \text{for} \quad t > t_o \end{cases}$$

$$\int_0^\infty \frac{\sin \Omega t \cos \Omega t_o}{\Omega} \, d\Omega \qquad \begin{cases} o & \text{for} \quad t < t_o \\ \frac{\pi}{2} & \text{for} \quad t > t_o \end{cases}$$

$$\int_0^\infty \frac{\sin \Omega t}{\Omega} \, d\Omega \qquad \begin{cases} \frac{\pi}{2} & \text{for} \quad t > o \\ -\frac{\pi}{2} & \text{for} \quad t < o \end{cases}$$

$$\int_0^\infty \frac{\sin \Omega t \left[1 - \cos \Omega t_o \right]}{\Omega^3} \, d\Omega \qquad \begin{cases} \frac{\pi}{4} t (2t_o - t) & \text{for} \quad t \leq t_o \\ \frac{\pi}{4} t_o^2 & \text{for} \quad t \geq t_o \end{cases}$$

$$\int_0^\infty \frac{\sin \Omega t_o \cos \Omega t}{\Omega^3} \, d\Omega \qquad \begin{cases} -\frac{\pi}{4} (t^2 + t_o^2) & \text{for} \quad t < t_o \\ -\frac{\pi}{2} t \cdot t_o & \text{for} \quad t > t_o \end{cases}$$

$$\int_0^\infty \frac{\Omega \cos \Omega t \sin \Omega t_o}{\omega_n^2 - \Omega^2} \, d\Omega \qquad \begin{cases} -\frac{\pi}{2} \cos \omega_n t \cos \omega_n t_o & \text{for} \quad t < t_o \\ \frac{\pi}{2} \sin \omega_n t \sin \omega_n t_o & \text{for} \quad t > t_o \end{cases}$$

$$\int_0^\infty \frac{\Omega \sin \Omega t \cos \Omega t_o}{\omega_n^2 - \Omega^2} \, d\Omega \qquad \begin{cases} \frac{\pi}{2} \sin \omega_n t \sin \omega_n t_o & \text{for } t < t_o \\ -\frac{\pi}{2} \cos \omega_n t \cos \omega_n t_o & \text{for } t > t_o \end{cases}$$

$$\int_0^\infty \frac{\Omega \sin \Omega t}{\omega_n^2 - \Omega^2} \, d\Omega \qquad \begin{cases} -\frac{\pi}{2} \cos \omega_n t & \text{for } t > o \\ o & \text{for } t < o \end{cases}$$

With these results, the velocity potential for excitation caused by a single rectangular pulse of the container wall y = a is given by:

$$\Phi(y,x,t) = v_o \left[\begin{Bmatrix} 1 \\ 0 \end{Bmatrix} \left[\frac{y^2}{2a} - \frac{a}{6} - \frac{1}{2a}(x^2 + 2hx) \right] + \frac{gh}{4a} \begin{Bmatrix} 2t^2 - 2tt_o + t_o^2 \\ 2tt_o - t_o^2 \end{Bmatrix} \right. \tag{3.2}$$

$$\left. - \frac{a}{\pi^2} \sum_{n=1}^{\infty} (-1)^n \frac{\cosh\left[\frac{n\pi}{a}(x+h)\right] \cos\left(\frac{n\pi}{a} y\right)}{n^2 \cosh\left(\frac{n\pi h}{a}\right)} \begin{Bmatrix} \cos\omega_n(t_o - t) + \cos\omega_n t \\ \cos\omega_n t - \cos\omega_n(t - t_o) \end{Bmatrix} \right]$$

where the upper line corresponds to values $t < t_o$ and the lower line, to the time $t > t_o$.

The free fluid surface displacement is

$$\bar{x} = -\frac{h}{a} v_o \begin{Bmatrix} t - t_o/2 \\ t_o/2 \end{Bmatrix} - \frac{a v_o}{g\pi^2} \sum_{n=1}^{\infty} (-1)^n \frac{\omega_n \cos\left(\frac{n\pi}{a} y\right)}{n^2} F(t) \tag{3.3}$$

where $F(t) = \sin \omega_n t \pm \sin \omega_n (t - t_o)$; the upper sign belongs to the time interval $t < t_o$ while the lower sign belongs to $t > t_o$.

The pressure in the container at a depth (-x) is given by

$$p = -\rho g x - \rho v_o \left[\frac{gh}{a} \left\{ \begin{matrix} t - \frac{t_o}{2} \\ \\ \frac{t_o}{2} \end{matrix} \right\} + \frac{a}{\pi^2} \sum_{n=1}^{\infty} (-1)^n \frac{\omega n \cosh\left[\frac{n\pi}{a}(x+h)\right] \cos\left(\frac{n\pi}{a} y\right)}{n^2 \cosh\left(\frac{\pi n h}{a}\right)} F(t) \right] \quad (3.4)$$

At the tank wall $y = 0$ the pressure distribution yields

$$p_{y=o} = -\rho g x - p v_o \left[\frac{gh}{a} \left\{ \begin{matrix} t - \frac{t_o}{2} \\ \\ \frac{t_o}{2} \end{matrix} \right\} + \frac{a}{\pi^2} \sum_{n=1}^{\infty} (-1)^n \frac{\omega n \cosh\left[\frac{n\pi}{a}(x+h)\right]}{n^2 \cosh\left(\frac{n\pi h}{a}\right)} F(t) \right] \quad (3.5)$$

and at the container wall $x = a$ the pressure distribution is

$$p_{y=a} = -\rho g x - \rho v_o \left[\frac{gh}{a} \left\{ \begin{matrix} t - \frac{t_o}{2} \\ \\ \frac{t_o}{2} \end{matrix} \right\} + \frac{a}{\pi^2} \sum_{n=1}^{\infty} \frac{\omega n \cosh\left[\frac{n\pi}{a}(x+h)\right]}{n^2 \cosh\left(\frac{n\pi h}{a}\right)} F(t) \right] . \quad (3.6)$$

At the container bottom $x = -h$ the pressure distribution yields

$$p_{bottom} = \rho gh - \rho v_o \left[\frac{gh}{a} \begin{Bmatrix} t - \frac{t_o}{2} \\ \frac{t_o}{2} \end{Bmatrix} + \frac{a}{\pi^2} \sum_{n=1}^{\infty} (-1)^n \frac{\omega_n \cos\left(\frac{n\pi}{a} y\right)}{n^2 \cosh\left(\frac{n\pi h}{a}\right)} F(t) \right] . \quad (3.7)$$

By integration of the appropriate pressure components, the liquid force and moment can be obtained. The force in y-direction becomes

$$F_y = -mv_o \left[\frac{2}{\pi^2} \sum_{n=1}^{\infty} \frac{\omega_{2n-1} \tanh\left[\frac{(2n-1)\pi h}{a}\right]}{(2n-1)^3 \pi \, h/a} F(t) \right] . \quad (3.8)$$

The fluid moment about an axis parallel to the z-axis through the center of gravity of the undisturbed liquid is

$$M_z = \frac{mav_o}{\pi^3} \sum_{n=1}^{\infty} \frac{\omega_{2n-1}}{(2n-1)^3} \left[\tanh\left[\frac{(2n-1)\pi h}{a}\right] + \frac{2}{(2n-1)\pi h/a} \left[\frac{2}{\cosh\left[(2n-1)\pi h/a\right]} - 1 \right] \right] F(t) . \quad (3.9)$$

The velocity distribution in y-direction is given by

$$u = \frac{\partial \Phi}{\partial y} = v_o \left[\frac{y}{a} \begin{Bmatrix} 1 \\ 0 \end{Bmatrix} + \frac{1}{\pi} \sum_{n=1}^{\infty} (-1)^n \frac{\cosh\left[\frac{n\pi}{a}(x+h)\right]}{n \cosh\left(\frac{n\pi h}{a}\right)} \sin\left(\frac{n\pi y}{a}\right) \begin{Bmatrix} \cos\omega_n(t_o - t) + \cos\omega_n t \\ \cos\omega_n t - \cos\omega_n(t - t_o) \end{Bmatrix} \right]$$

and in x-direction it is

$$u = \frac{\partial \Phi}{\partial x} = v_o \left[- \frac{x+h}{a} \begin{Bmatrix} 1 \\ 0 \end{Bmatrix} \right.$$

$$\left. - \frac{1}{\pi} \sum_{n=1}^{\infty} (-1)^n \frac{\sinh\left[\frac{n\pi}{a}(x+h)\right]}{n \cosh\left(\frac{n\pi h}{a}\right)} \cos\left(\frac{n\pi y}{a}\right) \begin{Bmatrix} \cos\omega_n(t_o - t) + \cos\omega_n t \\ \cos\omega_n t - \cos\omega_n(t - t_o) \end{Bmatrix} \right]$$

B. RESPONSE OF LIQUID DUE TO A DOUBLE RECTANGULAR PULSE

In considering a rectangular double pulse, i.e., a pulse of constant magnitude v_o for a duration of t_o seconds with a constant magnitude $-v_1$ for a duration of t_1 seconds (Fig. 11),

$$v(t) = \begin{Bmatrix} v_o & \text{for} & 0 < t < t_o \\ -v_1 & \text{for} & t_o < t < t_o + t_1 \\ 0 & \text{for all} & t > t_o + t_1 \end{Bmatrix} .$$

This pulse can be described by the Fourier-Integral

$$v(t) = \frac{(v_o + v_1)}{\pi} \int_o^{\infty} \frac{\cos \Omega t \sin \Omega t_o}{\Omega} d\Omega + \frac{(v_o + v_1)}{\pi} \int_o^{\infty} \frac{\sin \Omega t (1 - \cos \Omega t_o)}{\Omega} d\Omega$$

$$- \frac{v_1}{\pi} \int_o^{\infty} \frac{\cos \Omega t \sin \Omega (t_o + t_1)}{\Omega} d\Omega - \frac{v_1}{\pi} \int_o^{\infty} \frac{\sin \Omega t \left[1 - \cos \Omega (t_o + t_1)\right]}{\Omega} d\Omega .$$

The velocity potential for this pulse is then:

$$\Phi(y,x,t) = \frac{(v_o + v_1)}{\pi} \int_o^\infty \left[\frac{y^2}{2a} - \frac{a}{6} - \frac{1}{2a}(x^2 + 2hx)\right] \frac{\cos \Omega t \sin \Omega t_o}{\Omega} d\Omega$$

$$- \frac{v_1}{\pi} \int_o^\infty \left[\frac{y^2}{2a} - \frac{a}{6} - \frac{1}{2a}(x^2 + 2hx)\right] \frac{\cos \Omega t \sin \Omega (t_o + t_1)}{\Omega} d\Omega$$

$$+ \frac{(v_o + v_1)}{\pi} \int_o^\infty \left[\frac{y^2}{2a} - \frac{a}{6} - \frac{1}{2a}(x^2 + 2hx)\right] \frac{\sin \Omega t \left[1 - \cos \Omega t_o\right]}{\Omega} d\Omega$$

$$- \frac{v_1}{\pi} \int_o^\infty \left[\frac{y^2}{2a} - \frac{a}{6} - \frac{1}{2a}(x^2 + 2hx)\right] \frac{\sin \Omega t \left[1 - \cos \Omega (t_o + t_1)\right]}{\Omega} d\Omega$$

$$- \frac{(v_o + v_1)}{\pi} g\left(\frac{h}{a}\right) \int_o^\infty \frac{\sin \Omega t_o \cos \Omega t}{\Omega^3} d\Omega$$

$$- \frac{(v_o + v_2)}{\pi} g\left(\frac{h}{a}\right) \int_o^\infty \frac{\sin \Omega t \left[1 - \cos \Omega t_o\right]}{\Omega^3} d\Omega$$

$$+ \frac{v_1}{\pi} g\left(\frac{h}{a}\right) \int_o^\infty \frac{\cos \Omega t \sin \Omega (t_o + t_1)}{\Omega^3} d\Omega$$

$$+ \frac{v_1}{\pi} g\left(\frac{h}{a}\right) \int_o^\infty \frac{\sin \Omega t \left[1 - \cos \Omega (t_o + t_1)\right]}{\Omega^3} d\Omega$$

$$+ \frac{2a}{\pi^3} (v_o + v_1) \sum_{n=1}^\infty (-1)^n \frac{\cosh\left[\frac{n\pi}{a}(x + h)\right] \cos\left(\frac{n\pi}{a} y\right)}{n^2 \cosh \frac{n\pi h}{a}} \int_o^\infty \frac{\Omega \cos \Omega t \sin \Omega t_o}{(\omega_n^2 - \Omega^2)} d\Omega$$

$$+ \frac{2a}{\pi^3} (v_o + v_1) \sum_{n=1}^\infty (-1)^n \frac{\cosh\left[\frac{n\pi}{a}(x + h)\right] \cos\left(\frac{n\pi}{a} y\right)}{n^2 \cosh \frac{n\pi}{a} h} \int_o^\infty \frac{\Omega \sin \Omega t \left[1 - \cos \Omega t_o\right]}{(\omega_n^2 - \Omega^2)} d\Omega$$

$$- \frac{2a}{\pi^3} v_1 \sum_{n=1}^\infty (-1)^n \frac{\cosh\left[\frac{n\pi}{a}(x + h)\right] \cos\left(\frac{n\pi}{a} y\right)}{n^2 \cosh \frac{n\pi h}{a}} \int_o^\infty \frac{\Omega \cos \Omega t \sin \Omega (t_o + t_1)}{(\omega_n^2 - \Omega^2)} d\Omega$$

$$- \frac{2a}{\pi^3} v_1 \sum_{n=1}^\infty (-1)^n \frac{\cosh\left[\frac{n\pi}{a}(x + h)\right] \cos\left(\frac{n\pi}{a} y\right)}{n^2 \cosh \frac{n\pi}{a} h} \int_o^\infty \frac{\Omega \sin \Omega t \left[1 - \cos \Omega (t_o + t_1)\right]}{(\omega_n^2 - \Omega^2)} d\Omega .$$

In addition to the previous integrals others occur which can be solved by the same complex method indicated in the appendix. These are:

$$\int_0^\infty \frac{\cos \Omega t \sin \Omega (t_o + t_1)}{\Omega} d\Omega \qquad \left\{ \begin{array}{lll} \pi/2 & \text{for} & t < t_o + t_1 \\ 0 & \text{for} & t > t_o + t_1 \end{array} \right\}$$

$$\int_0^\infty \frac{\sin \Omega t \left[1 - \cos \Omega (t_o + t_1)\right]}{\Omega} d\Omega \qquad \left\{ \begin{array}{lll} \pi/2 & \text{for} & t < t_o + t_1 \\ 0 & \text{for} & t > t_o + t_1 \end{array} \right\}$$

$$\int_0^\infty \frac{\sin \Omega t \left[1 - \cos \Omega (t_o + t_1)\right]}{\Omega^3} d\Omega \qquad \left\{ \begin{array}{ll} (\pi/4)\, t\, (2 t_o + 2t_1 - t) & \text{for } t < t_o + t_1 \\ (\pi/4)\, (t_o + t_1)^2 & \text{for } t > t_o + t_1 \end{array} \right\}$$

$$\int_0^\infty \frac{\Omega \cos \Omega t \sin \Omega (t_o + t_1)}{\omega_n^2 - \Omega^2} d\Omega \qquad \left\{ \begin{array}{ll} (-\pi/2) \cos\omega_n t \cos\omega_n (t_o + t_1) & \text{for } t < t_o + t_1 \\ (\pi/2) \sin\omega_n t \sin\omega_n (t_o + t_1) & \text{for } t > t_o + t_1 \end{array} \right\}$$

$$\int_0^\infty \frac{\sin \Omega (t_o + t_1) \cos \Omega t}{\Omega^3} d\Omega \qquad \left\{ \begin{array}{ll} (-\pi/4) \left[t^2 + (t_1 + t_o)^2\right] & \text{for } t < t_o + t_1 \\ (-\pi/2)\, t\, (t_o + t_1) & \text{for } t > t_o + t_1 \end{array} \right\}$$

$$\int_0^\infty \frac{\Omega \sin \Omega t \left[1 - \cos \Omega (t_o + t_1)\right]}{\omega_n^2 - \Omega^2} d\Omega =$$

$$\left\{ \begin{array}{lll} (-\pi/2) \left[\cos\omega_n t + \sin\omega_n t \sin\omega_n (t_o + t_1)\right] & \text{for} & t < t_o + t_1 \\ (-\pi/2) \left[\cos\omega_n t - \cos\omega_n t \cos\omega_n (t_o + t_1)\right] & \text{for} & t > t_o + t_1 \end{array} \right\}$$

With these results the velocity potential finally is found to be

$$\Phi(y,x,t) = \left[\frac{y^2}{2a} - \frac{a}{6} - \frac{1}{2a}(x^2+2hx)\right]\left[v_o\begin{Bmatrix}1\\0\\0\end{Bmatrix} + v_1\begin{Bmatrix}0\\-1\\0\end{Bmatrix}\right]$$

$$- \frac{gh}{a}\left[v_o\begin{Bmatrix}\frac{1}{4}(2tt_o - 2t^2 - t_o^2)\\ t_o/4\,(t_o - 2t)\\ t_o/4\,(t_o - 2t)\end{Bmatrix} + v_1\begin{Bmatrix}\frac{1}{4}\left[(t_o+t_1)^2 - 2t_1t - t_o^2\right]\\ \frac{1}{4}\left[t_o^2 - 4tt_o + 2t^2 - 2tt_1 + (t_o+t_1)^2\right]\\ \frac{1}{4}\left[t_o^2 + 2tt_1 - (t_o+t_1)^2\right]\end{Bmatrix}\right]$$

$$- \frac{av_o}{\pi^2}\sum_{n=1}^{\infty}\frac{(-1)^n \cosh\left[\frac{n\pi}{a}(x+h)\right]\cos\left(\frac{n\pi}{a}y\right)}{n^2\cosh\left(\frac{n\pi h}{a}\right)}\begin{Bmatrix}\cos\omega_n t + \cos\omega_n(t-t_o)\\ \cos\omega_n t - \cos\omega_n(t-t_o)\\ \cos\omega_n t - \cos\omega_n(t-t_o)\end{Bmatrix}$$

$$- \frac{av_1}{\pi^2}\sum_{n=1}^{\infty}\frac{(-1)^n \cosh\left[\frac{n\pi}{a}(x+h)\right]\cos\left(\frac{n\pi}{a}y\right)}{n^2\cosh\left(\frac{n\pi h}{a}\right)}\begin{Bmatrix}\cos\omega_n(t-t_o) - \cos\omega_n\left[t-(t_o+t_1)\right]\\ -\cos\omega_n(t-t_o) - \cos\omega_n\left[t-(t_o+t_1)\right]\\ \cos\omega_n\left[t-(t_o+t_1)\right] - \cos\omega_n(t-t_o)\end{Bmatrix}.$$

In this equation the first line corresponds to the time interval $0 < t < t_o$, the second, to the time interval $t_o < t < t_o + t_1$ and the third line corresponds to $t > t_o + t_1$.

In the symmetric case when the container wall at $y = a$ is moved the same amount and with the same velocity to the left and right, the time intervals are consecutively $0 < t < t_o$, $t_o < t < 2t_o$, and $t > 2t_o$. For this case $v_o = v_1$, $t_1 = t_o$ and the velocity potential is

$$\Phi(y,x,t) = \left[\frac{y^2}{2a} - \frac{a}{6} - \frac{1}{2a}(x^2+2hx)\right] v_o \begin{Bmatrix} 1 \\ -1 \\ 0 \end{Bmatrix}$$

$$- \frac{ghv_o}{2a} \begin{Bmatrix} t_o^2 - t^2 \\ t^2 - 4t_o t + 3t_o^2 \\ -t_o^2 \end{Bmatrix}$$

$$- \frac{av_o}{\pi^2} \sum_{n=1}^{\infty} (-1)^n \frac{\cosh\left[\frac{n\pi}{a}(x+h)\right]\cos\left(\frac{n\pi}{a}y\right)}{n^2 \cosh\left(\frac{n\pi h}{a}\right)}$$

$$\begin{Bmatrix} \cos\omega_n t + 2\cos\omega_n(t-t_o) - \cos\omega_n(t-2t_o) \\ \cos\omega_n t - 2\cos\omega_n(t-t_o) - \cos\omega_n(t-2t_o) \\ \cos\omega_n t - 2\cos\omega_n(t-t_o) + \cos\omega_n(t-2t_o) \end{Bmatrix} \tag{3.10}$$

The free fluid surface displacement is

$$\bar{x} = -\frac{v_o h}{a} \begin{Bmatrix} t \\ 2t_o - t \\ o \end{Bmatrix} + \frac{v_o a}{g\pi^2} \sum_{n=1}^{\infty} \frac{(-1)^{n+1}\omega_n \cos\left(\frac{n\pi}{a}y\right)}{n^2} F_n(t) \tag{3.11}$$

where

$$F_n(t) = \begin{Bmatrix} \sin\omega_n t + 2\sin\omega_n(t-t_o) - \sin\omega_n(t-2t_o) \\ \sin\omega_n t - 2\sin\omega_n(t-t_o) - \sin\omega_n(t-2t_o) \\ \sin\omega_n t - 2\sin\omega_n(t-t_o) + \sin\omega_n(t-2t_o) \end{Bmatrix}.$$

The upper line represents the time interval $0 < t < t_o$, the middle line, the interval $t_o < t < 2t_o$ and the lower line is valid for $t > 2t_o$. Considering only

the first term of the surface displacement, it can be seen that the surface level will sink during the time interval $0 < t < t_o$ and then rise again to its original level in the second time interval $t_o < t < 2\,t_o$. The pressure in the container at a depth $(-x)$ is given by

$$p = -\rho g x - \rho g \left(\frac{h}{a}\right) v_o \begin{Bmatrix} t \\ 2\,t_o - t \\ o \end{Bmatrix} - \frac{\rho v_o a}{\pi^2} \sum_{n=1}^{\infty} \frac{(-1)^n \omega_n \cosh\left[\frac{n\pi}{a}(x+h)\right] \cos\left(\frac{n\pi}{a} y\right)}{n^2 \cosh\left(\frac{n\pi\, h}{a}\right)} F_n(t). \qquad (3.12)$$

At the tank wall $y = 0$ the pressure distribution is

$$p_{y=o} = -\rho g x - \rho g \left(\frac{h}{a}\right) v_o \begin{Bmatrix} t \\ 2\,t_o - t \\ o \end{Bmatrix} - \frac{\rho v_o a}{\pi^2} \sum_{n=1}^{\infty} \frac{(-1)^n \omega_n \cosh\left[\frac{n\pi}{a}(x+h)\right]}{n^2 \cosh\left(\frac{n\pi\, h}{a}\right)} F_n(t) \qquad (3.13)$$

and at the container wall $x = a$ it yields

$$p_{y=a} = -\rho g x - \rho g \left(\frac{h}{a}\right) v_o \begin{Bmatrix} t \\ 2\,t_o - t \\ o \end{Bmatrix} - \frac{\rho v_o a}{\pi^2} \sum_{n=1}^{\infty} \frac{\omega_n \cosh\left[\frac{n\pi}{a}(x+h)\right]}{n^2 \cosh\left(\frac{n\pi\, h}{a}\right)} F_n(t). \qquad (3.14)$$

At the container bottom $x = -h$ the pressure distribution is

$$p_{bottom} = \rho g h - \rho g \left(\frac{h}{a}\right) v_o \begin{Bmatrix} t \\ 2t_o - t \\ o \end{Bmatrix}$$

$$- \frac{\rho v_o a}{\pi^2} \sum_{n=1}^{\infty} \frac{(-1)^n \omega_n \cos\left(\frac{n\pi}{a} y\right)}{n^2 \cosh\left(\frac{n\pi h}{a}\right)} F_n(t) \quad . \tag{3.15}$$

The fluid force in y-direction is

$$F_y = \frac{-2mv_o}{\pi^2} \sum_{n=1}^{\infty} \frac{\omega_{2n-1} \tanh\left(\frac{(2n-1)\pi h}{a}\right)}{(2n-1)^3 \pi \ (h/a)} F_{2n-1}(t) \tag{3.16}$$

and the moment of the liquid about an axis parallel to the z-axis through the center of gravity of the quiescent fluid is

$$M_z = \frac{mav_o}{\pi^3} \sum_{n=1}^{\infty} \frac{\omega_{2n-1}}{(2n-1)^3} \left[\tanh\left(\frac{(2n-1)\pi h}{a}\right) \right.$$

$$\left. + \frac{2}{(2n-1)\frac{\pi h}{a}} \left[\frac{2}{\cosh\left[\frac{(2n-1)\pi h}{a}\right]} - 1 \right] \right] F_{2n-1}(t) . \tag{3.17}$$

The velocity distribution in y-direction yields

$$v = \frac{y}{a} v_o \begin{Bmatrix} 1 \\ -1 \\ o \end{Bmatrix} + \frac{v_o}{\pi} \sum_{n=1}^{\infty} \frac{(-1)^n \cosh\left[\frac{n\pi}{a}(x+h)\right] \sin\left(\frac{n\pi}{a} y\right)}{n \cosh\left(\frac{n\pi h}{a}\right)} G_n(t)$$

which vanishes for the left container wall $y = 0$; for the right container wall $y = a$ it exhibits the value v_o during the time interval $0 < t < t_o$ and the value $-v_o$ during the time interval $t_o < t < 2t_o$, and vanishes for the time $t > 2t_o$, as prescribed by the boundary conditions.

$G_n(t)$ represents the time function as given in the infinite series of the potential (3.10). The velocity distribution in x-direction is

$$u = -\frac{(x+h)}{a} v_0 \begin{Bmatrix} 1 \\ -1 \\ 0 \end{Bmatrix} - \frac{v_0}{\pi} \sum_{n=1}^{\infty} \frac{(-1)^n \sinh\left[\frac{n\pi}{a}(x+h)\right] \cos\left(\frac{n\pi}{a} y\right)}{n \cosh\left(\frac{n\pi h}{a}\right)} G_n(t).$$

The first term in these expressions indicates the motion of the liquid without sloshing since the geometry of the container changes, The liquid has to flow down during the time interval $0 < t < t_o$ and flow up again during the time interval $t_o < t < 2t_o$ as the wall moves back to its original position.

C. RESPONSE OF LIQUID DUE TO SINUSOIDAL PULSE

A sinusoidal pulse consisting of one single sine-wave (Fig. 11) of the form $v_o \sin(2\pi t/t_o)$, with t_o seconds duration as given by

$$v(t) = \begin{cases} v_o \sin(2\pi t/t_o) & \text{for} \quad o \le t \le t_o, \\ o & \text{elsewhere} \end{cases}$$

can be represented by the Fourier-Integral

$$v(t) = \frac{2v_o}{t_o} \int_o^{\infty} \frac{\left[\cos \Omega t_o - 1\right] \cos \Omega t}{(\Omega^2 - 4\pi^2/t_o^2)} \, d\Omega$$

$$+ \frac{2v_o}{t_o} \int_o^{\infty} \frac{\sin \Omega t_o \sin \Omega t}{(\Omega^2 - 4\pi^2/t_o^2)} \, d\Omega.$$

The potential is, therefore,

$$\Phi(y,x,t) = \frac{2v_o}{t_o}\int_o^\infty \left[\frac{y^2}{2a} - \frac{a}{6} - \frac{1}{2a}(x^2+2hx)\right]\left[\frac{\sin\Omega t_o \sin\Omega t}{(\Omega^2 - 4\pi^2/t_o^2)} - \frac{\cos\Omega t\left[1-\cos\Omega t_o\right]}{(\Omega^2 - 4\pi^2/t_o^2)}\right]d\Omega - \frac{2v_o gh}{t_o a}\int_o^\infty \frac{\sin\Omega t_o \sin\Omega t}{\Omega^2(\Omega^2 - 4\pi^2/t_o^2)}\,d\Omega$$

$$+ \frac{2v_o gh}{t_o a}\int_o^\infty \frac{\cos\Omega t\left[1-\cos\Omega t_o\right]}{\Omega^2\left[\Omega^2 - 4\pi^2/t_o^2\right]}\,d\Omega$$

$$+ \frac{4av_o}{\pi^2 t_o}\sum_{n=1}^{\infty}(-1)^n \frac{\cosh\left[\frac{n\pi}{a}(x+h)\right]}{n^2\cosh\left(\frac{n\pi h}{a}\right)}\cos\left(\frac{n\pi}{a}y\right)\int_o^\infty \left[\frac{\Omega^2\sin\Omega t_o \sin\Omega t}{(\Omega^2 - 4\pi^2/t_o^2)(\omega_n^2 - \Omega^2)} - \frac{\Omega^2\cos\Omega t\left[1-\cos\Omega t_o\right]}{(\Omega^2 - 4\pi^2/t_o^2)(\omega_n^2 - \Omega^2)}\right]d\Omega .$$

The occurring integrals are

$$\int_o^\infty \frac{\sin\Omega t \sin\Omega t_o}{(\Omega^2 - 4\pi^2/t_o^2)}\,d\Omega = \begin{cases} \frac{t_o}{4}\sin\frac{2\pi t}{t_o} & \text{for } t < t_o \\ 0 & \text{for } t > t_o \end{cases}$$

$$\int_o^\infty \frac{\cos\Omega t\left[1-\cos\Omega t_o\right]}{(\Omega^2 - 4\pi^2/t_o^2)}\,d\Omega = \begin{cases} -\frac{t_o}{4}\sin\frac{2\pi t}{t_o} & \text{for } t < t_o \\ 0 & \text{for } t > t_o \end{cases}$$

$$\int_o^\infty \frac{\sin\Omega t \sin\Omega t_o}{\Omega^2(\Omega^2 - 4\pi^2/t_o^2)}\,d\Omega = \begin{cases} \frac{t_o^2}{4\pi^2}\left[\frac{t_o}{4}\sin\left(\frac{2\pi t}{t_o}\right) - \frac{\pi t}{2}\right] & \text{for } t < t_o \\ -\frac{t_o^3}{8\pi} & \text{for } t > t_o \end{cases}$$

$$\int_0^\infty \frac{\Omega^2 \sin \Omega t \sin \Omega t_o}{(\omega_n^2 - \Omega^2)\left(\Omega^2 - 4\pi^2/t_o^2\right)} d\Omega =$$

$$\left\{ \begin{array}{ll} \dfrac{-\omega_n \pi}{2(\omega_n^2 - 4\pi^2/t_o^2)} \left[\sin \omega_n t \cdot \cos \omega_n t_o\right] + \dfrac{\pi^2 \sin\left(\dfrac{2\pi}{t_o} t\right)}{t_o(\omega_n^2 - 4\pi^2/t_o^2)} & \text{for } t < t_o \\ -\dfrac{\omega_n \pi}{2(\omega_n^2 - 4\pi^2/t_o^2)} \cos \omega_n t \sin \omega_n t_o & \text{for } t > t_o \end{array} \right\}$$

$$\int_0^\infty \frac{\cos \Omega t \left[1 - \cos \Omega t_o\right]}{\Omega^2 (\Omega^2 - 4\pi^2/t_o^2)} d\Omega =$$

$$\left\{ \begin{array}{ll} + \dfrac{t_o^2}{8\pi}(t - t_o) - \dfrac{t_o^3}{16\pi^2} \sin\left(\dfrac{2\pi t}{t_o}\right) & \text{for } t < t_o \\ 0 & \text{for } t > t_o \end{array} \right\}$$

$$\int_0^\infty \frac{\Omega^2 \cos \Omega t \left[1 - \cos \Omega t_o\right]}{(\omega_n^2 - \Omega^2)(\Omega^2 - 4\pi^2/t_o^2)} d\Omega =$$

$$\left\{ \begin{array}{ll} \dfrac{\pm \pi \omega_n}{2(\omega_n^2 - 4\pi^2/t_o^2)} \left[\sin \omega_n t \mp \cos \omega_n t \sin \omega_n t_o\right] - \dfrac{\pi^2 \sin\left(\dfrac{2\pi}{t_o} t\right)}{t_o(\omega_n^2 - 4\pi^2/t_o^2)} & \text{for } t < t_o \\ \dfrac{\pm \pi \omega_n}{2(\omega_n^2 - 4\pi^2/t_o^2)} \left[\sin \omega_n t \mp \sin \omega_n t \cos \omega_n t_o\right] & \text{for } t > t_o \end{array} \right\}$$

With these results the velocity potential due to a sinusoidal pulse is

$$\Phi(y,x,t) = v_o\left[\frac{y^2}{2a} - \frac{a}{6} - \frac{1}{2a}(x^2+2hx)\right]\begin{Bmatrix}1\\0\end{Bmatrix}\sin\left(\frac{2\pi t}{t_o}\right)$$

$$-\frac{2v_o g t_o^2 h}{a}\begin{Bmatrix}\dfrac{\sin\frac{2\pi t}{t_o}}{8\pi^2} + \dfrac{1}{8\pi} - \dfrac{t}{4\pi t_o}\\ -\dfrac{1}{8\pi}\end{Bmatrix}$$

$$+\frac{4av_o}{\pi^2 t_o}\sum_{n=1}^{\infty}(-1)^n\frac{\cosh\left[\frac{n\pi}{a}(x+h)\right]\cos\left(\frac{n\pi}{a}y\right)}{n^2\cosh\left(\frac{n\pi h}{a}\right)}\,\bar{G}_n(t) \qquad (3.18)$$

where

$$\bar{G}_n(t) = \begin{cases}\dfrac{-\pi\omega_n}{2(\omega_n^2 - 4\pi^2/t_o^2)}\left[\sin\omega_n t + \sin\omega_n(t_o - t)\right] + \dfrac{2\pi^2\sin\left(\frac{2\pi t}{t_o}\right)}{t_o(\omega_n^2 - 4\pi^2/t_o^2)} & \text{for } t < t_o\\ \dfrac{\pi\omega_n}{2(\omega_n^2 - 4\pi^2/t_o^2)}\left[-\sin\omega_n t + \sin\omega_n(t - t_o)\right] & \text{for } t > t_o\end{cases}.$$

The free fluid surface displacement is

$$\bar{x} = -\frac{2v_o\pi}{g t_o}\left(\frac{y^2}{2a} - \frac{a}{6}\right)\begin{Bmatrix}1\\0\end{Bmatrix}\cos\left(\frac{2\pi t}{t_o}\right) + \frac{v_o h t_o}{2a\pi}\begin{Bmatrix}1\\0\end{Bmatrix}\left[\cos\left(\frac{2\pi t}{t_o}\right) - 1\right]$$

$$-\frac{2v_o a}{\pi g t_o}\sum_{n=1}^{\infty}(-1)^n\frac{\cos\left(\frac{n\pi}{a}y\right)}{n^2(\omega_n^2 - 4\pi^2/t_o^2)}\,\bar{F}_n(t) \qquad (3.19)$$

where

$$\bar{F}_n(t) = \begin{cases}-\omega_n^2\left[\cos\omega_n t - \cos\omega_n(t - t_o)\right] + \dfrac{8\pi^2}{t_o^2}\cos\dfrac{2\pi t}{t_o} & \text{for } t < t_o\\ \omega_n^2\left[-\cos\omega_n t + \cos\omega_n(t - t_o)\right] & \text{for } t > t_o\end{cases}.$$

The pressure in the container at a depth (-x) is given by

$$p = -\rho g x - \frac{2\rho v_o \pi}{t_o}\left[\frac{y^2}{2a} - \frac{a}{6} - \frac{1}{2a}(x^2 + 2hx)\right]\begin{Bmatrix}1\\0\end{Bmatrix}\cos\left(\frac{2\pi t}{t_o}\right)$$

$$+ \frac{\rho v_o g h t_o}{2\pi a}\begin{Bmatrix}1\\0\end{Bmatrix}\left[\cos\left(\frac{2\pi t}{t_o}\right) - 1\right]$$

$$- \frac{2\rho a(u_o)}{\pi t_o}\sum_{n=1}^{\infty}\frac{(-1)^n \cosh\left[\frac{n\pi}{a}(x+h)\right]\cos\left(\frac{n\pi}{a}y\right)}{n^2\cosh\left(\frac{n\pi h}{a}\right)\left(\omega_n^2 - 4\pi^2/t_o^2\right)}\ \bar{F}_n(t). \qquad (3.20)$$

At the tank wall y = 0 the pressure distribution is:

$$p_{y=o} = -\rho g x + \frac{2\rho v_o \pi}{t_o}\left[\frac{a}{6} + \frac{1}{2a}(x^2 + 2hx)\right]\begin{Bmatrix}1\\0\end{Bmatrix}\cos\left(\frac{2\pi t}{t_o}\right)$$

$$+ \frac{\rho v_o g h t_o}{2a\pi}\begin{Bmatrix}\left[\cos\frac{2\pi t}{t_o} - 1\right]\\0\end{Bmatrix}$$

$$- \frac{2\rho v_o a}{\pi t_o}\sum_{n=1}^{\infty}(-1)^n\frac{\cosh\left[\frac{\pi n}{a}(x+h)\right]}{n^2\cosh\left(\frac{n\pi h}{a}\right)\left(\omega_n^2 - \frac{4\pi^2}{t_o^2}\right)}\ \bar{F}_n(t) \qquad (3.21)$$

and at the container wall y = a the pressure distribution yields

$$p_{y=a} = -\rho g x - \frac{2\rho v_o \pi}{t_o}\left[\frac{a}{3} - \frac{1}{2a}(x^2 + 2hx)\right]\begin{Bmatrix}\cos(2\pi t/t_o)\\0\end{Bmatrix}$$

$$+ \frac{\rho v_o g h t_o}{2\pi a}\begin{Bmatrix}\left[\cos(2\pi t/t_o) - 1\right]\\0\end{Bmatrix}$$

$$- \frac{2\rho v_o a}{\pi t_o}\sum_{n=1}^{\infty}\frac{\cosh\left[\frac{n\pi}{a}(x+h)\right]}{n^2\cosh\left(\frac{n\pi h}{a}\right)(\omega_n^2 - 4\pi^2/t_o^2)}\ \bar{F}_n(t). \qquad (3.22)$$

The pressure at the bottom (x = -h) yields

$$p_{bottom} = \rho g h - \frac{2\rho v_o \pi}{t_o}\left[\frac{y^2}{2a} - \frac{a}{6} + \frac{h^2}{2a}\right]\begin{Bmatrix}\cos(2\pi t/t_o)\\ 0\end{Bmatrix} + \frac{\rho v_o g h t_o}{2\pi a}\begin{Bmatrix}[\cos(2\pi t/t_o) - 1]\\ 0\end{Bmatrix} - \frac{2\rho v_o a}{\pi t_o}\sum_{n=1}^{\infty}\frac{(-1)^n \cos\left(\frac{n\pi}{a}y\right)}{n^2 \cosh\left(\frac{n\pi h}{a}\right)\left(\omega_n^2 - 4\pi^2/t_o^2\right)}\,\bar{F}_n(t) \quad . \tag{3.23}$$

The liquid force in y-direction is

$$F_y = -\frac{v_o \pi m}{t_o}\begin{Bmatrix}\cos(2\pi t/t_o)\\ 0\end{Bmatrix} - \frac{4 v_o m}{\pi t_o}\sum_{n=1}^{\infty}\frac{\tanh\left(\frac{(2n-1)\pi h}{a}\right)}{\pi\left(\frac{h}{a}\right)(2n-1)^3(\omega_{2n-1}^2 - 4\pi^2/t_o^2)}\,\bar{F}_{2n-1}(t). \tag{3.24}$$

and the fluid moment yields

$$M_z = ma^2\left[\frac{v_o \pi}{t_o}, \frac{1}{6\left(\frac{h}{a}\right)}\begin{Bmatrix}\cos(2\pi t/t_o)\\ 0\end{Bmatrix} + \frac{4v_o}{\pi^2 a t_o}\sum_{n=1}^{\infty}\frac{F_{2n-1}(t)\left[\frac{\tanh\left(\frac{(2n-1)\pi h}{a}\right)}{2} + \frac{\left\{\frac{2}{\cosh\left(\frac{(2n-1)\pi h}{a}\right)} - 1\right\}}{(2n-1)\,\frac{\pi h}{a}}\right]}{(2n-1)^3(\omega_{2n-1}^2 - 4\pi^2/t_o^2)}\right]. \tag{3.25}$$

Finally, the velocity distribution in y-direction is

$$v = v_o \left[\frac{y}{a} \begin{Bmatrix} 1 \\ 0 \end{Bmatrix} \sin \frac{2\pi t}{t_o} \right] -$$

$$- \frac{4v_o}{\pi t_o} \sum_{n=1}^{\infty} \frac{(-1)^n \cosh\left(\frac{n\pi}{a}(x+h)\right)}{n \cosh\left(\frac{n\pi}{a} h\right)} \sin\left(\frac{n\pi}{a} y\right) \bar{G}_n(t) .$$

It vanishes for the left wall $y = 0$ and exhibits for the right container wall $y = a$ the expression $v_o \frac{y}{a} \begin{Bmatrix} 1 \\ 0 \end{Bmatrix} \sin (2\pi t / t_o)$, as given in the boundary conditions.

In x-direction it is

$$u = -v_o \frac{(x+h)}{a} \begin{Bmatrix} 1 \\ 0 \end{Bmatrix} \sin\left(\frac{2\pi t}{t_o}\right)$$

$$+ \frac{4v_o}{t_o} \sum_{n=1}^{\infty} \frac{(-1)^n \sinh\left(\frac{n\pi}{a}(x+h)\right)}{n \cosh\left(\frac{n\pi h}{a}\right)} \cos\left(\frac{n\pi}{a} y\right) \bar{G}_n(t) .$$

which satisfies the boundary condition at the container bottom $x = -h$.

SECTION IV. NUMERICAL EVALUATION AND CONCLUSIONS

The behavior of the liquid caused by harmonic excitation of one container wall does not present any new effects compared to those of the excitation of the total container. At the natural frequencies ω_n the free fluid surface displacement, fluid force and moment, etc., exhibit singularities. For this reason the number of graphs showing this type of excitation has been held to a minimum. However, it is interesting to note that in the case of harmonic excitation of one side wall the nodal line of the free fluid surface no longer remains at $y = a/2$, as in the case of excitation of the total container. For an excitation frequency Ω below first resonance, the nodal line is in the right half

of the free fluid surface, while above resonance it is in the left half of the free surface. Figure 12 exhibits the shape of the free fluid for excitation frequencies $\Omega = 0.9\,\omega_1$, $1.1\,\omega_1$ and $0.9\,\omega_3$.

The character of the height of the free liquid surface is well presented by the formulas for double rectangular and sinusoidal pulses (Equations 3.11 and 3.19). The first one probably best describes the effect of the rocket firing. Both excitations, however, should yield a similar liquid response in spite of the different analytical expressions. The disturbance of one container wall acts like a line source emitting waves of all wavelengths and frequencies. The numerical results are given for a tank of length a = 250 feet and a liquid height h = 16 feet. The natural frequencies for this container are given in Table 1 for n = 1, 2, ...30.

A rectangular double pulse with a duration of one second is considered. During the first half-second of the pulse the container wall moves to the right and the liquid moves down the moving wall, while during the second half of the pulse duration the container wall moves to the left and the liquid moves up, forming a valley in front of the wall. After the pulse is completed, the liquid is still moving toward the left, separating from the wall and starting to build up wave packages. As the first wave of the package moves towards the left, it decreases its height and the energy thus released is used to form other waves. The first wave valley of larger wave length initially created by the motion of the container wall moves faster away from the disturbance than the waves of smaller wave length in the wave package. The free fluid surface elevation of the liquid in the container is shown in Figures 13 through 24 at various times; the abscissa is (y/a) and the ordinate is $\overline{x}/v_o$.

It can be seen that after completion of the pulse the liquid reaches a height of $\overline{x} = 0.41v_o$, while the valley exhibits a magnitude of $\overline{x} = -0.042v_o$ and is at a location $y \approx 0.95a$. One second afterward, the valley has moved to $y = 0.87a$ and has decreased its magnitude to about $\overline{x} = -0.038v_o$. At the same time, the peak amplitude of the wave which separated from the wall has moved only by 0.02a and has decreased its amplitude to a value of $\overline{x} = 0.212\,v_o$. As time increases, other waves are generated on the right side of the container, while the amplitudes of the present waves decrease continuously.

At three seconds, i.e., two seconds after the disturbing pulse has been completed, the original valley has a depth of $\overline{x} = 0.028\,v_o$ and is located

further to the left at y = 0.77a. A second wave has been formed very close to the first one. The positive displacement of the first wave is reduced again to a value of approximately $\bar{x} = 0.125\ v_o$, while its negative displacement is $\bar{x} = -0.18\ v_o$. As time elapses, the waves move with different speeds toward the other container wall. The first valley needs about eleven seconds to traverse the container.

At time four seconds, the first valley has further decreased its magnitude (to $\bar{x} = -0.023 v_o$) and is located at y = 0.69a. The magnitude of the first wave has decreased to $\bar{x} = 0.087 v_o$ and is located at y = 0.87a. A third wave has been formed and the second wave has a negative displacement of $\bar{x} = -0.145a$. As the first valley travels toward the left container wall its geometric shape becomes flatter and its depth decreases. The first waves separate more and more from the wave package, decreasing their amplitude, while others are still formed.

At the time of six to seven seconds after completion of the pulse, the liquid on the left wall experiences a decrease in level. A few seconds later the first wave package seems to be completed. The first valley finally reaches the left wall at about eleven seconds with a magnitude of $\bar{x} = -0.22\ v_o$, is reflected within two seconds and in the fifteenth second exhibits an amplitude of $\bar{x} = 0.055\ v_o$. The reflected wave is running toward the right into the first waves of the wave package.

At this time, about one-tenth of the container surface from the right hand wall is about at the equilibrium position $\bar{x} = 0$. The first of the reflected waves increases in magnitude, then decreases during the time the waves work at each other. During that same time period, one-tenth of the liquid level on the right hand side container wall sinks slowly to a value of $\bar{x} = -0.01\ v_o$ at twenty-one seconds, and forms a curved surface with more negative displacement at the right container wall, while on the left container wall large liquid oscillations ($\bar{x} = -0.06 v_o$) take place. With increasing time the liquid level on the right container wall rises again to a level of about $\bar{x} = 0.012 v_o$, which stretches to about one-fifth of the fluid surface area from the right container wall into the liquid.

During the time period from twenty-five to twenty-seven seconds, the liquid surface rises at y = a but decreases at y = 0.8a exhibiting an amplitude at y = a of about $\overline{x} = 0.036\ v_o$, then swings back to the negative side to an amplitude of $\overline{x} = -0.04\ v_o$, and so on. On the left hand wall of the container the amplitude increases to a value of about $0.12\ v_o$ as time proceeds, while in the center of the container a "confused" wave motion takes place.

At forty-nine seconds the amplitude of the liquid at the right container wall (y = a) exhibits a value $\overline{x} = 0.068\ v_o$ and shows a wave of larger wave length in its vicinity. It should be noted, however, that for a fairly large value of $v_o = 10$ feet per second, the original wave height at separation from the moving container wall would be 4.1 feet, while the initial valley is only 0.42 foot in depth. The maximum wave height at the left container wall would be about 0.7 foot.

Although the liquid motion can still be described for long periods after completion of the excitation pulse, in reality the motion may have damped out due to viscous forces of the fluid. Therefore, no further attempt is made to ascribe real significance to the wave motion which takes place after the first wave has reached the opposite container wall.

Before proceeding to the description of the liquid behavior at a fixed location in the container, the results of the sinusoidal pulse excitation will be investigated and discussed. It should again be mentioned that no energy dissipation has been considered during the liquid motion, indicating that the energy introduced into the system by the wall motion remains indefinitely in the liquid. This, of course, is not in agreement with daily experience.

The response of the free fluid surface to a sinusoidal pulse of the form $v_o \sin(2\pi\ t/\ t_o)$ of the container wall at y = a can also be presented at a fixed time after the pulse. Most of the results will be omitted here and only a few graphs are presented. (Figs. 25-30).

The total pulse duration is again $t_o = 1$ second. During half of the pulse duration the liquid will move down on the right container wall, while during the second half of the pulse, when the right container wall moves toward the left again to its initial position, the fluid moves up the wall. At time one and one-fourth seconds, i.e., one-fourth second after the pulse has been completed,

the valley exhibits a depth of $\bar{x} = -0.032\ v_o$ (which for $v_o = 10$ feet per second is a valley of 0.32 foot). The wave which moves away from the right hand wall has height of $\bar{x} = 0.25\ v_o$ (2.5 feet for $v_o = 10$ feet per second.

A comparison of these results with those for the rectangular pulse shows that the valley and the first wave height exhibit about sixteen percent larger values in the rectangular pulse case. Essentially the same liquid behavior is observed in these results. The first wave of the wave package moves with decreasing height but increasing wave length toward the left wall of the container, while new waves are added to the wave package as time elapses. The first created valley and waves move faster toward the left container wall than those of the interior of the wave package.

At about six seconds the liquid level on the left container wall starts to sink until the first valley which decreased its original magnitude of $\bar{x} = -0.032\ v_o$ to a value below $-0.01\ v_o$, increases it slightly again to about $\bar{x} = -0.014\ v_o$ at eleven seconds, at which time the reflection starts. Approximately one-tenth of the liquid level on the right container wall is in the equilibrium position at that time. As the amplitude of the reflected wave on the left container wall increases to positive values of magnitude $\bar{x} = 0.035\ v_o$, the liquid on the right hand side performs no motion at all from $y = 0.9a$ to $y = a$.

As time progresses, the reflected waves work against the wave package while the flat liquid surface area on the right hand side of the container increases its area from $y = a$ to $y \approx 0.85a$ and sinks like a straight surface. In the center of the container a violent wave motion takes place. The wave height on the left container wall increases to $\bar{x} = \pm 0.04\ v_o$, while the right-hand side surface curves to larger depths for $y = a$, swings first up at $y = 0.8a$ and is then followed by an increase of surface elevation at $y = a$ to a magnitude of about $\bar{x} = 0.01\ v_o$ at twenty-five seconds. In the time proceeding, the free fluid surface elevation at $y = 0.8a$ decreases to negative values, while it increases at the right container wall to a magnitude of about $0.024\ v_o$ at twenty-seven seconds. On the left container wall the amplitude is increasing with time and shows a value of $\bar{x} = 0.07\ v_o$ at forty-two seconds. On the right container wall, a wave of larger wave length forms.

The sequence of these motions can be seen in a 16mm movie, which was produced from the computer results.* It should be mentioned again, that the liquid motion is subjected to internal as well as to wall friction; therefore, the motion will be damped out soon and probably will not continue for the time length indicated in the graphs or the film. It should also be mentioned that the scale in the direction of the ordinate is greatly magnified. While the distance between the left and the right container wall is 250 feet, the height of the waves is only three to four feet.

The flow rate of 4000 feet^3 per second during the firing of the rocket engines is simulated by a velocity v_o of the right container wall of

$$v_o = 1.67/t_o.$$

With this relation, the velocity amplitude v_o of the right container wall during a double rectangular pulse for a half-pulse duration of t_o seconds has to be

$v_o = 6.7$ ft/sec. for $t_o = \frac{1}{4}$ second

$v_o = 3.4$ ft/sec. for $t_o = \frac{1}{2}$ second

$v_o = 1.67$ ft/sec. for $t_o = 1$ second.

For a sinusoidal pulse, the value for v_o can be obtained from

$$16 \text{ ft} \times 150 \text{ ft.} \times \int_0^{t_o/2} v_o \sin\left(\frac{2\pi t}{t_o}\right) dt = 4000 \text{ ft}^3$$

(the width of the container is 150 feet)

---

* The motion picture can be obtained on a loan basis from F. Kramer of MSFC, Test-Division.

which yields

$$v_o = \frac{1.67\pi}{t_o} = \frac{5.25}{t_o} \quad .$$

With this result the velocity amplitude v_o of the container wall during a sinusoidal pulse of duration t_o seconds is obtained as

$v_o = 10.5$ ft/ sec for $t_o = \frac{1}{2}$ second

$v_o = 5.25$ ft/ sec for $t_o = 1$ second

$v_o = 2.63$ ft/ sec for $t_o = 2$ seconds.

For a rectangular double pulse the original wave height at separation of the disturbing container wall would be $\bar{x} = 2.74$ feet, while the maximum liquid height at the left container wall is about 0.48 foot for double-pulse duration of one second. For a half-second duration, these values represent only the magnitude of 2.2 feet and 0.37 foot respectively.

Similar results are obtained for a sinusoidal pulse; only those for the one-second duration are presented here. The liquid height at the right container wall is 1.3 feet at the time of pulse completion, while the maximum wave height at the left container wall is about 0.37 foot. It may be mentioned that the sinusoidal excitation mode with one-second duration ($t_o = 1$ second) was used for the film. Figure 31 shows the surface elevation at the left wall, as a function of time.

The pressure distribution at the left container wall $y = 0$ is given for the rectangular pulse with a total duration of one-half, one and two seconds respectively, for various locations along that wall. The fluid height in this case is $h_3 = 16$ feet. For the pulse duration of one-half second, the pressure distribution $\frac{p_{y=o} + \rho g z}{\rho a u_o}$ at the left wall $y = 0$ is given at the free fluid surface,

at half the depth of the liquid and at the container bottom (Shown in Figs. 37 through 39). It can be seen that no dynamic pressure exists during the first few seconds that the wave is travelling from the right to the left container wall. At about nine seconds the pressure is indicated for the first time and continues to grow until it reaches (in a kind of sinusoidal fashion) a maximum of about $0.0035\ \rho\ a\ v_o$ at the free fluid surface, $0.0014\ \rho\ a\ v_o + \rho\ g\ 0.032a$ at half the liquid depth and $0.0013\ \rho\ v_o\ a + \rho\ g\ 0.064a$ at the container bottom.

However, these peak pressures are reached at various times, as seen in Figures 32-40 for various pulse durations. With the mass density $\rho = 0.973$ lbs sec^2/ ft^4 and the specific weight of $\gamma = \rho\ g = 62.4$ lbs$/ ft^3$, the total peak pressures at the left container wall for a rectangular double pulse are

(a) for $t_o = \frac{1}{4}$ second by

11.7 lbs$/ ft^2$	at $x = 0$	(at the free fluid surface)
504.7 lbs$/ ft^2$	at $x = -\frac{1}{2}h_3$	(at half the depth)
1004.7 lbs$/ ft^2$	at $x = -h_3$	(at the container bottom)

(b) for $t_o = \frac{1}{2}$ second by

21 lbs$/ ft^2$	at $x = 0$	(at the free fluid surface)
511.7 lbs$/ ft^2$	at $x = -h_3/_2$	(at half the depth)
1008.4 lbs$/ ft^2$	at $x = -h_3$	(at the container bottom)

(c) for $t_o = 1$ second by

27 lbs$/ ft^2$	at $x = 0$	(at the free fluid surface)
518.5 lbs$/ ft^2$	at $x = -h_3/_2$	(at half the depth)
1017 lbs$/ ft^2$	at $x = -h_3$	(at the container bottom) .

It can be seen, that the pressure at the bottom of the container (Fig. 41) coincides with the pressure at the wall ($y = 0$ for $x = -h$) (Fig. 39). In the center of the container at $y = a/2$, the pressure $\left(\frac{p_{Bottom} - \rho gh}{av_o\rho} \right)$ versus time is presented in Figures 44, 45, and 48 for $t_o = 1/4$, $1/2$ and 1 second. The peak pressure at the container bottom at $y = a/2$ is, therefore,

1002.7 lbs/ft^2 for t_o = 1/4 second

1005.2 lbs/ft^2 for t_o = 1/2 second

1009.6 lbs/ft^2 for t_o = 1 second .

The fluid force F_y is exhibited in the Figures 50 through 52 for $t_o = \frac{1}{4}, \frac{1}{2}$ and 1 second. For $t_o = \frac{1}{4}$ second, the force per foot of tank width in y-direction drops from a value of 113 pounds per foot to 61 pounds per foot. For a tank width of 150 feet this yields a total force on the container in y-direction of 17000 pounds at $t = \frac{1}{2}$ sec., i.e., exactly at the end of the pulse, and 9100 pounds at about 48.5 seconds. For a half-pulse duration $t_o = \frac{1}{2}$ second, the force per foot drops from 205 pounds per feet at t = 1 second to 115 pounds per feet at about 48.5 seconds. This corresponds to a total force 30, 800 pounds and 17, 200 pounds, respectively. For t_o = 1 second, i.e., a pulse duration of two seconds, the force per foot yields 263 pounds per foot at t = 2 seconds and drops to 182 pounds per foot at about 49 seconds. This corresponds to a total force of 39, 400 pounds and 27, 300 pounds, respectively.

The liquid moment is presented in Figures 53 through 55. For $t_o = \frac{1}{4}$ second, the maximum value of the moment per foot of liquid is 6700 pounds, which corresponds to a total moment of 10^6 foot-pounds. For $t_o = \frac{1}{2}$ second the maximum value is 14, 300 pounds corresponding to a total moment about the center of gravity of the undisturbed liquid of 2, 142, 000 foot-pounds. For t_o = 1 second the maximum value of the moment per unit width of the container is 26, 300 pounds. This corresponds to a total moment of M_z = 3, 950, 000 foot-pounds.

SECTION V. RECOMMENDATIONS

According to the theory presented and its numerical evaluation, it can be recommended that the walls of the container should be at least three feet higher than the liquid height to prevent any liquid loss during the operation of the system. The wall structure of the liquid reservoir should be designed according to the maximum pressures listed on page 35.

Since it was found that the liquid force and moments for pulses caused by one-wall-excitation are considerably smaller than those of a harmonic excitation of the complete container, further design specifications can be found only by treating the total system of liquid and structure. This has been done for various wind inputs and the result is presented in the report "Interaction of Structure and Liquid in the Sound Suppressor System."

George C. Marshall Space Flight Center,
National Aeronautics and Space Administration
Huntsville, Alabama, September 30, 1965.

TABLE I. NATURAL CIRCULAR FREQUENCIES

	y-Direction			z-Direction			
ω_n	h_1/a_1	h_2/a_1	h_3/a_1	h_1/a_2	h_2/a_2	h_3/a_2	fluid height ratio
ω_1	0.2248	0.2558	0.2832	0.4293	0.4863	0.5319	
ω_2	0.4461	0.5051	0.5555	0.8354	0.9305	1.0044	
ω_3	0.6608	0.7422	0.8087	1.2024	1.3104	1.3837	
ω_4	0.8663	0.9634	1.0380	1.5243	1.6358	1.6851	
ω_5	1.0609	1.1666	1.2425	1.8028	1.8880	1.9306	
ω_6	1.2435	1.3515	1.4236	2.0439	2.1104	2.1389	
ω_7	1.4136	1.5191	1.5842	2.2548	2.3042	2.3223	
ω_8	1.5716	1.6710	1.7276	2.4421	2.4774	2.4886	
ω_9	1.7180	1.8090	1.8569	2.6111	2.6358	2.6425	
ω_{10}	1.8538	1.9353	1.9748	2.7660	2.7829	2.7869	
ω_{11}	1.9797	2.0515	2.0835	2.9098	2.9213	2.9236	
ω_{12}	2.0970	2.1592	2.1848	3.0450	3.0526	3.0539	
ω_{13}	2.2066	2.2598	2.2801	3.1730	3.1780	3.1788	
ω_{14}	2.3094	2.3545	2.3704	3.2951	3.2984	3.2988	
ω_{15}	2.4062	2.4441	2.4565	3.4123	3.4144	3.4147	
ω_{16}	2.4979	2.5295	2.5390	3.5251	3.5265	3.5267	
ω_{17}	2.5851	2.6113	2.6186	3.6342	3.6351	3.6352	
ω_{18}	2.6683	2.6899	2.6955	3.7400	3.7406	3.7406	
ω_{19}	2.7480	2.7657	2.7700	3.8427	3.8431	3.8431	
ω_{20}	2.8247	2.8392	2.8424	3.9427	3.9429	3.9429	
ω_{21}	2.8987	2.9105	2.9129	4.0402	4.0403	4.0403	
ω_{22}	2.9073	2.9798	2.9817	4.1353	4.1354	4.1354	
ω_{23}	3.0397	3.0474	3.0488	4.2283	4.2283	4.2283	
ω_{24}	3.1072	3.1135	3.1145	4.3192	4.3193	4.3193	

TABLE I. (Concluded)

	y-Direction			z-Direction			
ω_n	h_1/a_1	h_2/a_1	h_3/a_1	h_1/a_2	h_2/a_2	h_3/a_2	fluid height ratio
ω_{25}	3.1730	3.1780	3.1788	4.4083	4.4084	4.4084	
ω_{26}	3.2372	3.2412	3.2418	4.4956	4.4957	4.4957	
ω_{27}	3.2999	3.3031	3.3036	4.5813	4.5813	4.5813	
ω_{28}	3.3613	3.3639	3.3642	4.6654	4.6654	4.6654	
ω_{29}	3.4214	3.4235	3.4238	4.7479	4.7479	4.7479	
ω_{30}	3.4805	3.4821	3.4823	4.8291	4.8291	4.8291	

$h_1 = 10$ feet
$h_2 = 12$ feet
$h_3 = 16$ feet

$a_1 = 250$ feet
$a_2 = 150$ feet

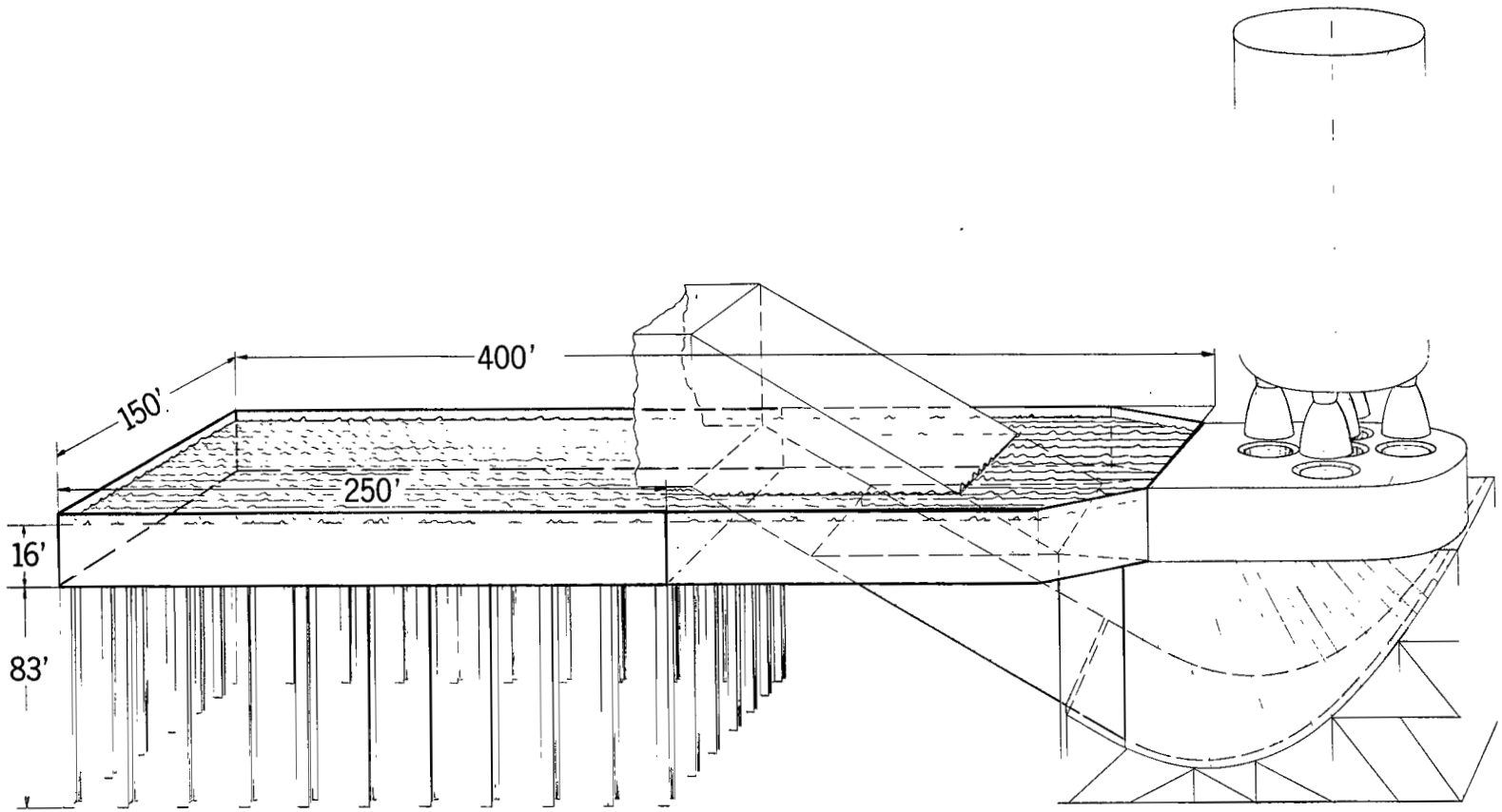

FIGURE 1. SCHEMATIC OF TANK SYSTEM, SATURN V SOUND SUPPRESSOR

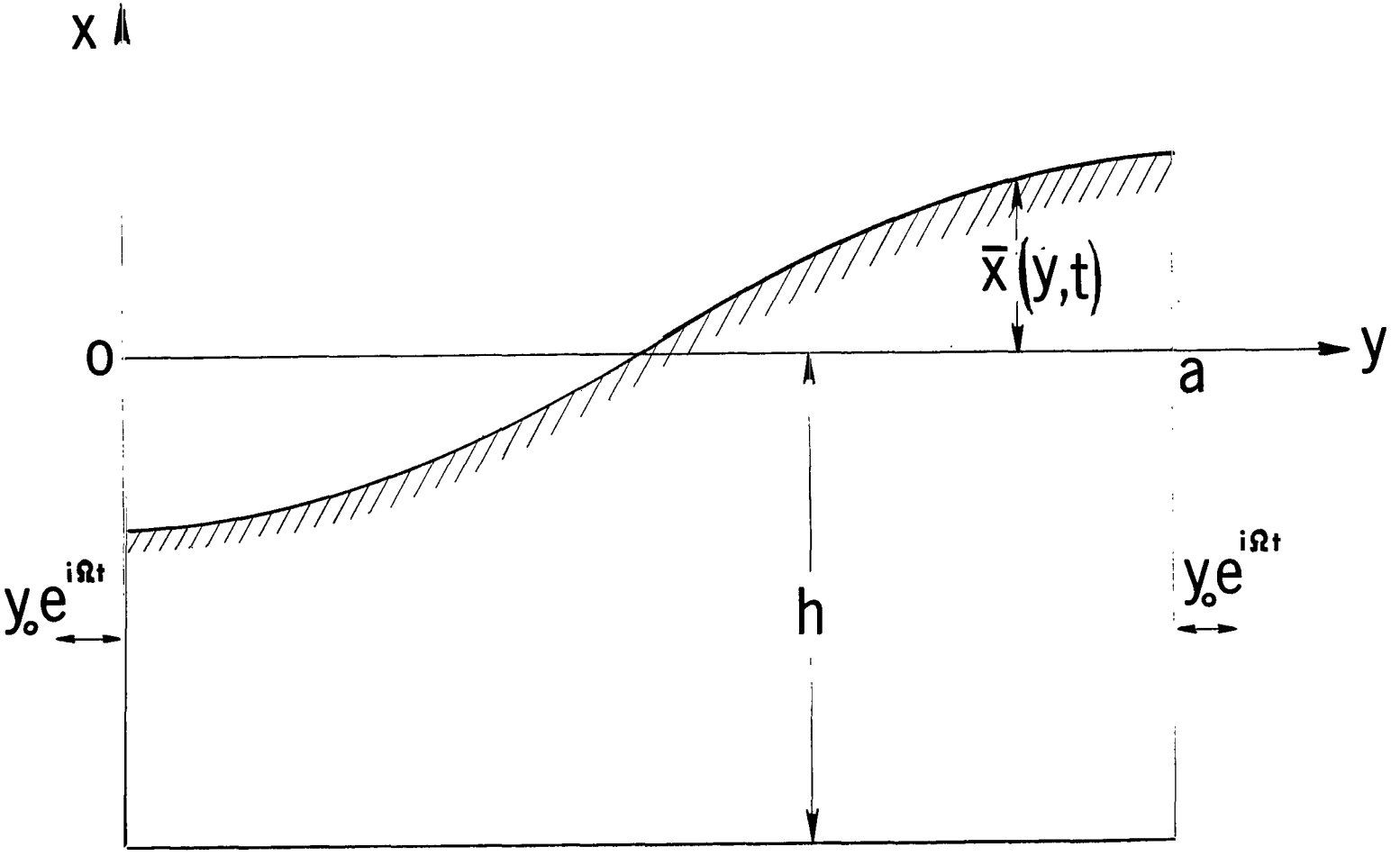

FIGURE 2. TANK GEOMETRY AND COORDINATE SYSTEM

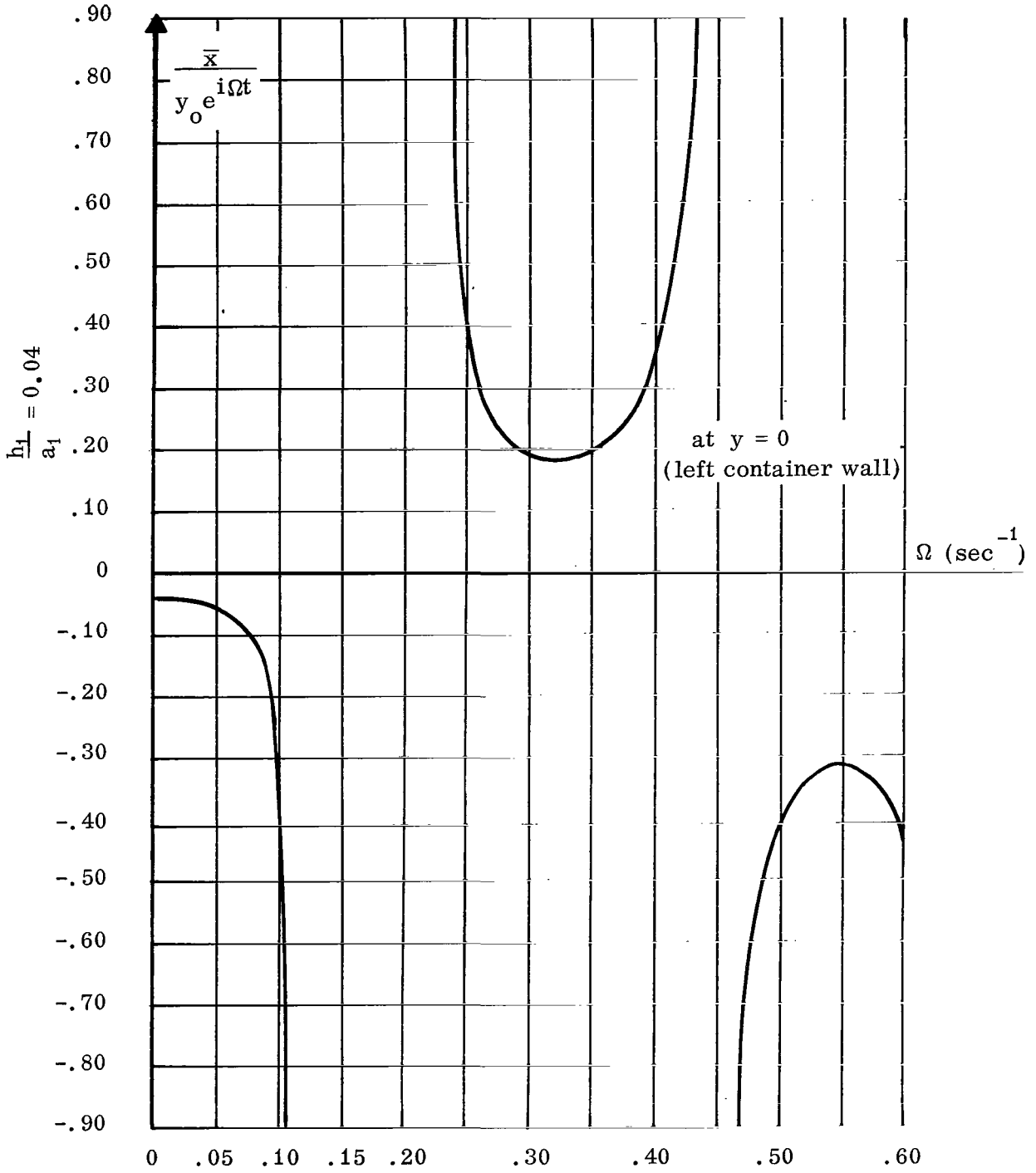

FIGURE 3. FREE FLUID SURFACE RESPONSE AT LEFT WALL

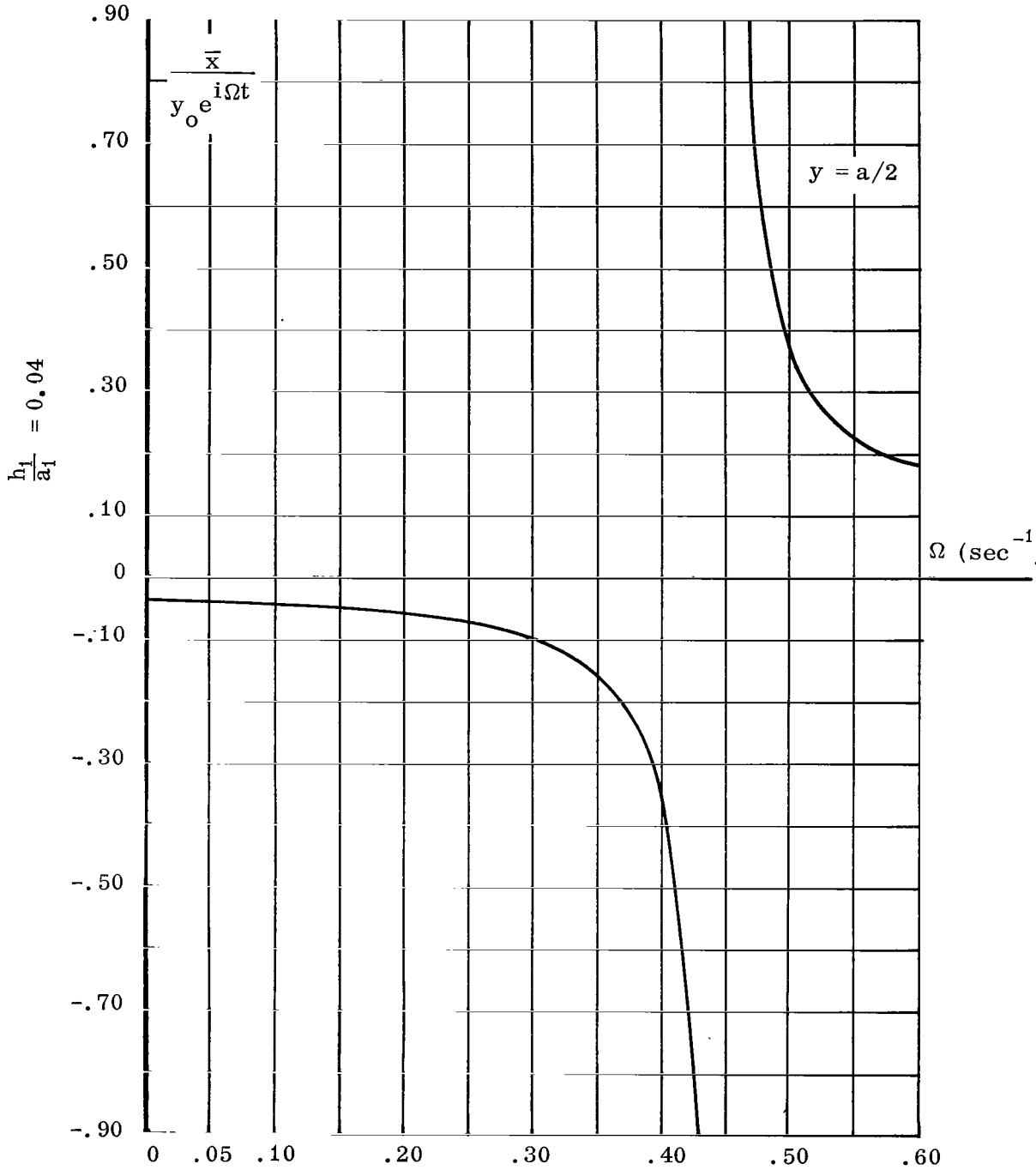

FIGURE 4. FREE FLUID SURFACE RESPONSE AT CENTER OF CONTAINER

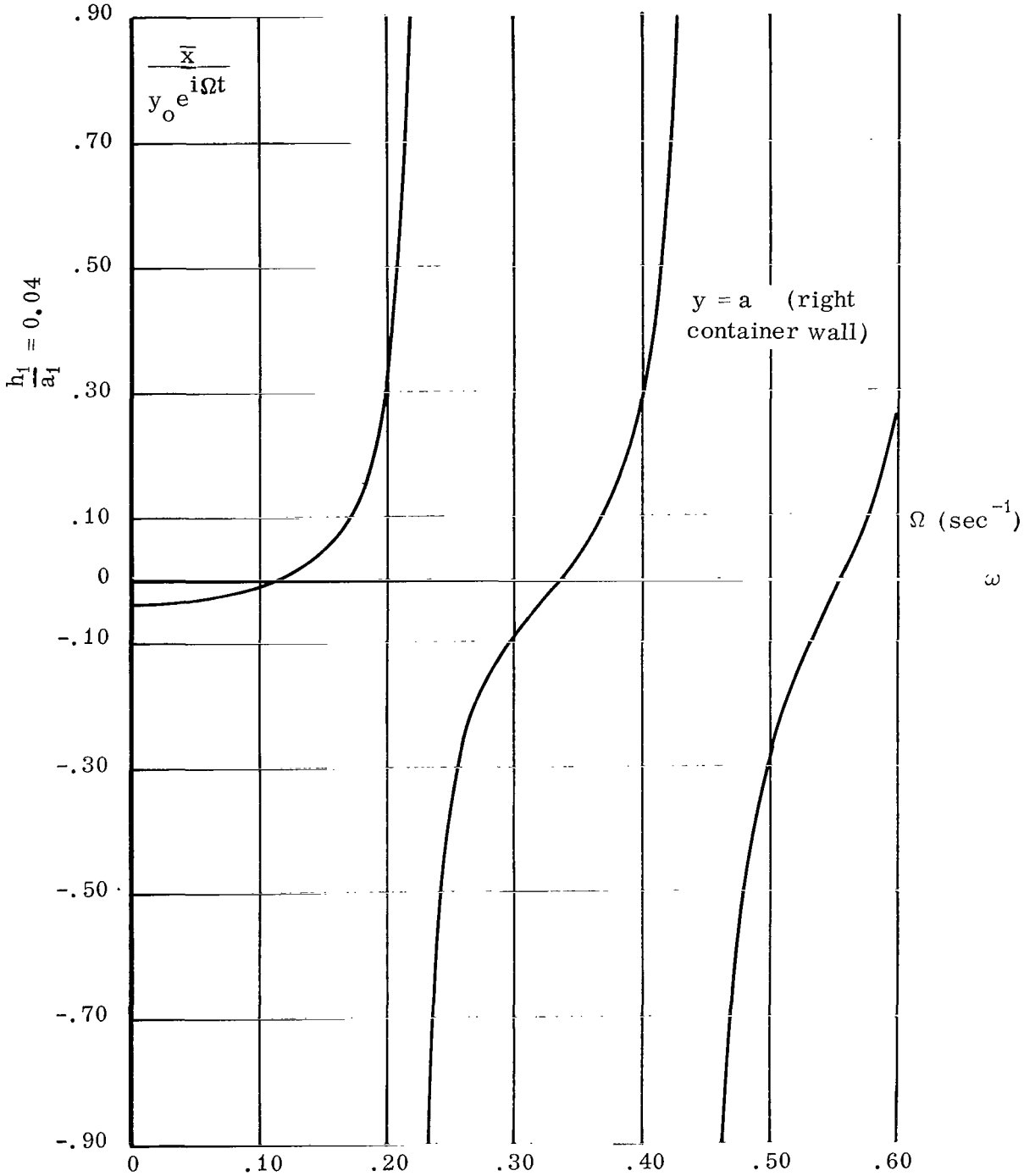

FIGURE 5. FREE FLUID SURFACE RESPONSE AT RIGHT WALL

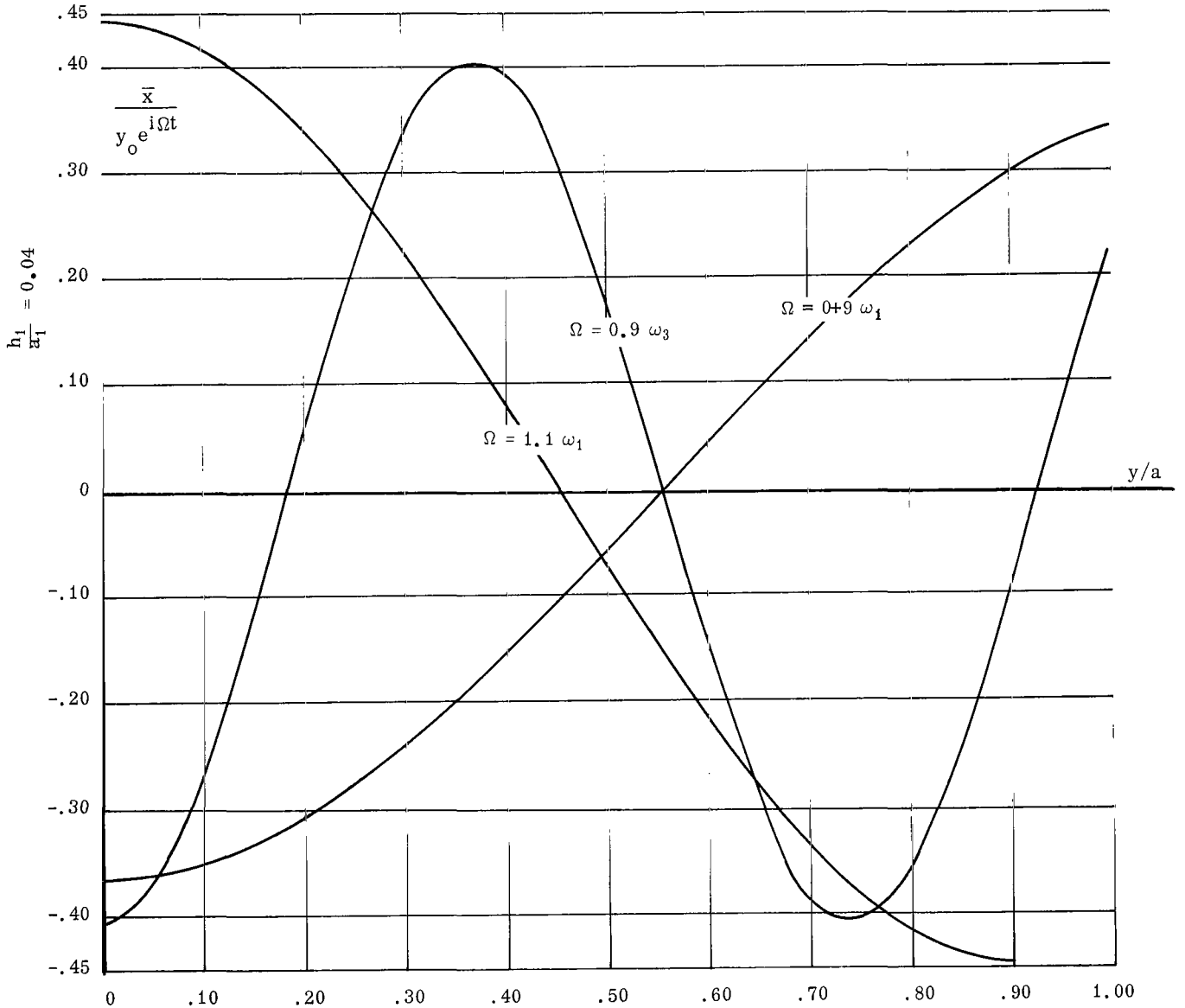

FIGURE 6. FREE FLUID SURFACE SHAPE FOR VARIOUS FORCING FREQUENCIES

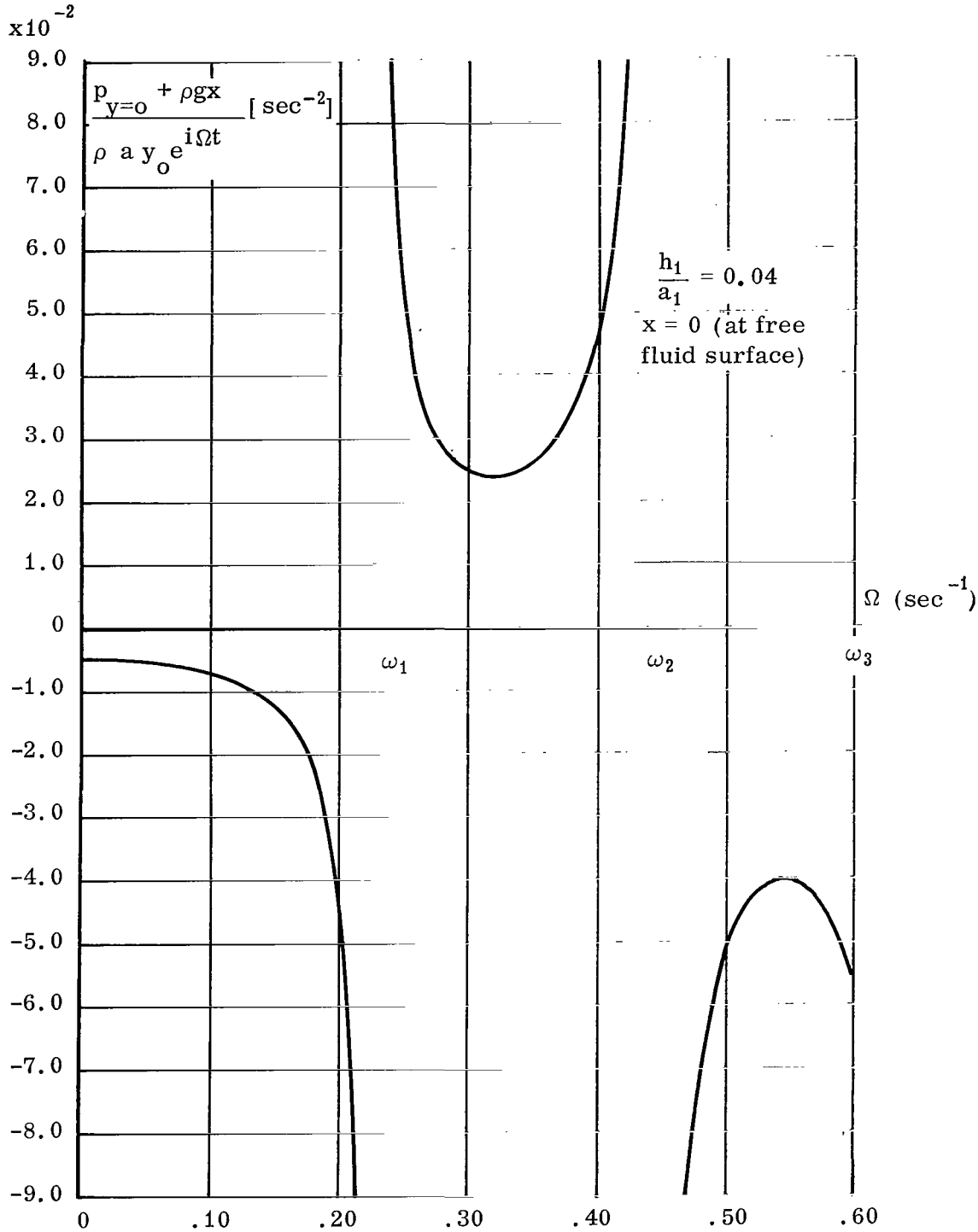

FIGURE 7. PRESSURE RESPONSE AT FREE FLUID SURFACE

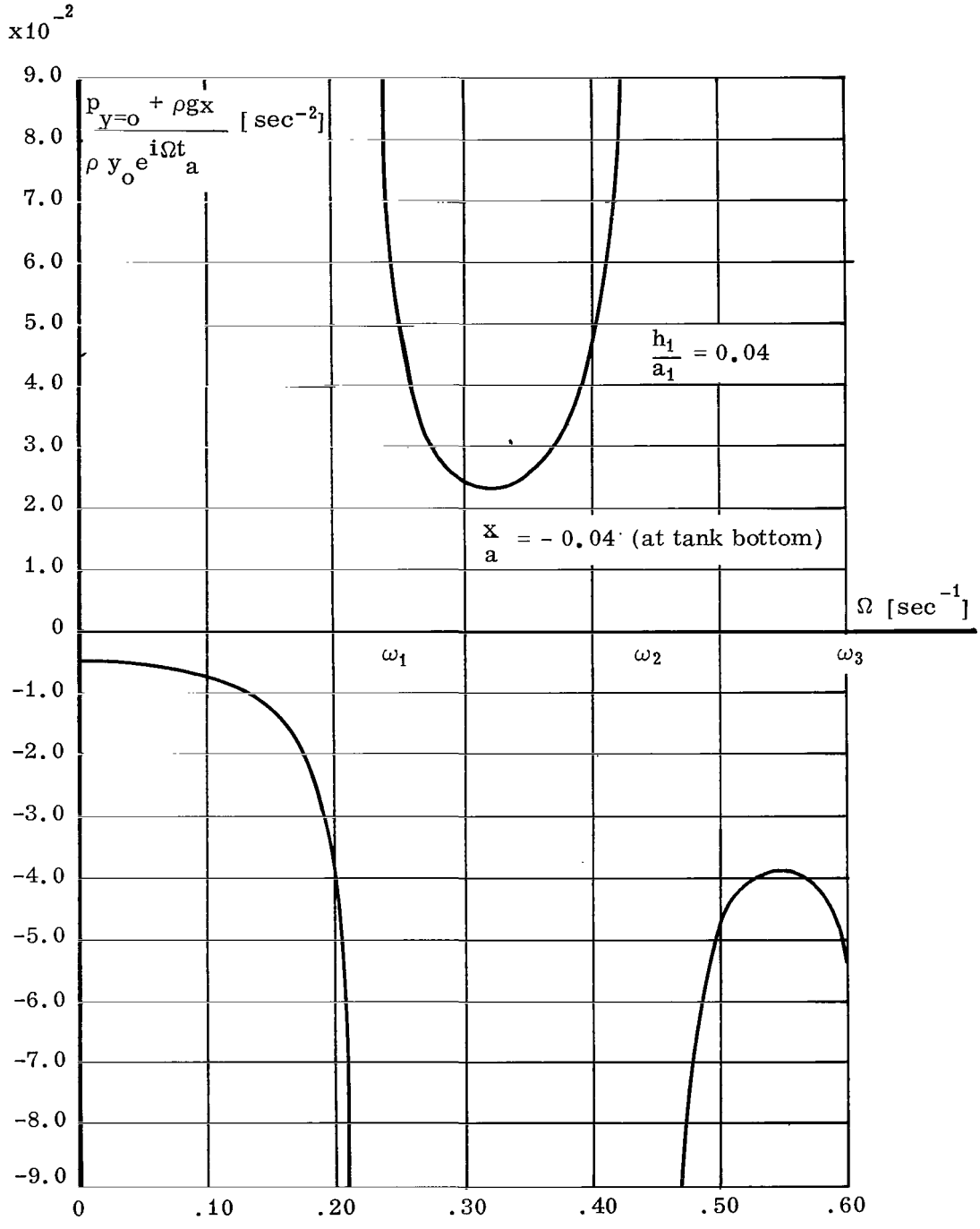

FIGURE 8. PRESSURE RESPONSE AT THE BOTTOM OF CONTAINER

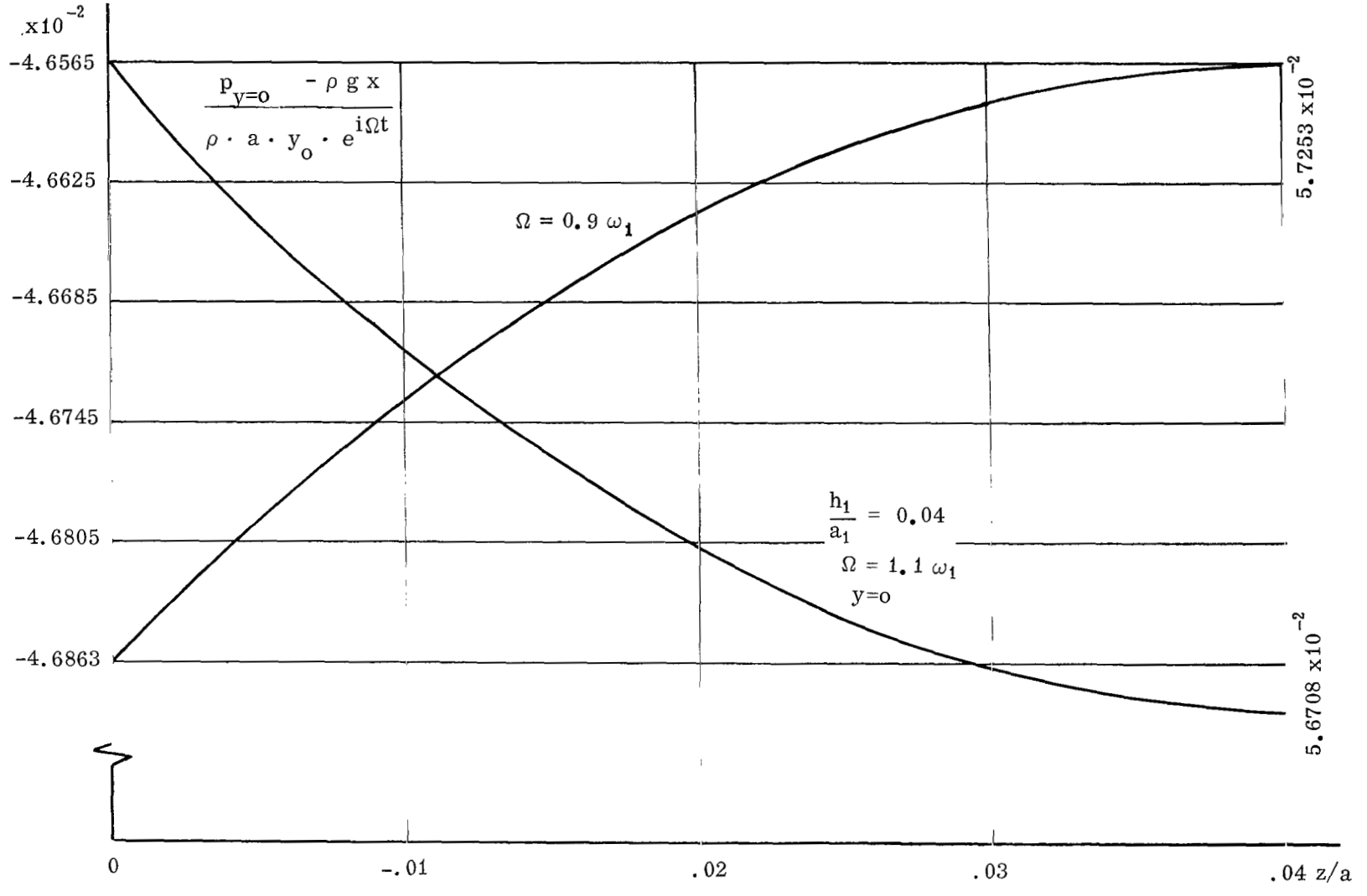

FIGURE 9. PRESSURE DISTRIBUTION FOR VARIOUS FORCING FREQUENCIES

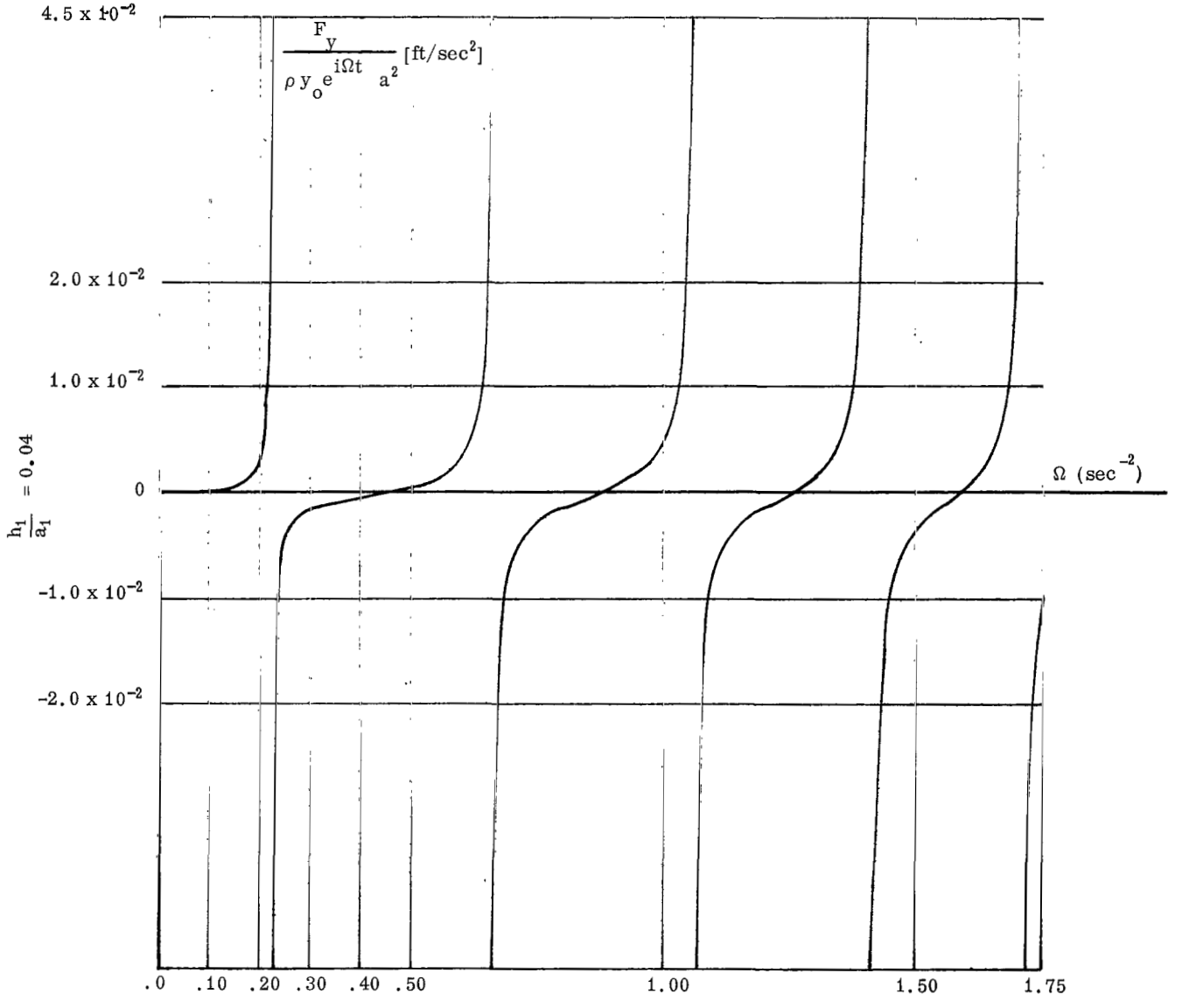

FIGURE 10. LIQUID FORCE RESPONSE

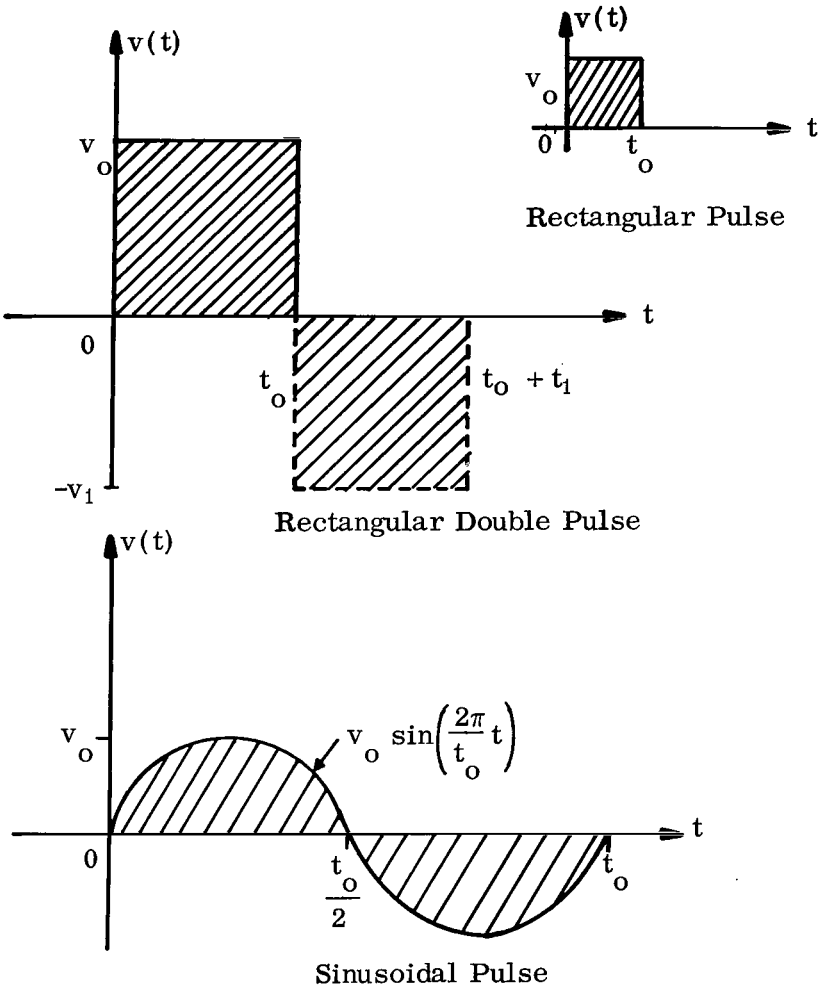

FIGURE 11. PULSE EXCITATIONS

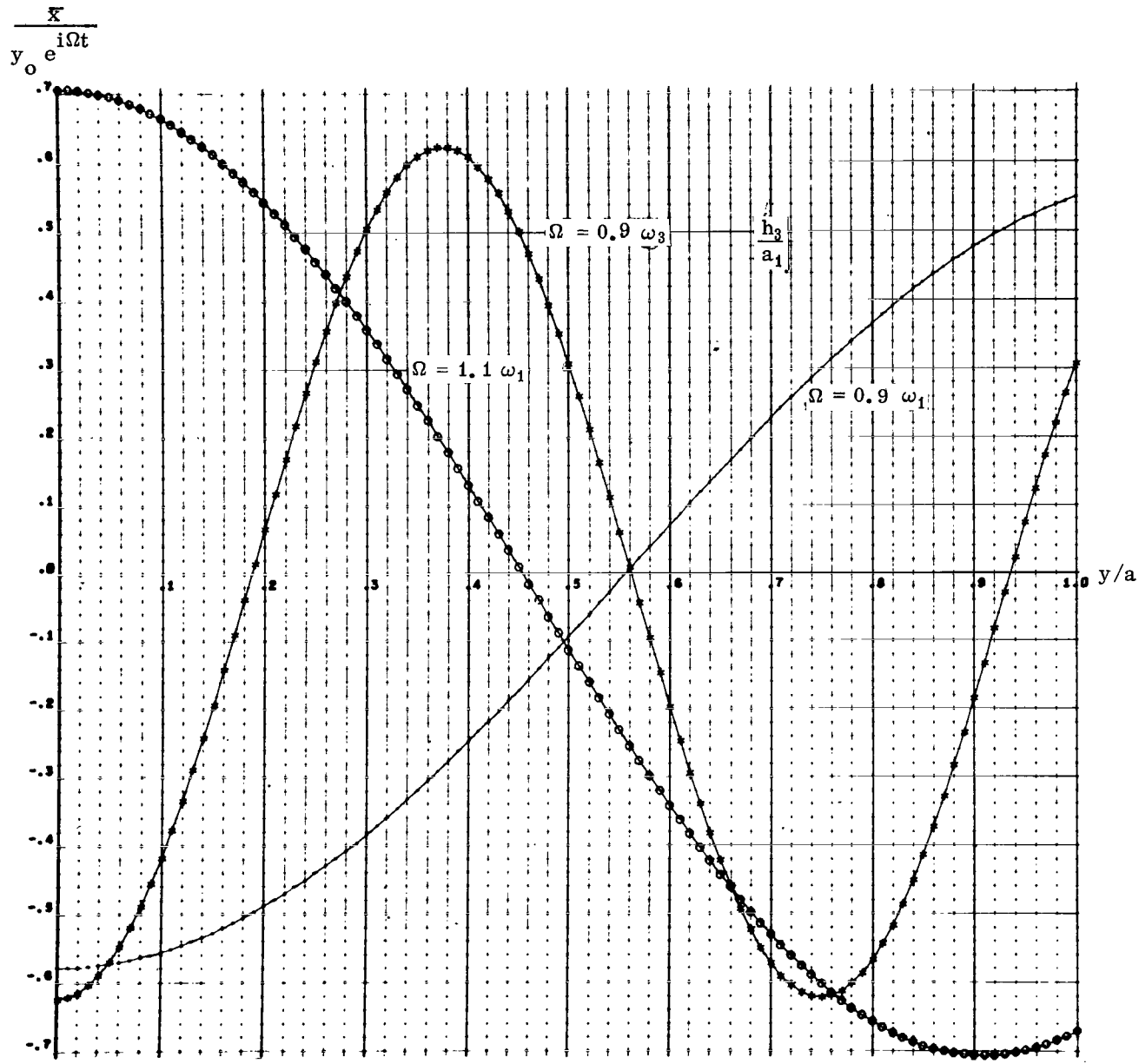

FIGURE 12. SHAPE OF FREE FLUID SURFACE FOR HARMONIC EXCITATION OF RIGHT SIDE WALL

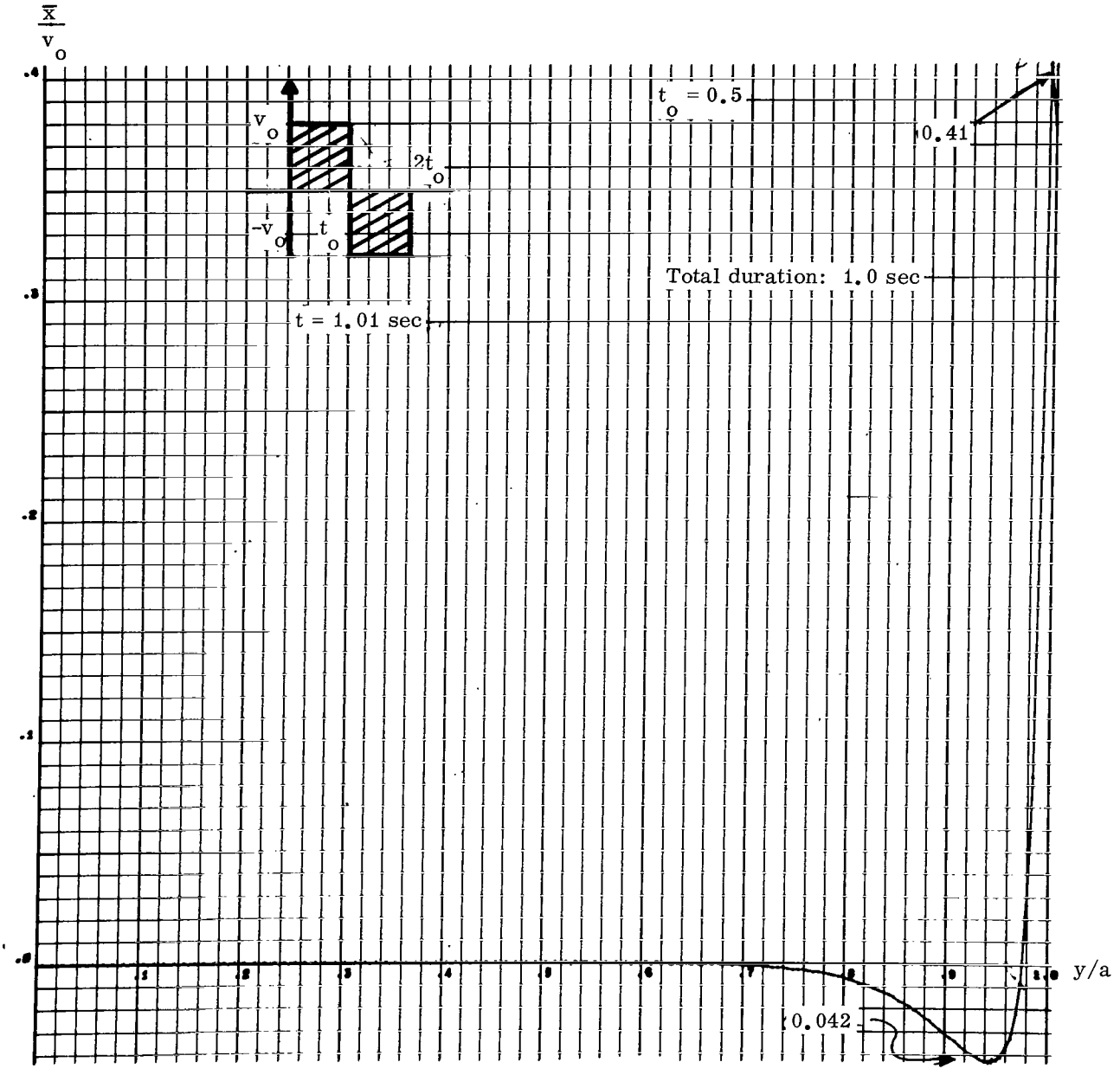

FIGURE 13. LIQUID SURFACE ELEVATION FOR RECTANGULAR DOUBLE PULSE OF ONE SECOND DURATION FOR VARIOUS TIMES

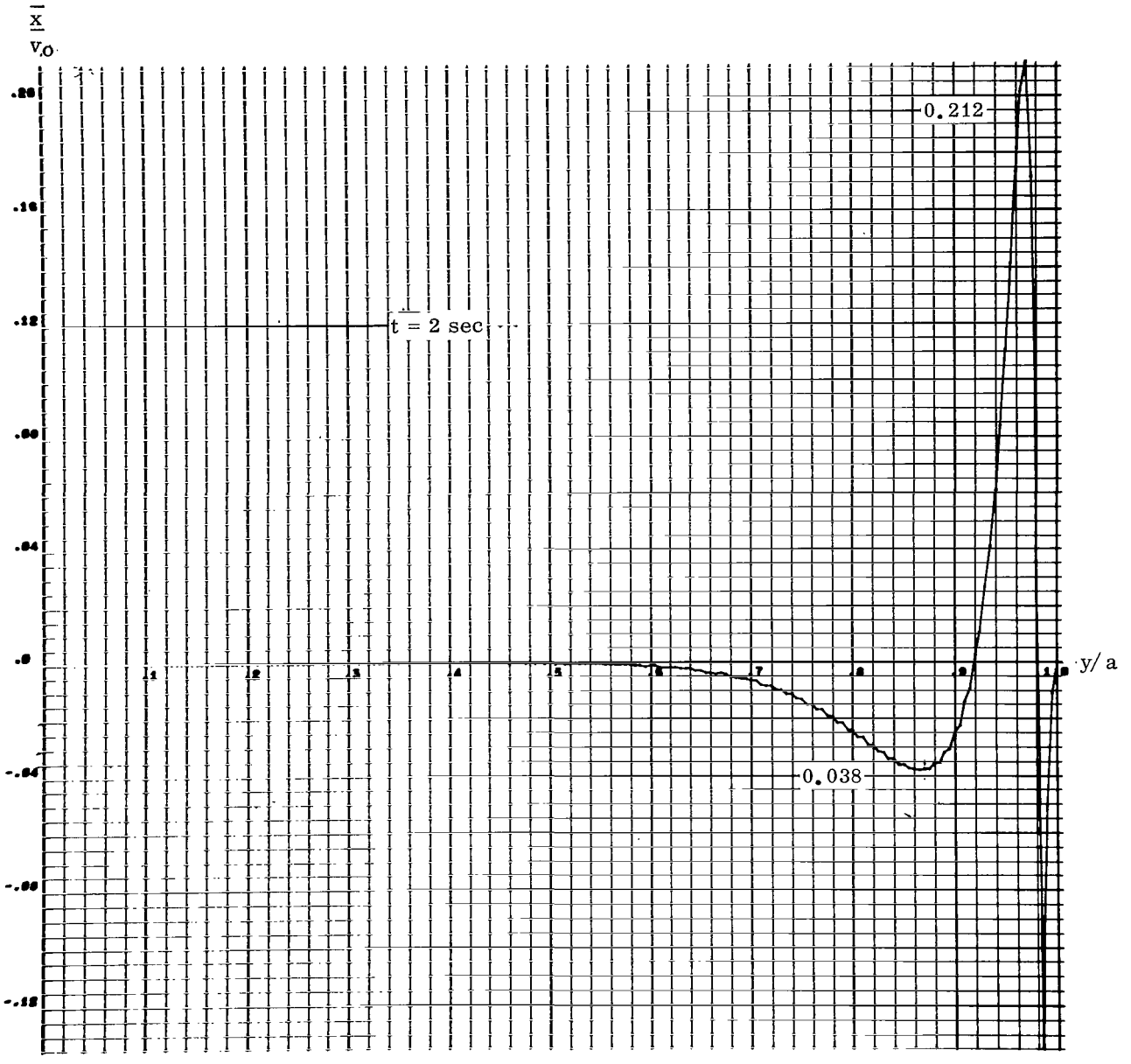

FIGURE 14. LIQUID SURFACE ELEVATION FOR RECTANGULAR DOUBLE PULSE OF ONE SECOND DURATION FOR VARIOUS TIMES

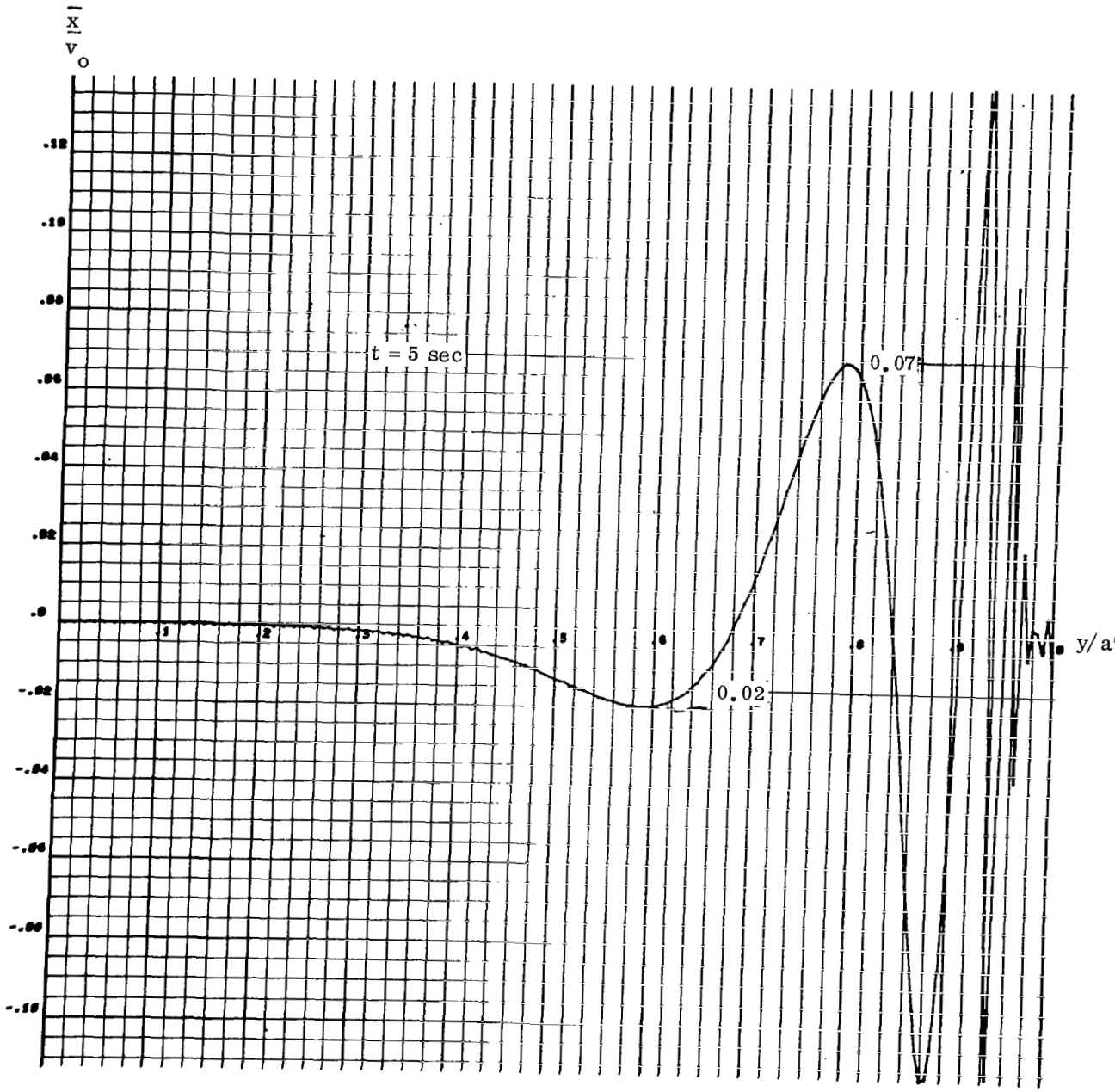

FIGURE 15. LIQUID SURFACE ELEVATION FOR RECTANGULAR DOUBLE PULSE OF ONE SECOND DURATION FOR VARIOUS TIMES

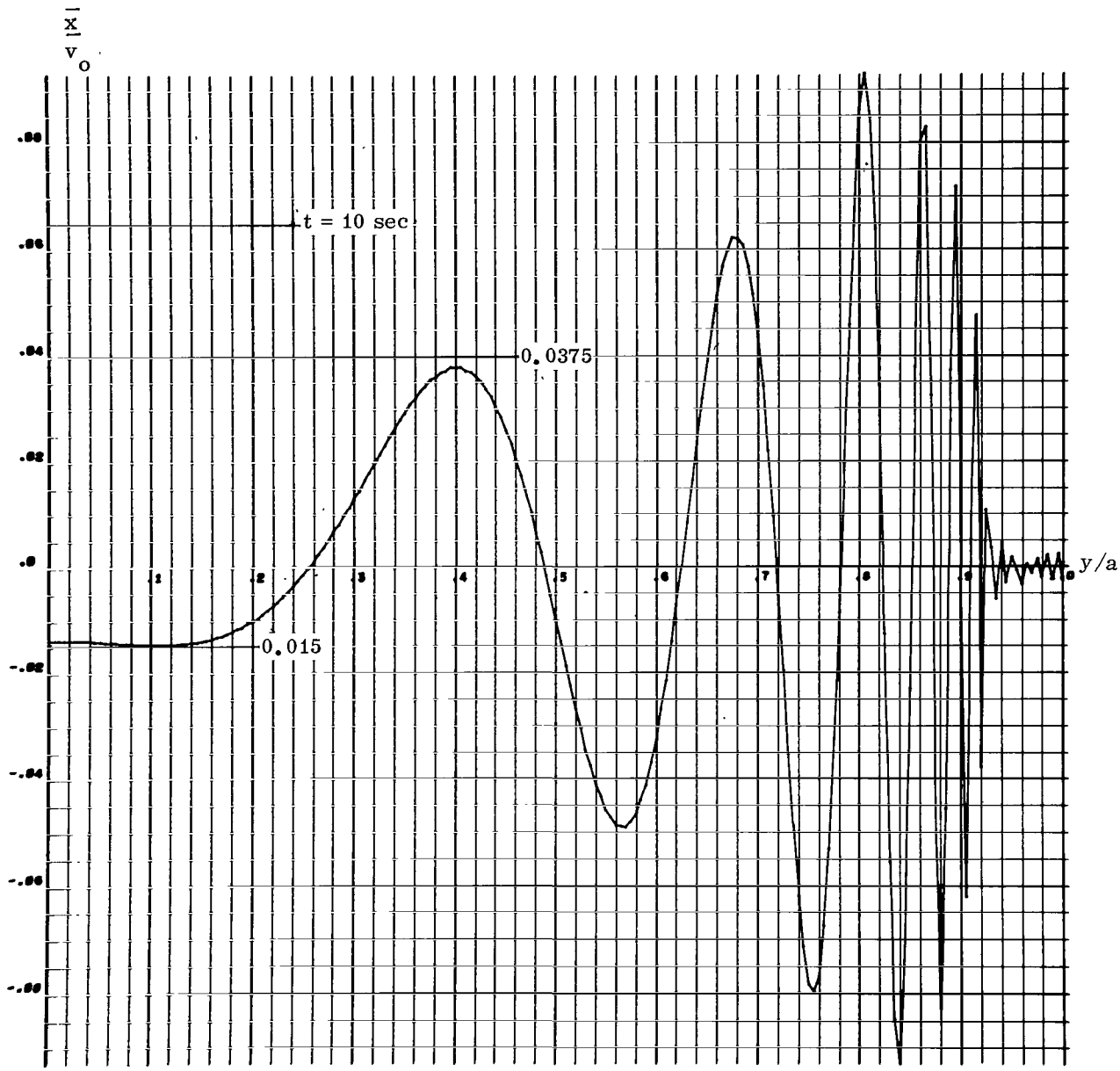

FIGURE 16. LIQUID SURFACE ELEVATION FOR RECTANGULAR DOUBLE PULSE OF ONE SECOND DURATION FOR VARIOUS TIMES

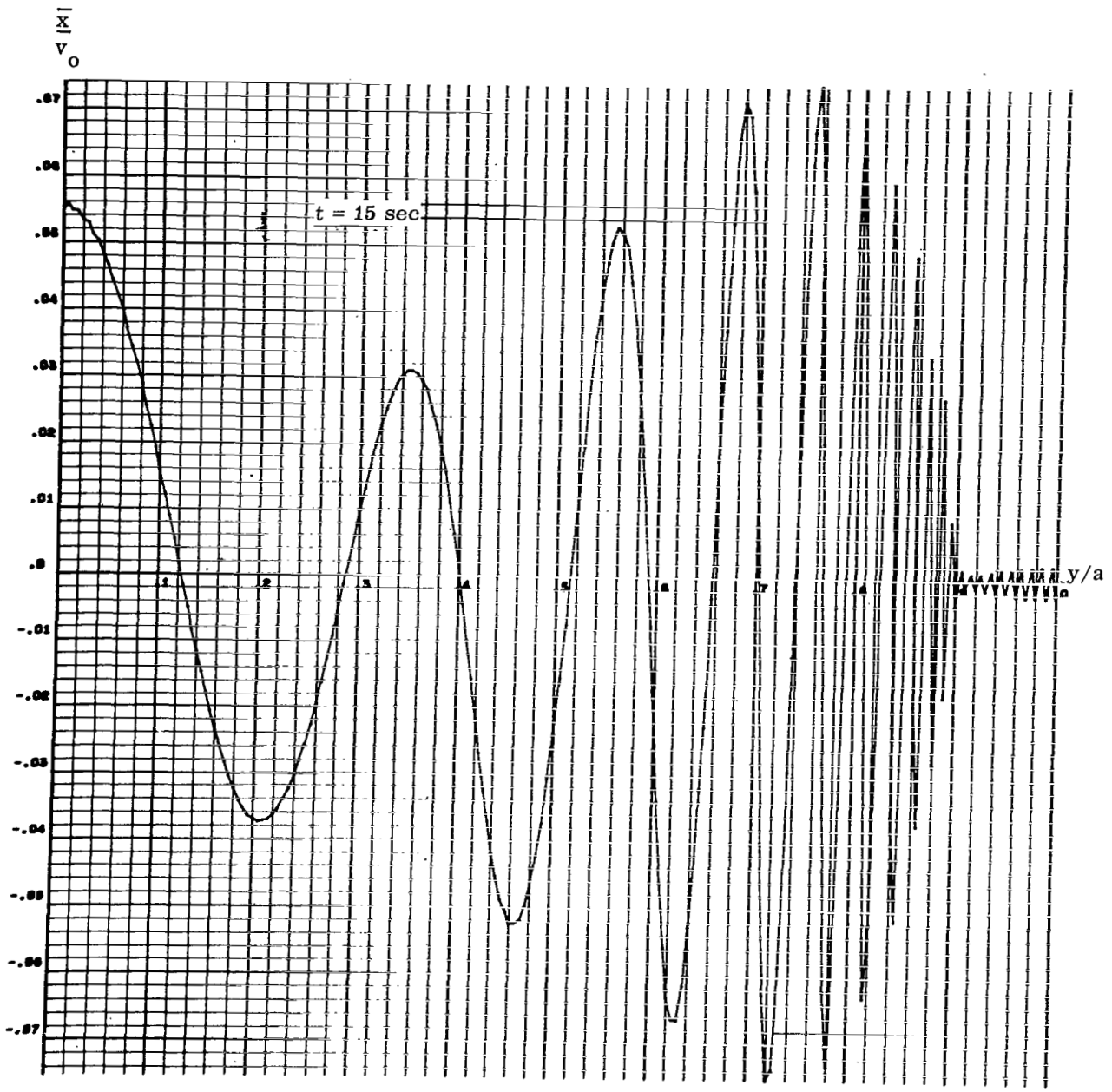

FIGURE 17. LIQUID SURFACE ELEVATION FOR RECTANGULAR DOUBLE PULSE OF ONE SECOND DURATION FOR VARIOUS TIMES

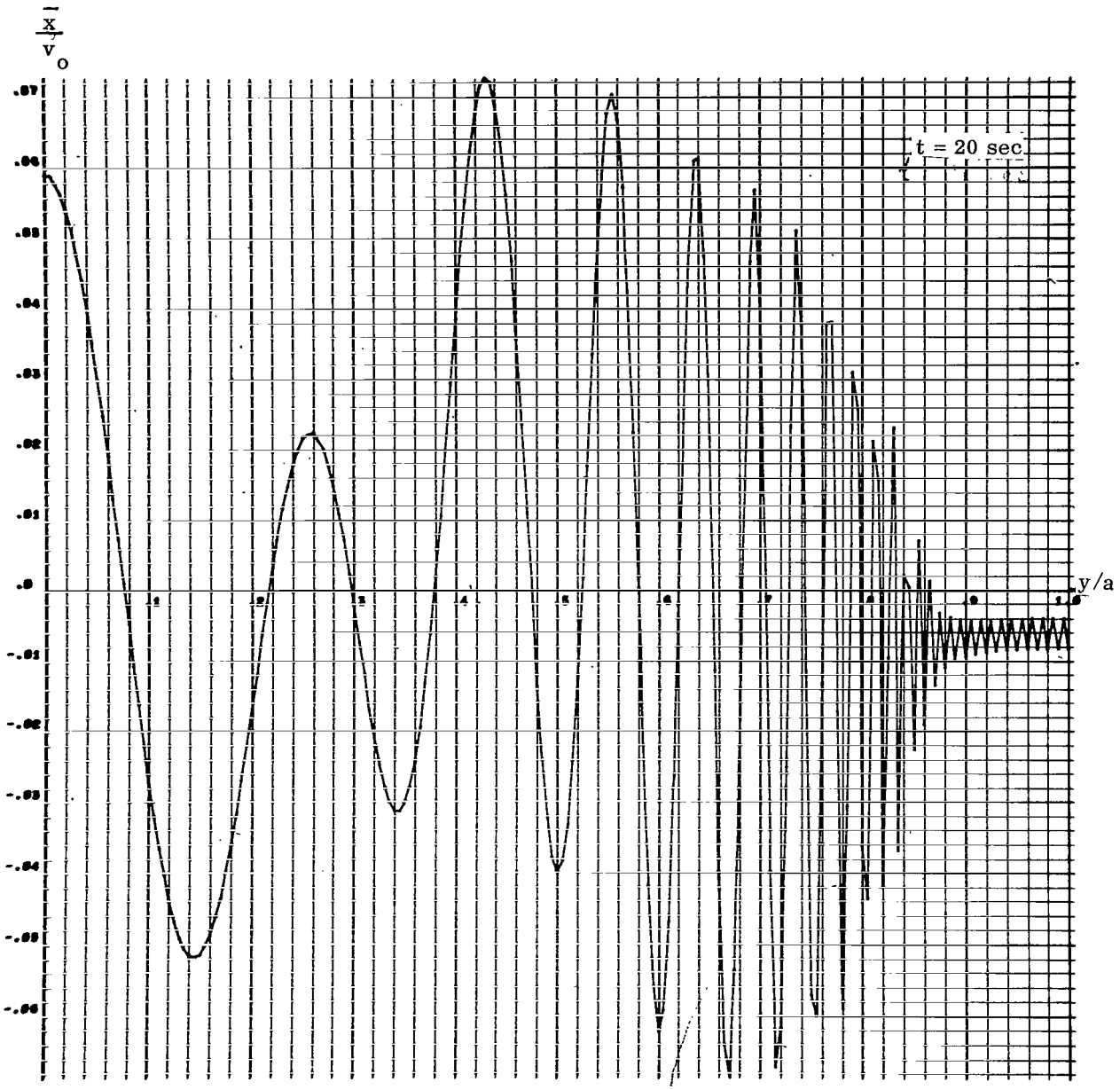

FIGURE 18. LIQUID SURFACE ELEVATION FOR RECTANGULAR DOUBLE PULSE OF ONE SECOND DURATION FOR VARIOUS TIMES

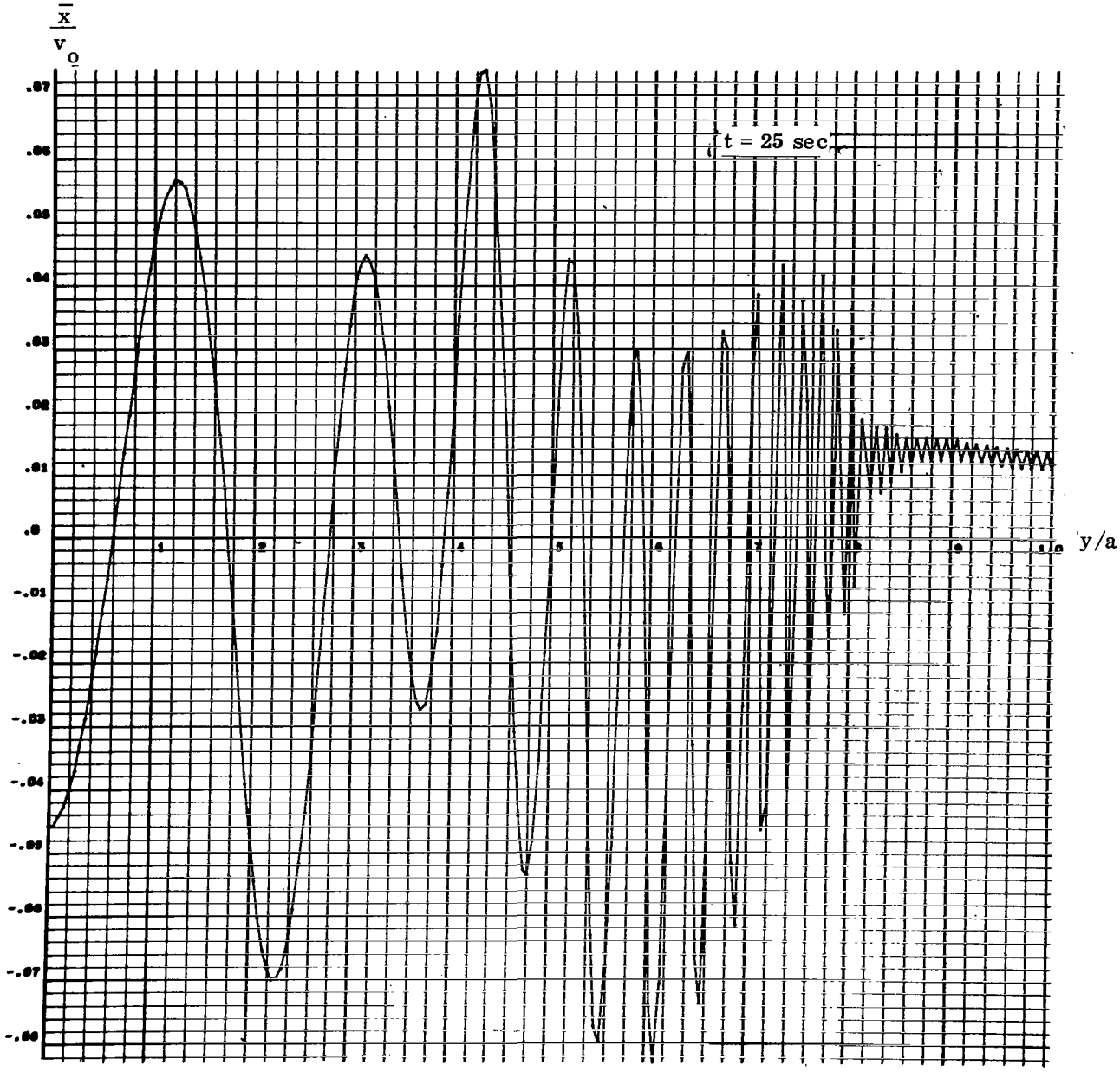

FIGURE 19. LIQUID SURFACE ELEVATION FOR RECTANGULAR DOUBLE PULSE OF ONE SECOND DURATION FOR VARIOUS TIMES

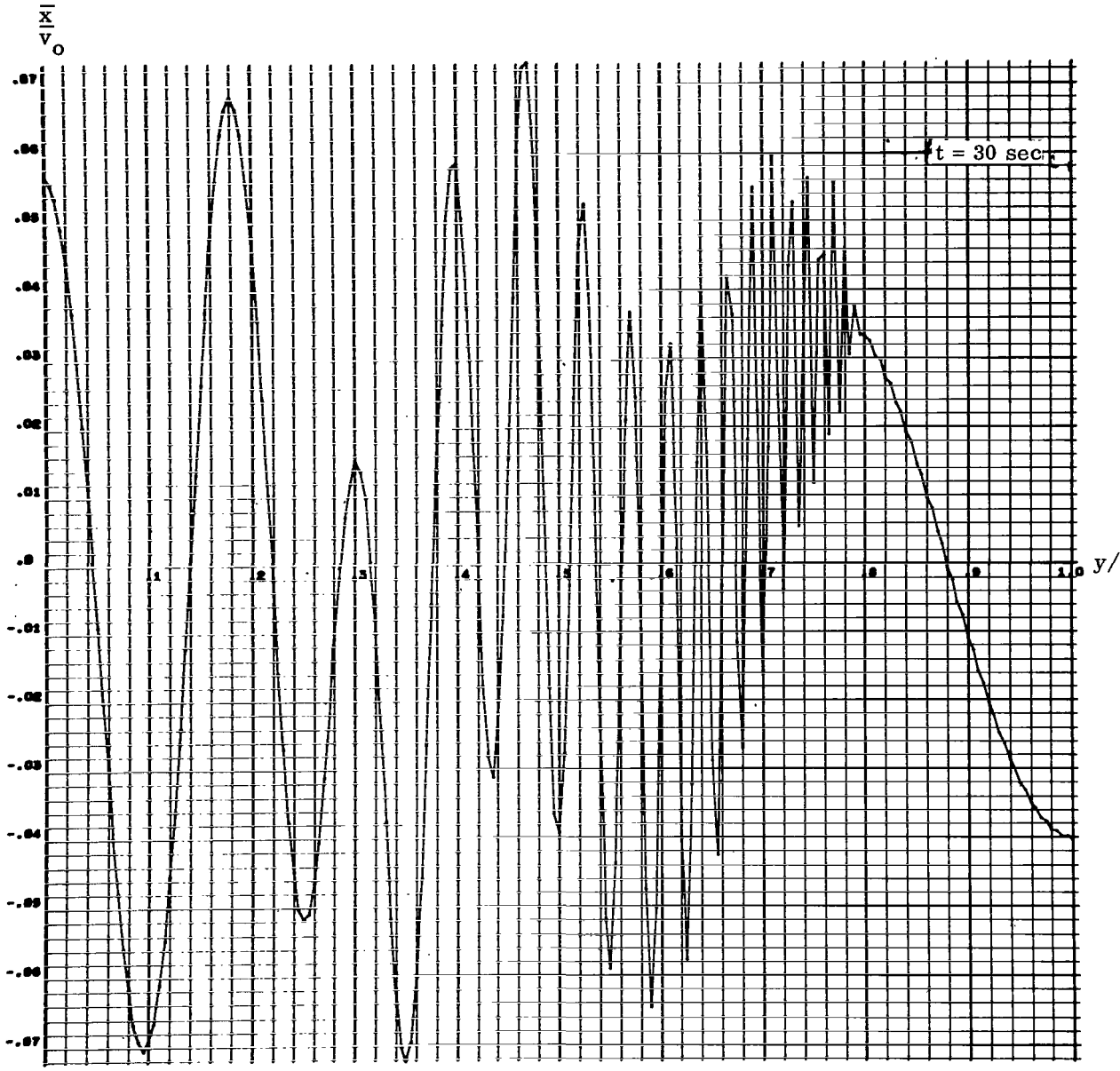

FIGURE 20. LIQUID SURFACE ELEVATION FOR RECTANGULAR DOUBLE PULSE OF ONE SECOND DURATION FOR VARIOUS TIMES

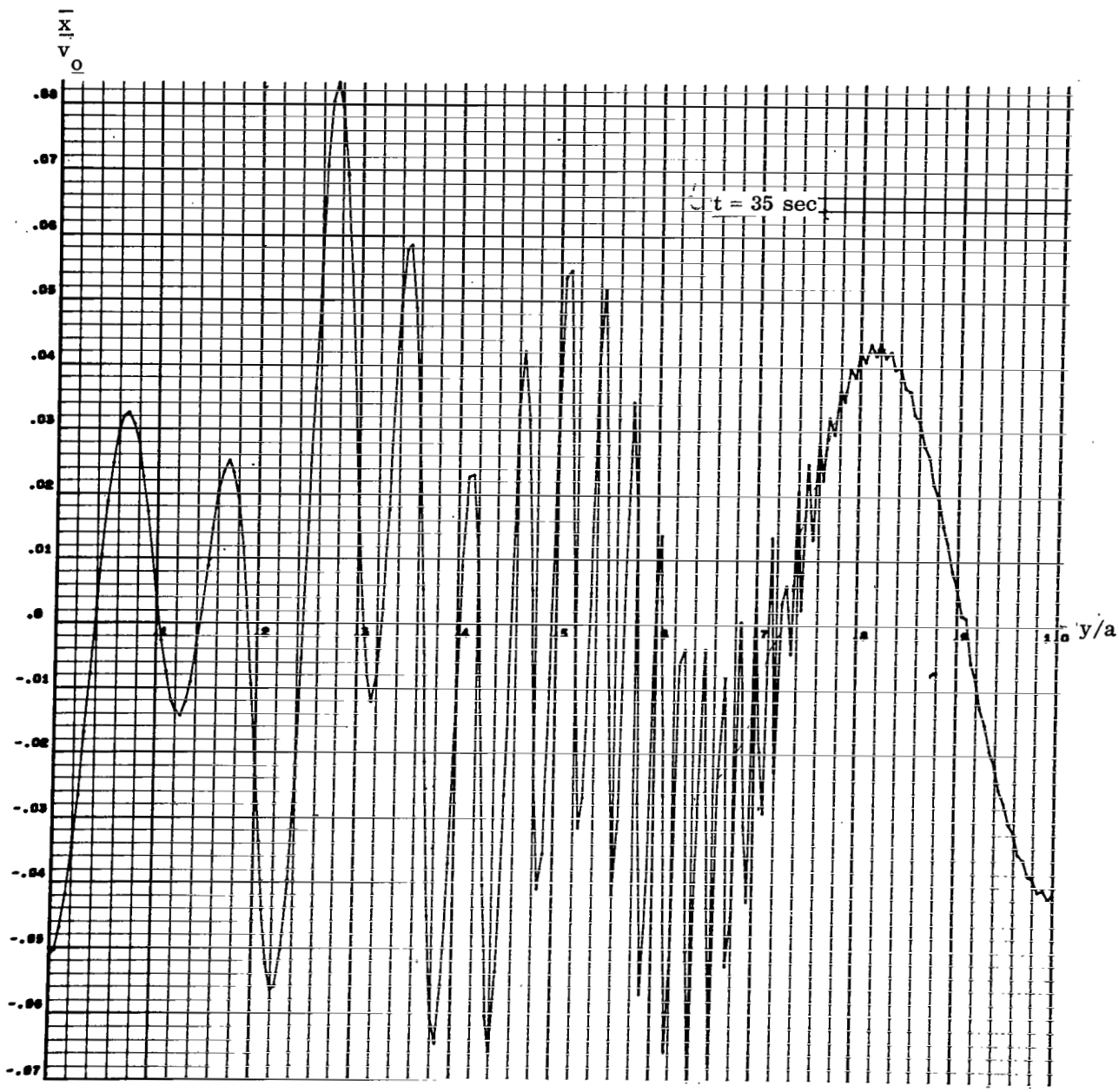

FIGURE 21. LIQUID SURFACE ELEVATION FOR RECTANGULAR DOUBLE PULSE OF ONE SECOND DURATION FOR VARIOUS TIMES

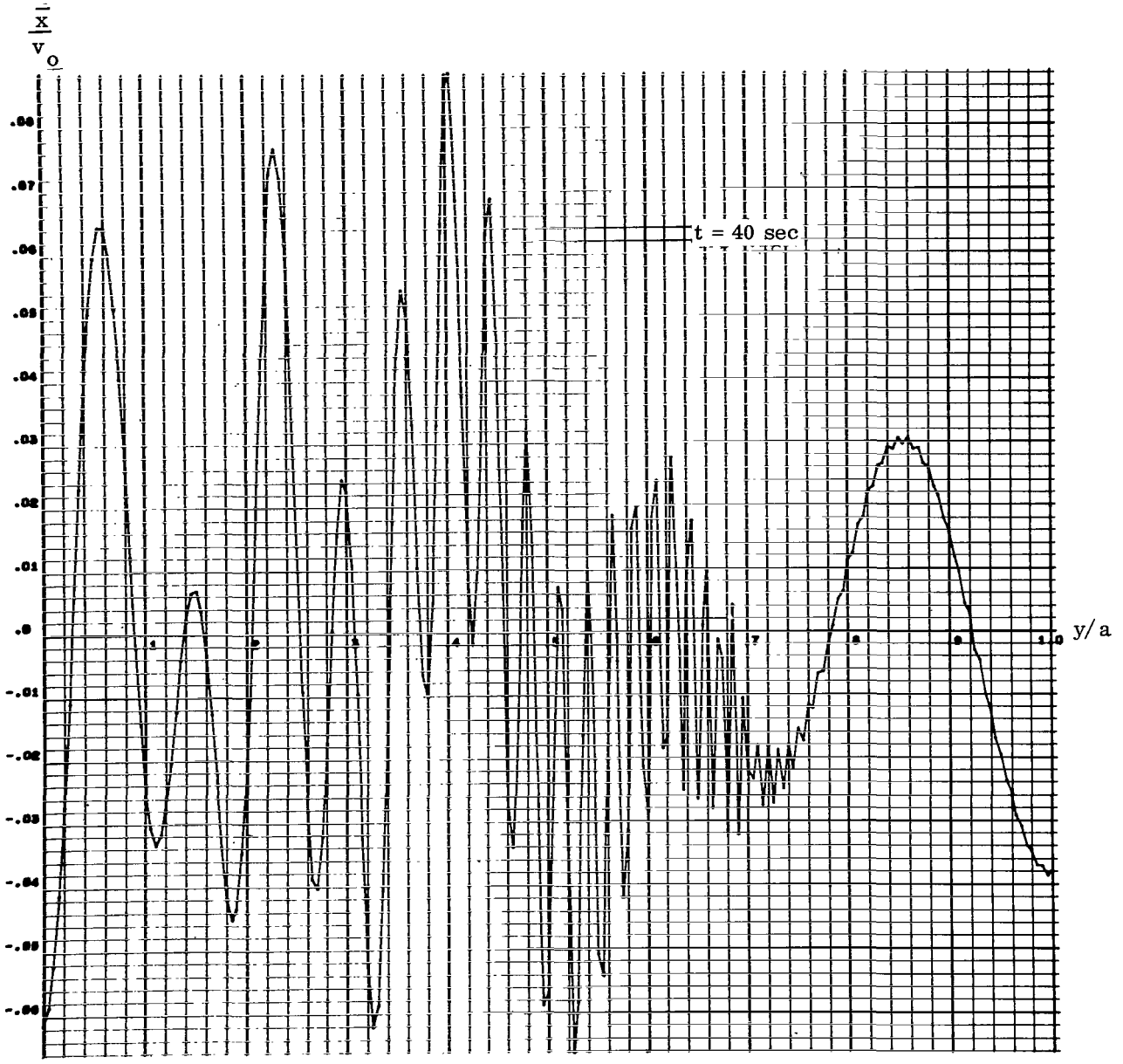

FIGURE 22. LIQUID SURFACE ELEVATION FOR RECTANGULAR DOUBLE PULSE OF ONE SECOND DURATION FOR VARIOUS TIMES

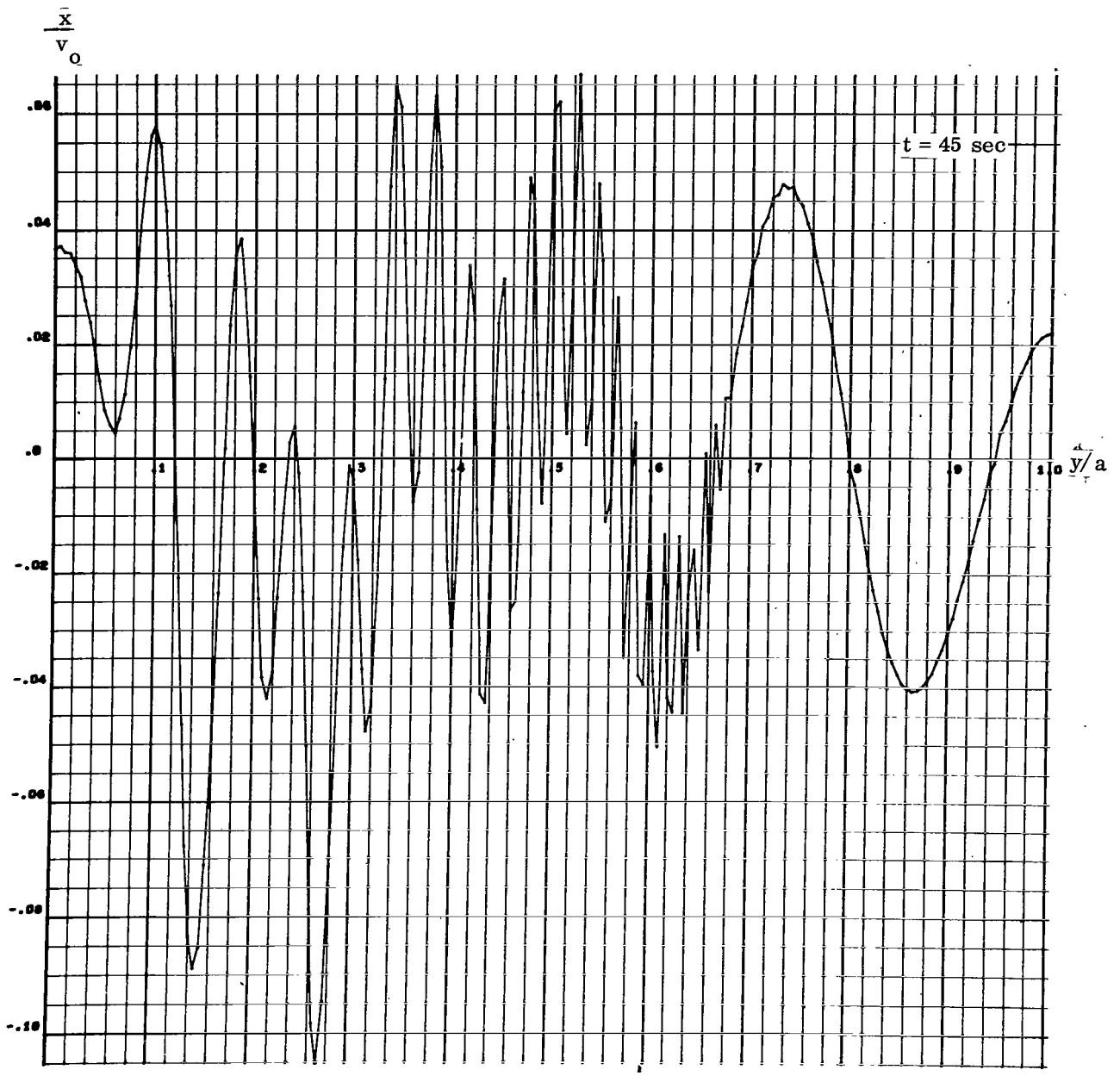

FIGURE 23. LIQUID SURFACE ELEVATION FOR RECTANGULAR DOUBLE PULSE OF ONE SECOND DURATION FOR VARIOUS TIMES

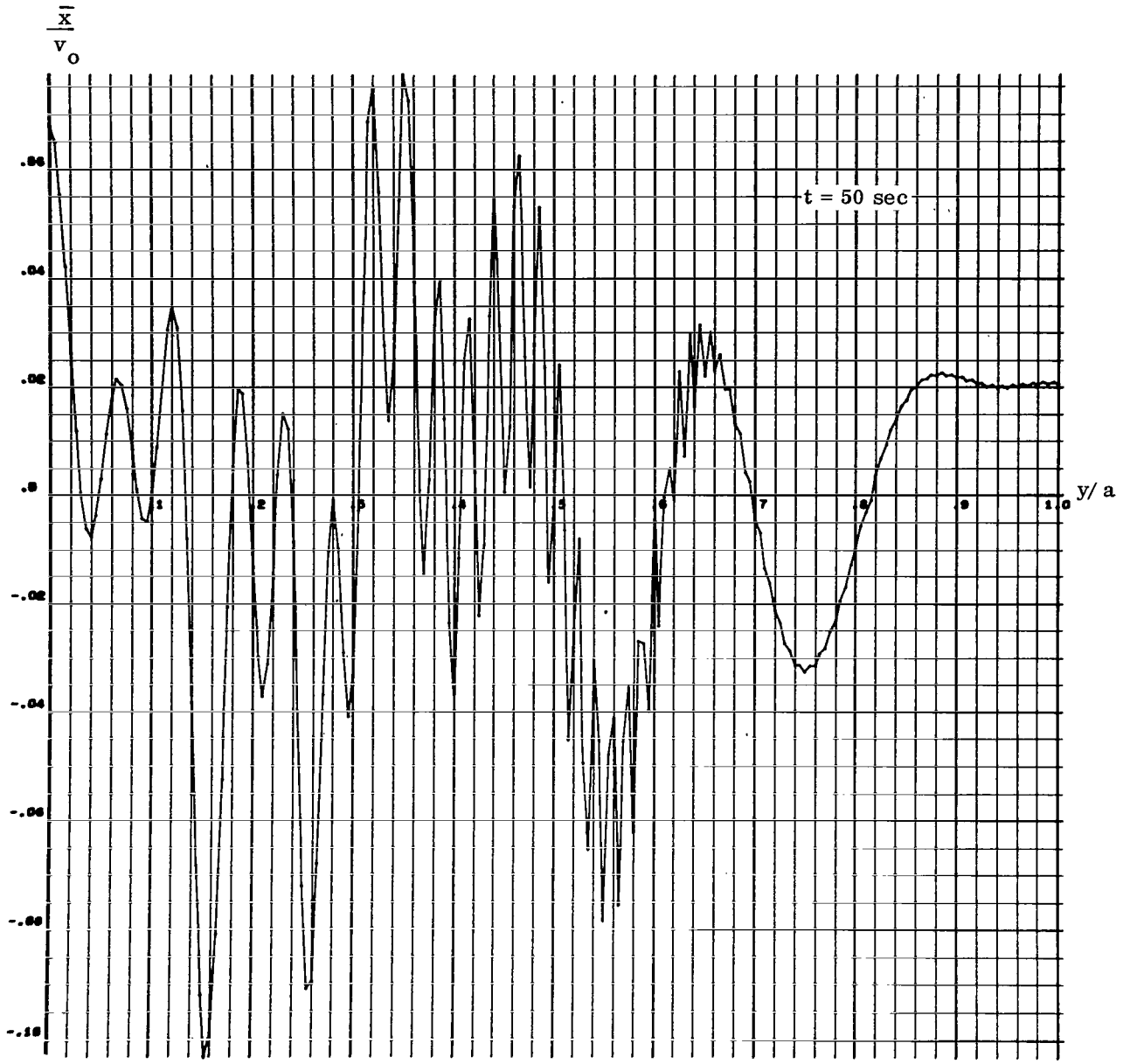

FIGURE 24. LIQUID SURFACE ELEVATION FOR RECTANGULAR DOUBLE PULSE OF ONE SECOND DURATION FOR VARIOUS TIMES

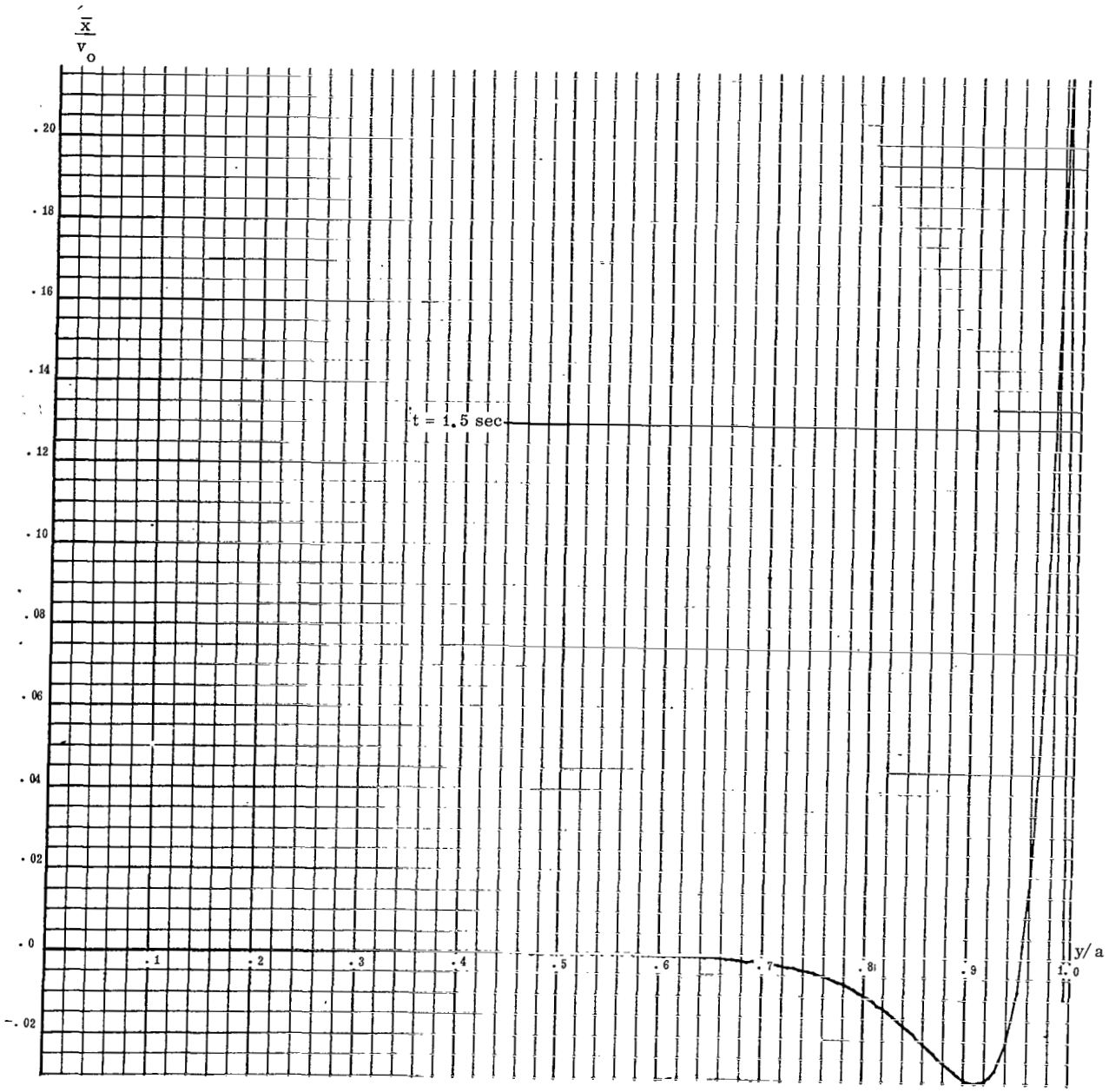

FIGURE 25. LIQUID SURFACE ELEVATION FOR SINUSOIDAL PULSE OF ONE SECOND DURATION FOR VARIOUS TIMES

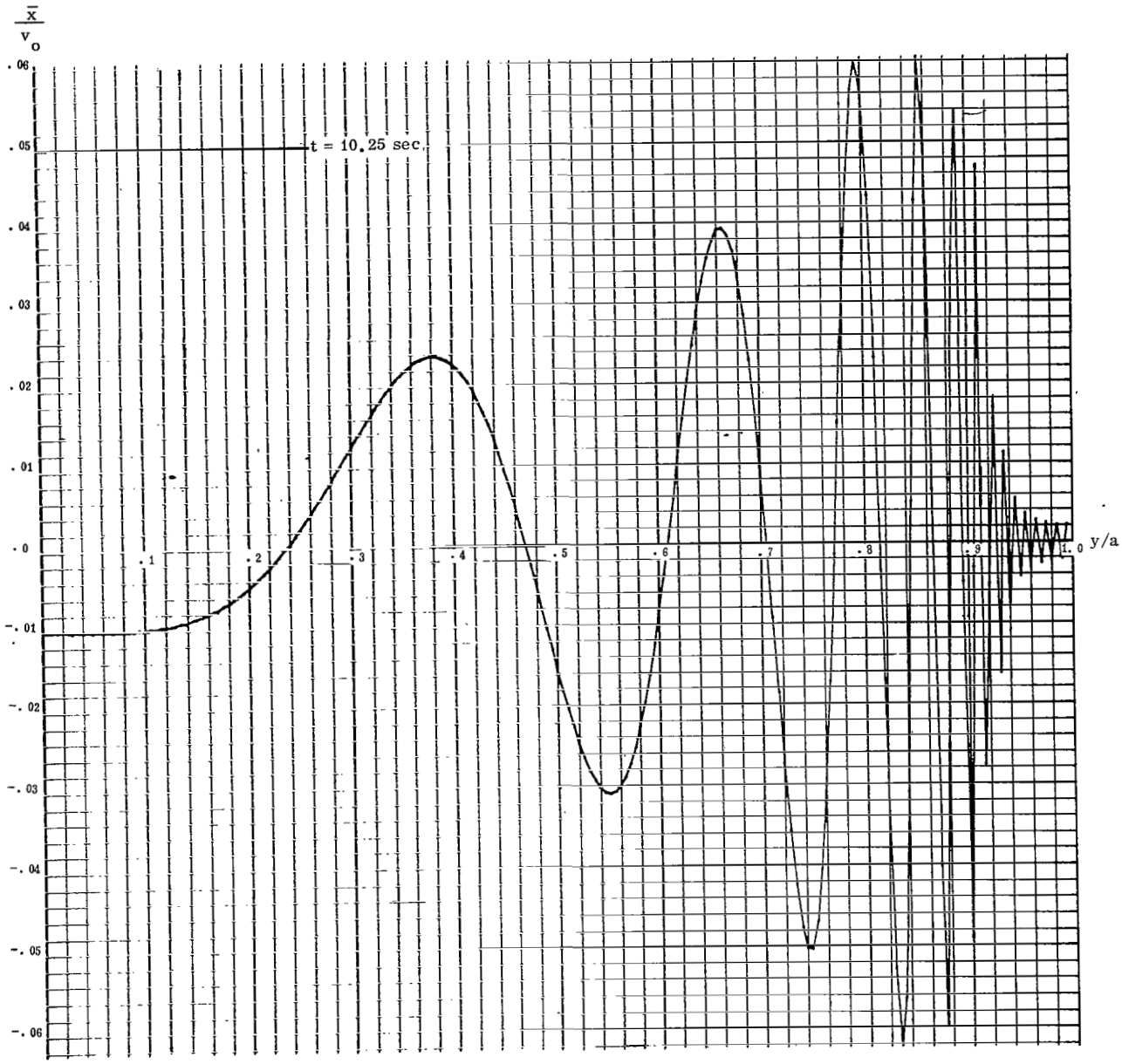

FIGURE 26. LIQUID SURFACE ELEVATION FOR SINUSOIDAL PULSE OF ONE SECOND DURATION FOR VARIOUS TIMES

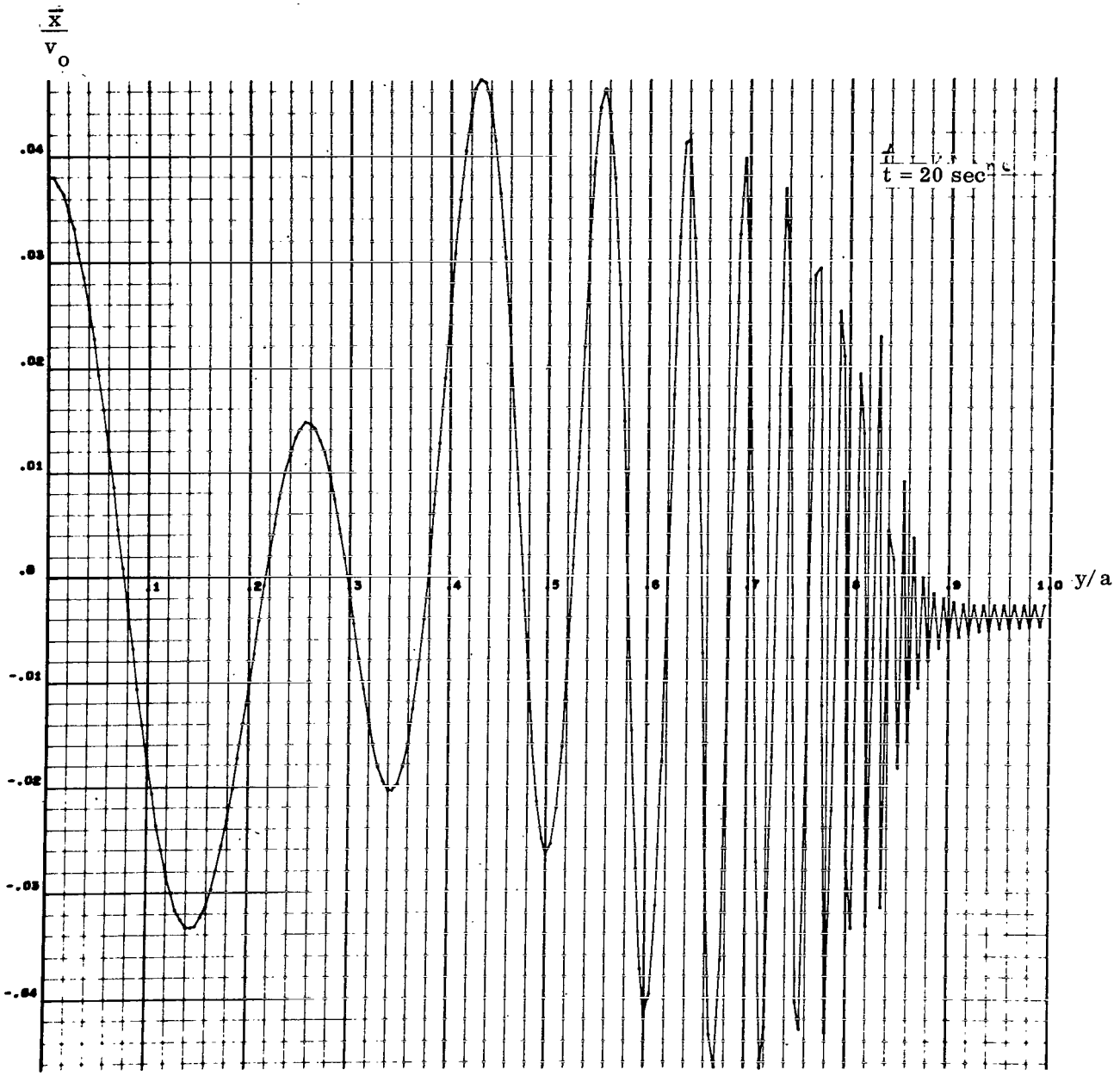

FIGURE 27. LIQUID SURFACE ELEVATION FOR SINUSOIDAL PULSE OF ONE SECOND DURATION FOR VARIOUS TIMES

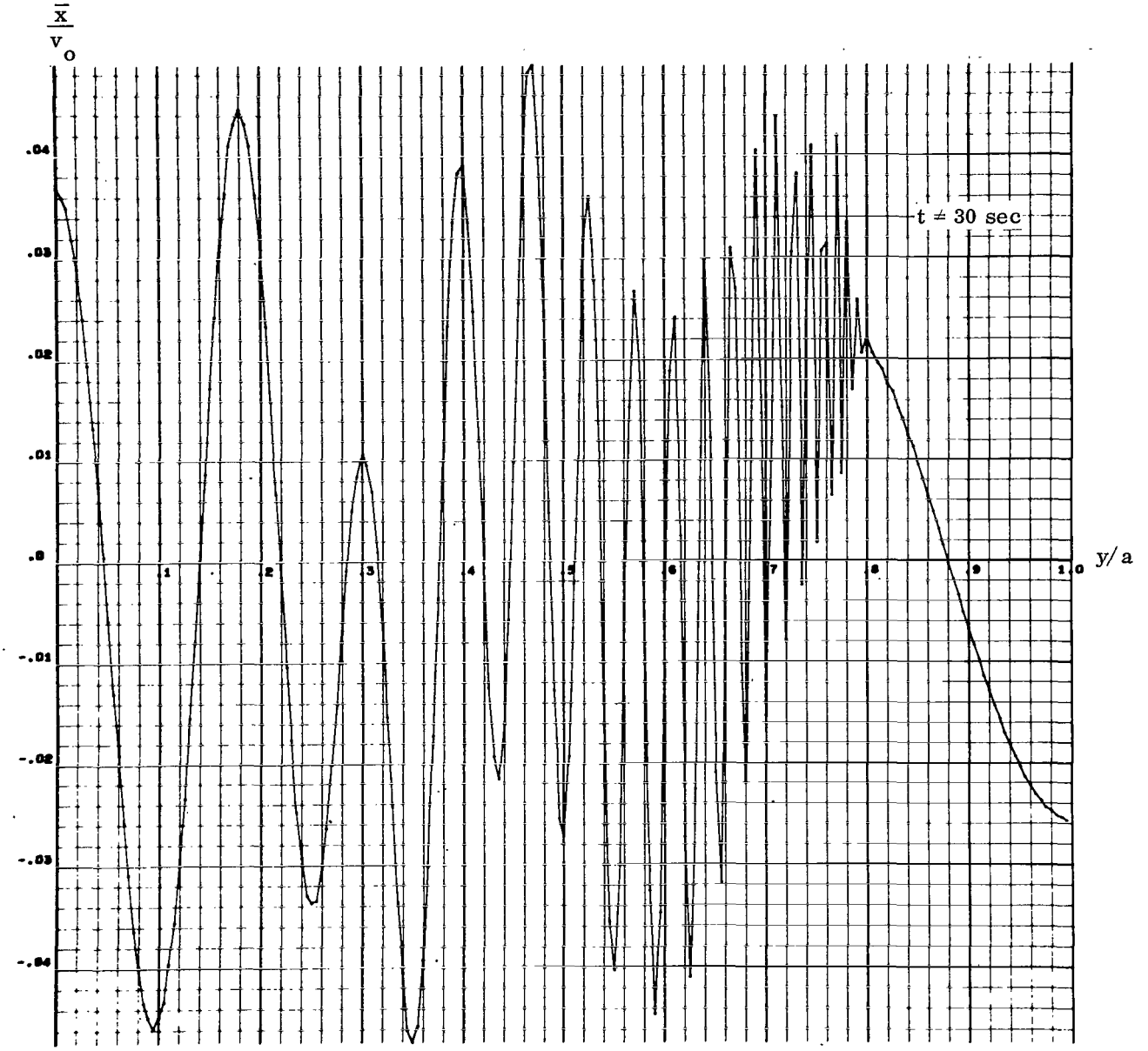

FIGURE 28. LIQUID SURFACE ELEVATION FOR SINUSOIDAL PULSE OF ONE SECOND DURATION FOR VARIOUS TIMES

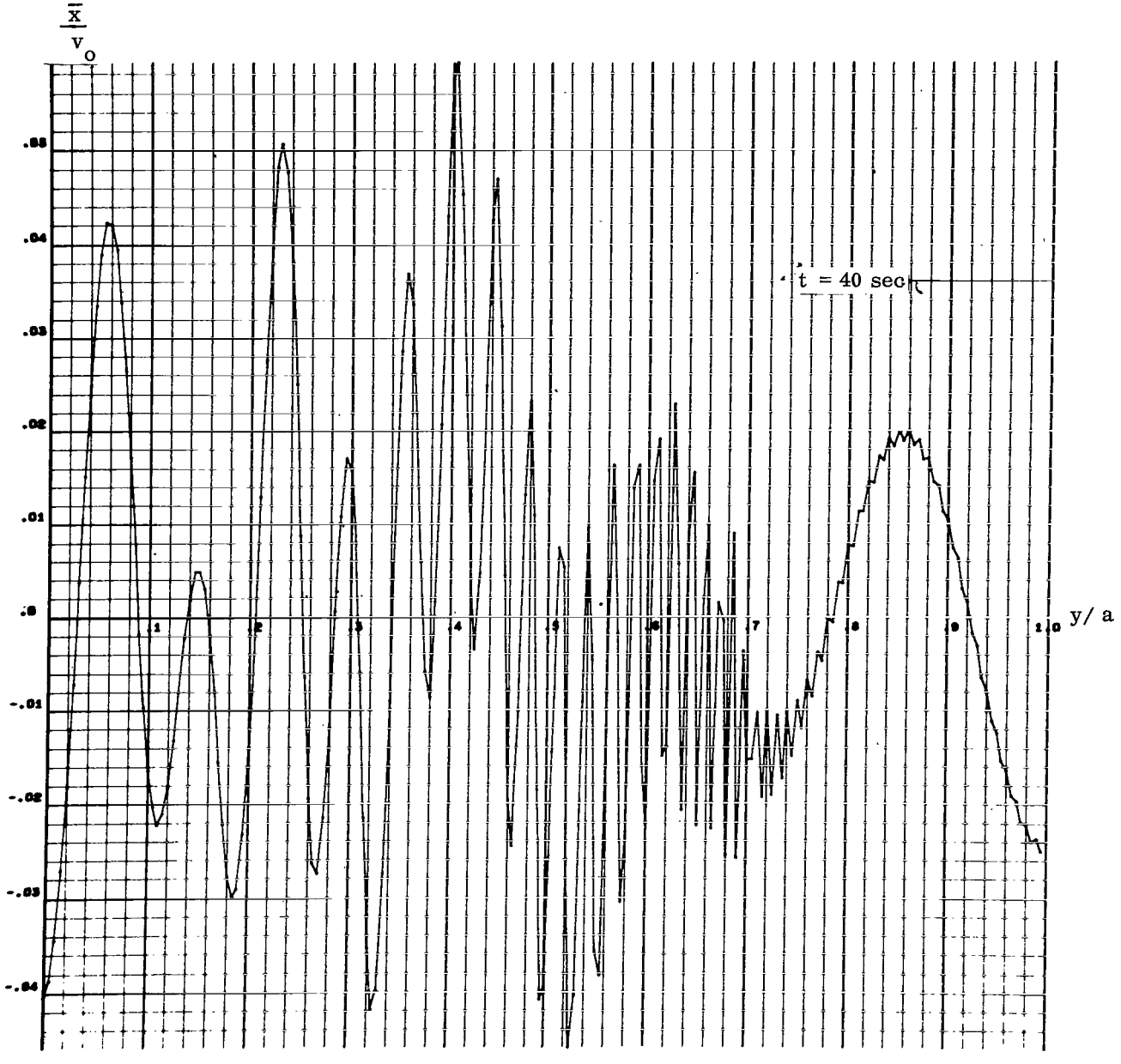

FIGURE 29. LIQUID SURFACE ELEVATION FOR SINUSOIDAL PULSE OF ONE SECOND DURATION FOR VARIOUS TIMES

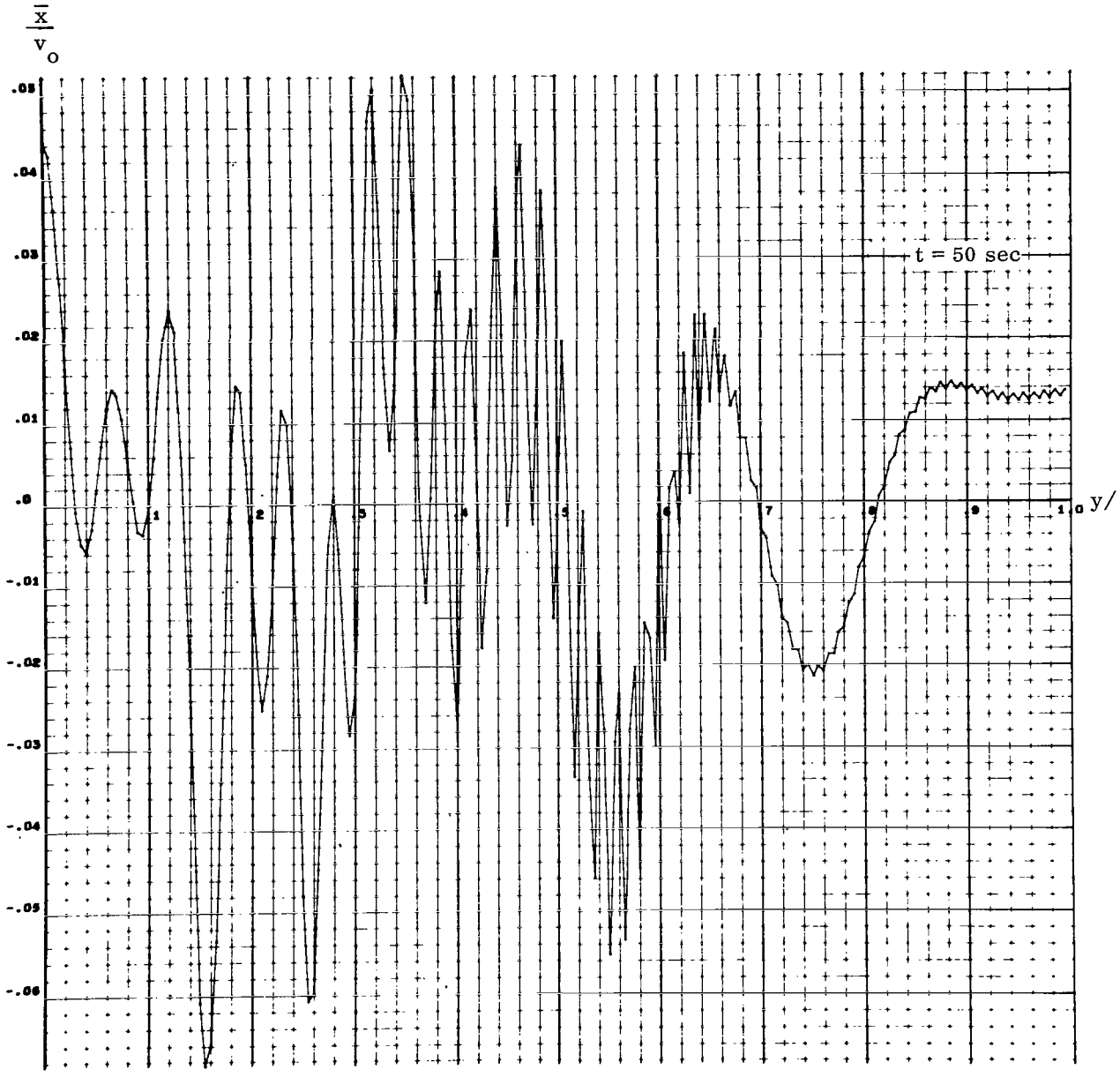

FIGURE 30. LIQUID SURFACE ELEVATION FOR SINUSOIDAL PULSE OF ONE SECOND DURATION FOR VARIOUS TIMES

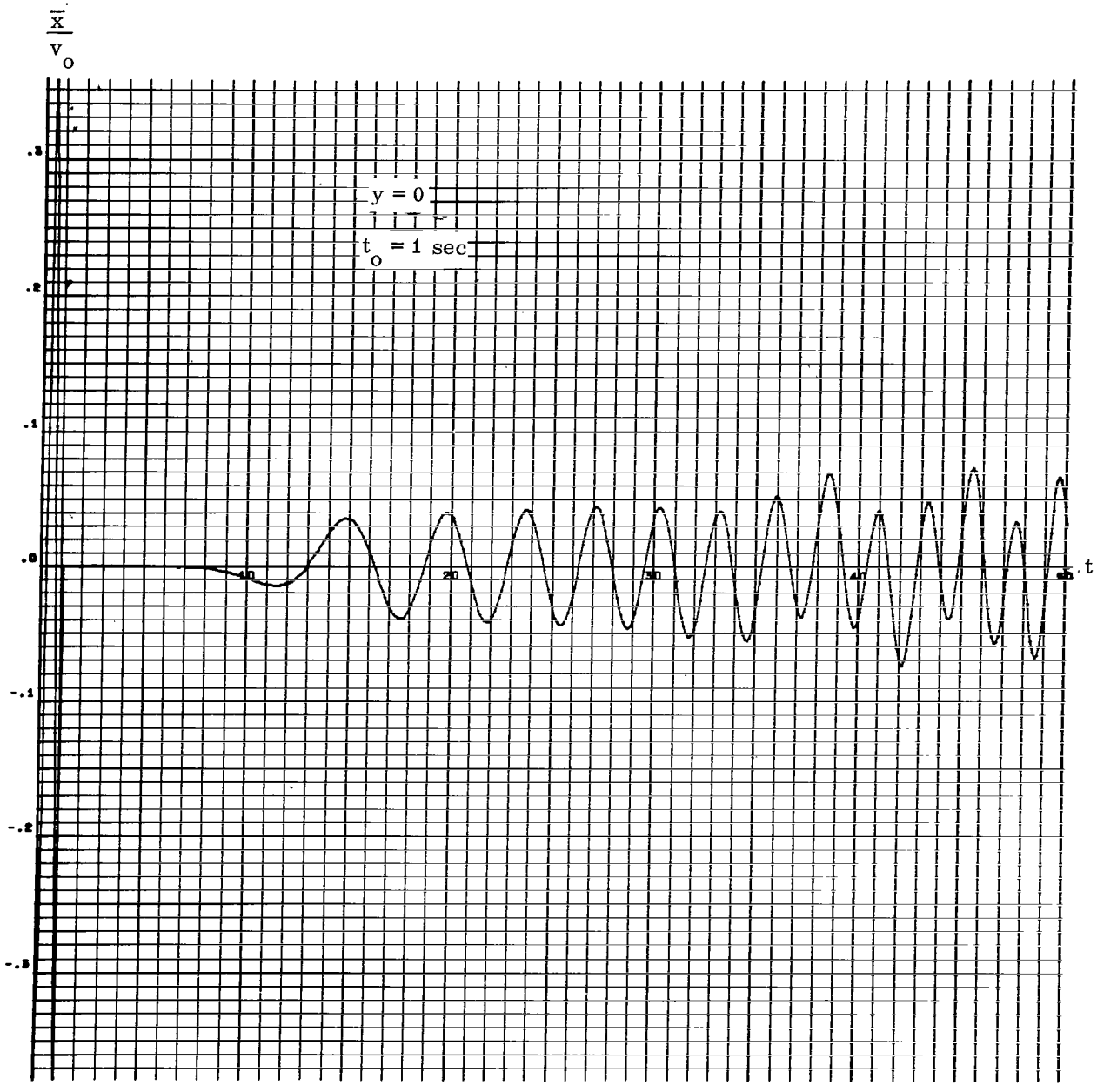

FIGURE 31. LIQUID ELEVATION VERSUS TIME AT y = 0 FOR RECTANGULAR DOUBLE PULSE

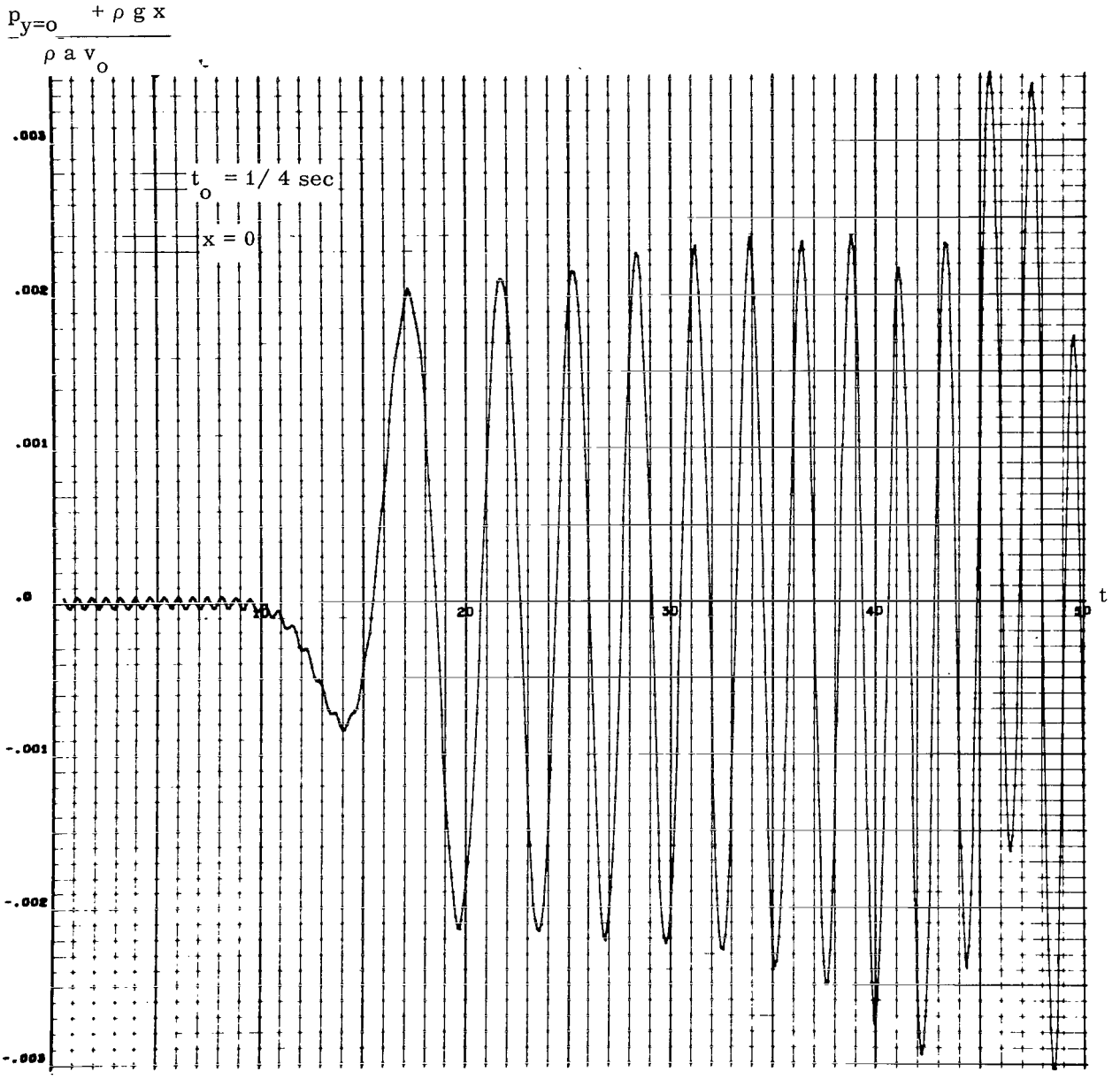

FIGURE 32. PRESSURE DISTRIBUTION AT THE LEFT CONTAINER WALL FOR RECTANGULAR DOUBLE PULSE FOR VARIOUS PULSE DURATIONS

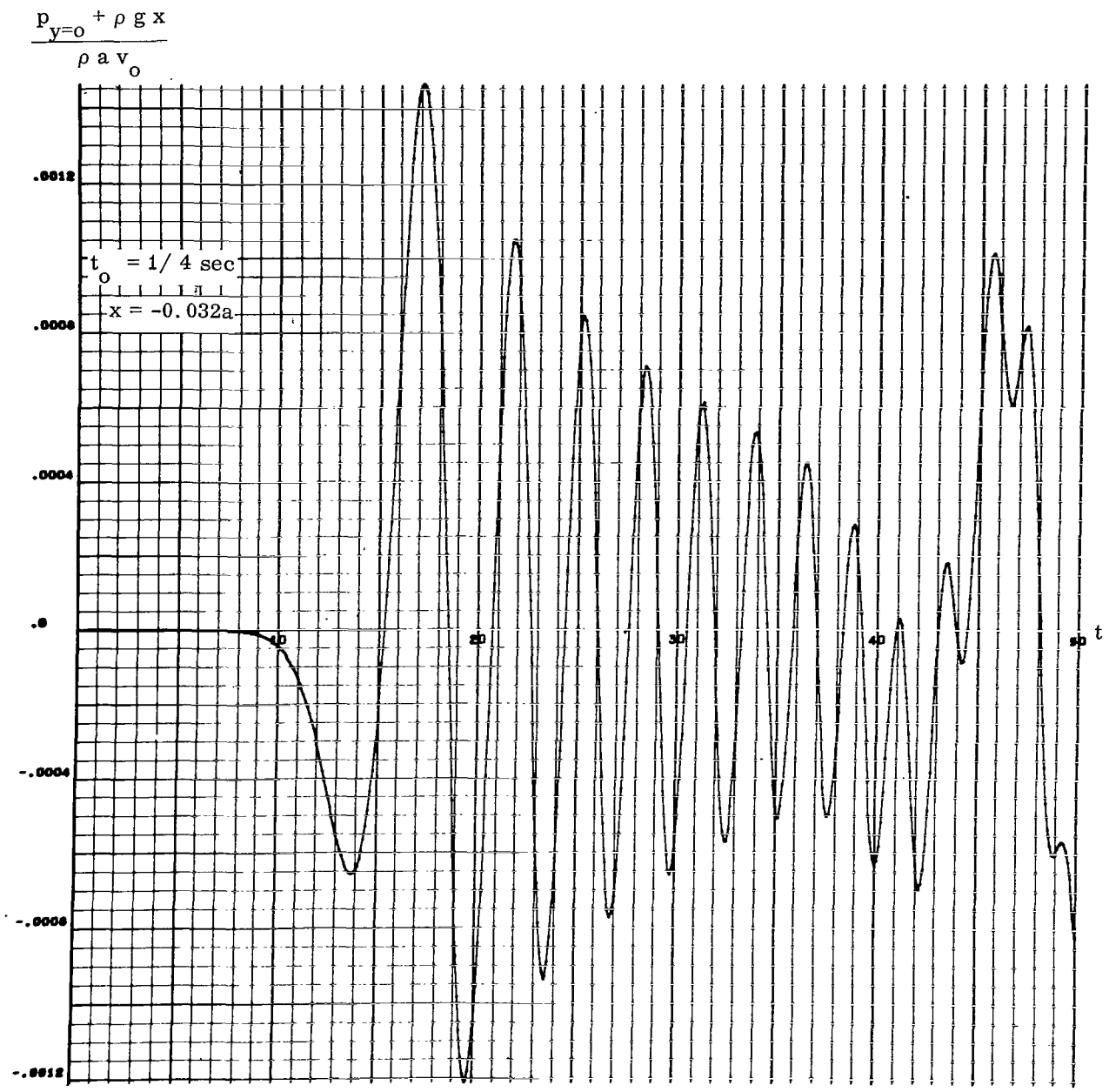

FIGURE 33. PRESSURE DISTRIBUTION AT THE LEFT CONTAINER WALL FOR RECTANGULAR DOUBLE PULSE FOR VARIOUS PULSE DURATIONS

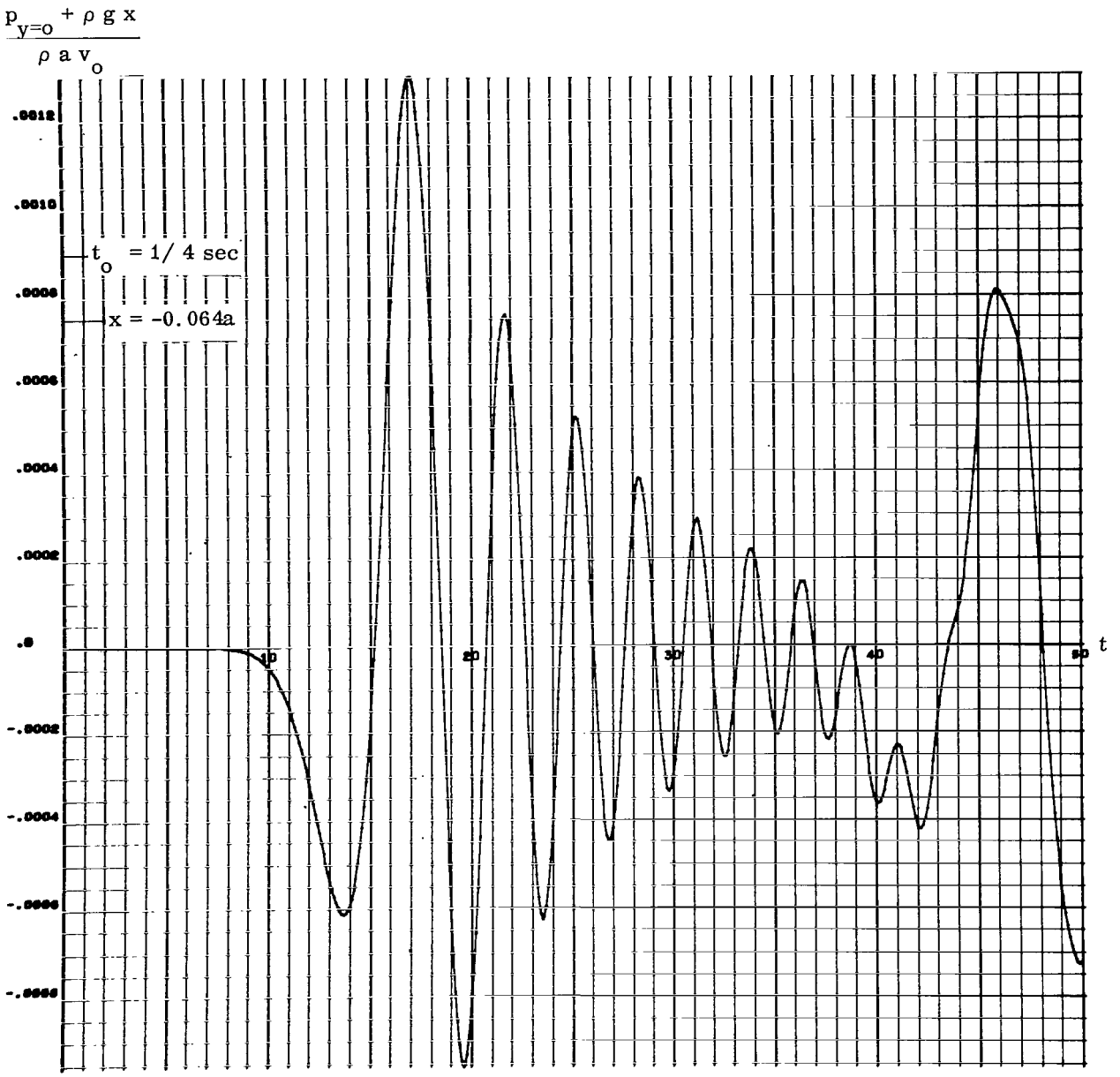

FIGURE 34. PRESSURE DISTRIBUTION AT THE LEFT CONTAINER WALL FOR RECTANGULAR DOUBLE PULSE FOR VARIOUS PULSE DURATIONS

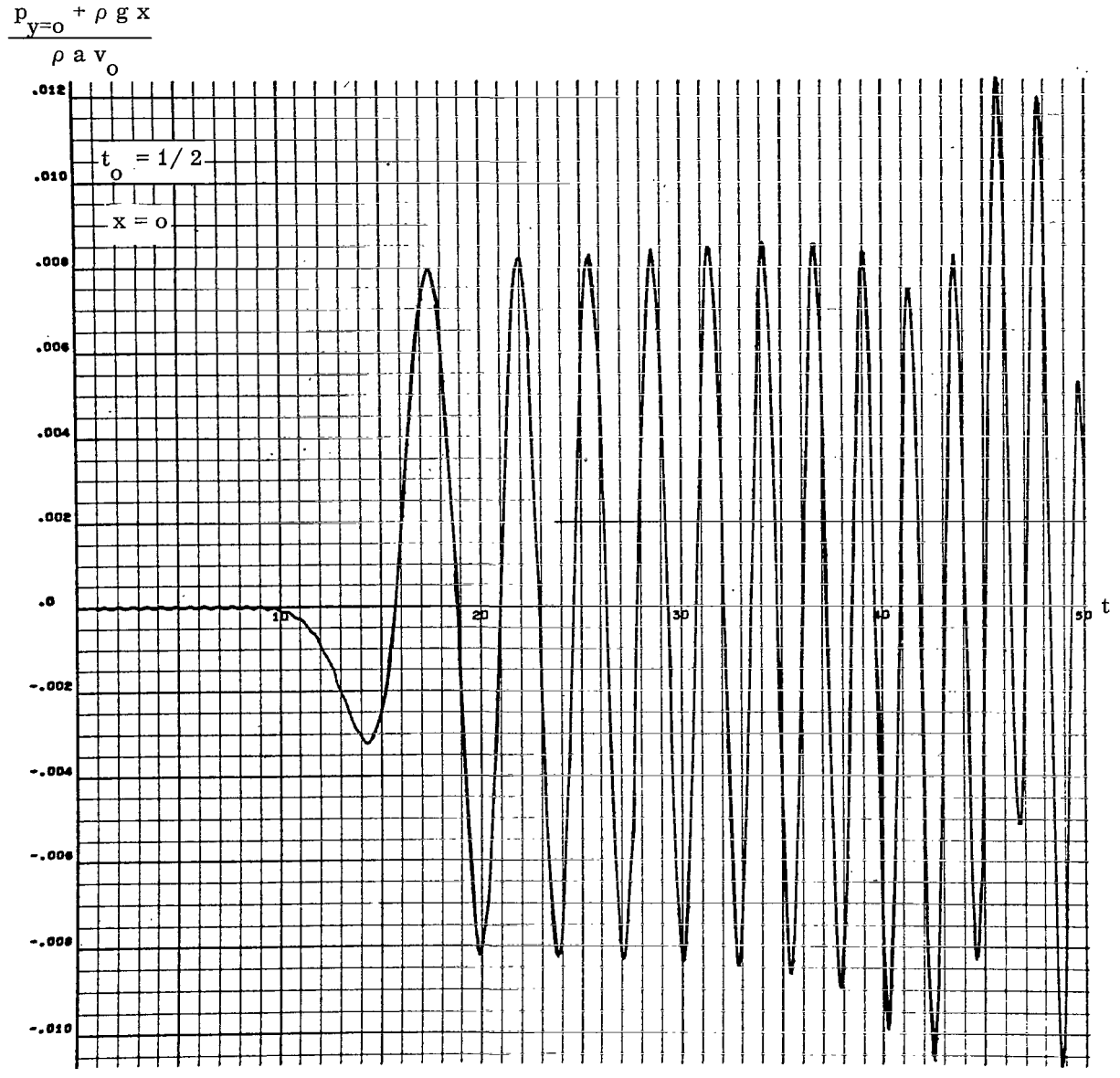

FIGURE 35. PRESSURE DISTRIBUTION AT THE LEFT CONTAINER WALL FOR RECTANGULAR DOUBLE PULSE FOR VARIOUS PULSE DURATIONS

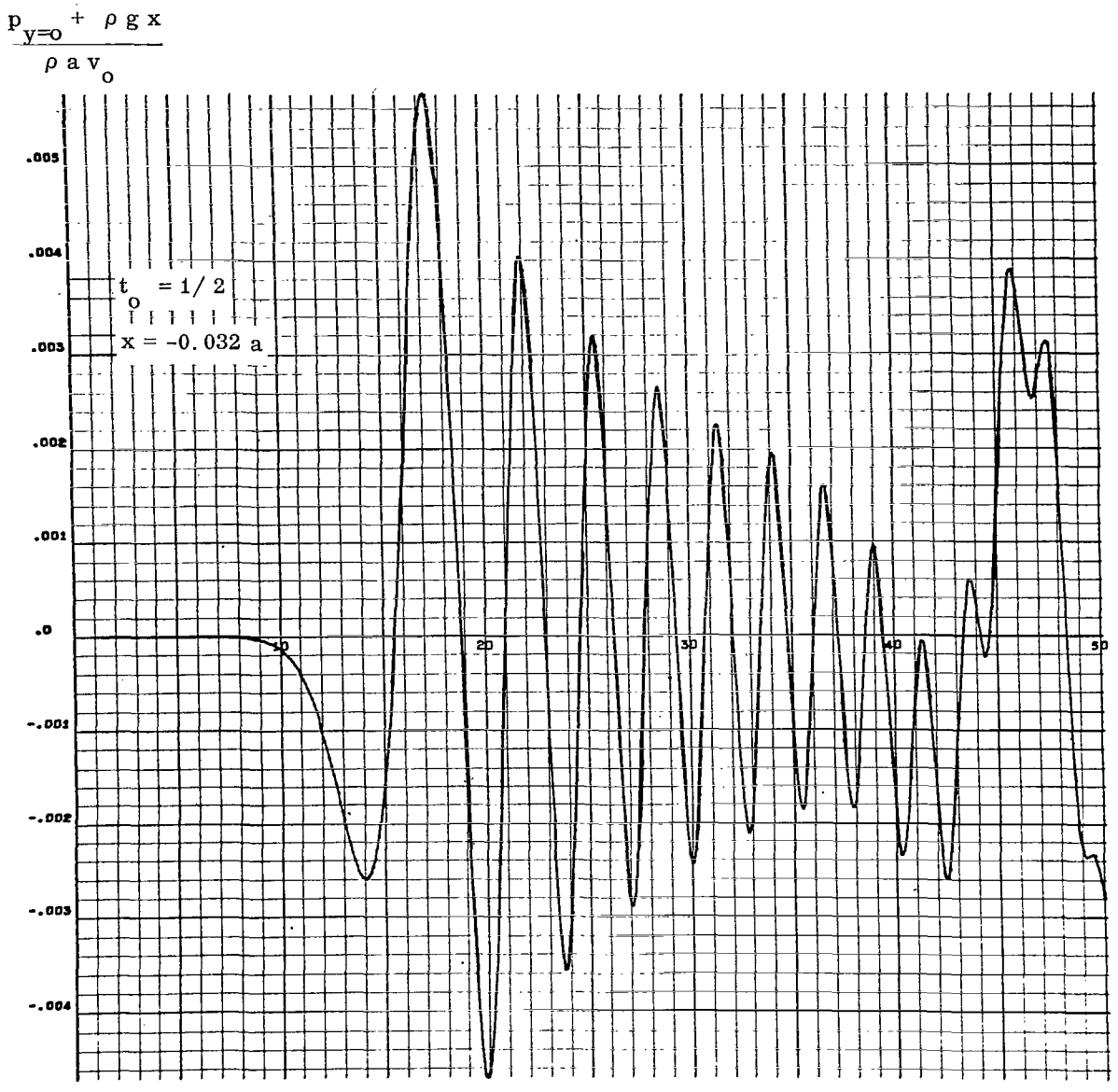

FIGURE 36. PRESSURE DISTRIBUTION AT THE LEFT CONTAINER WALL FOR RECTANGULAR DOUBLE PULSE FOR VARIOUS PULSE DURATIONS

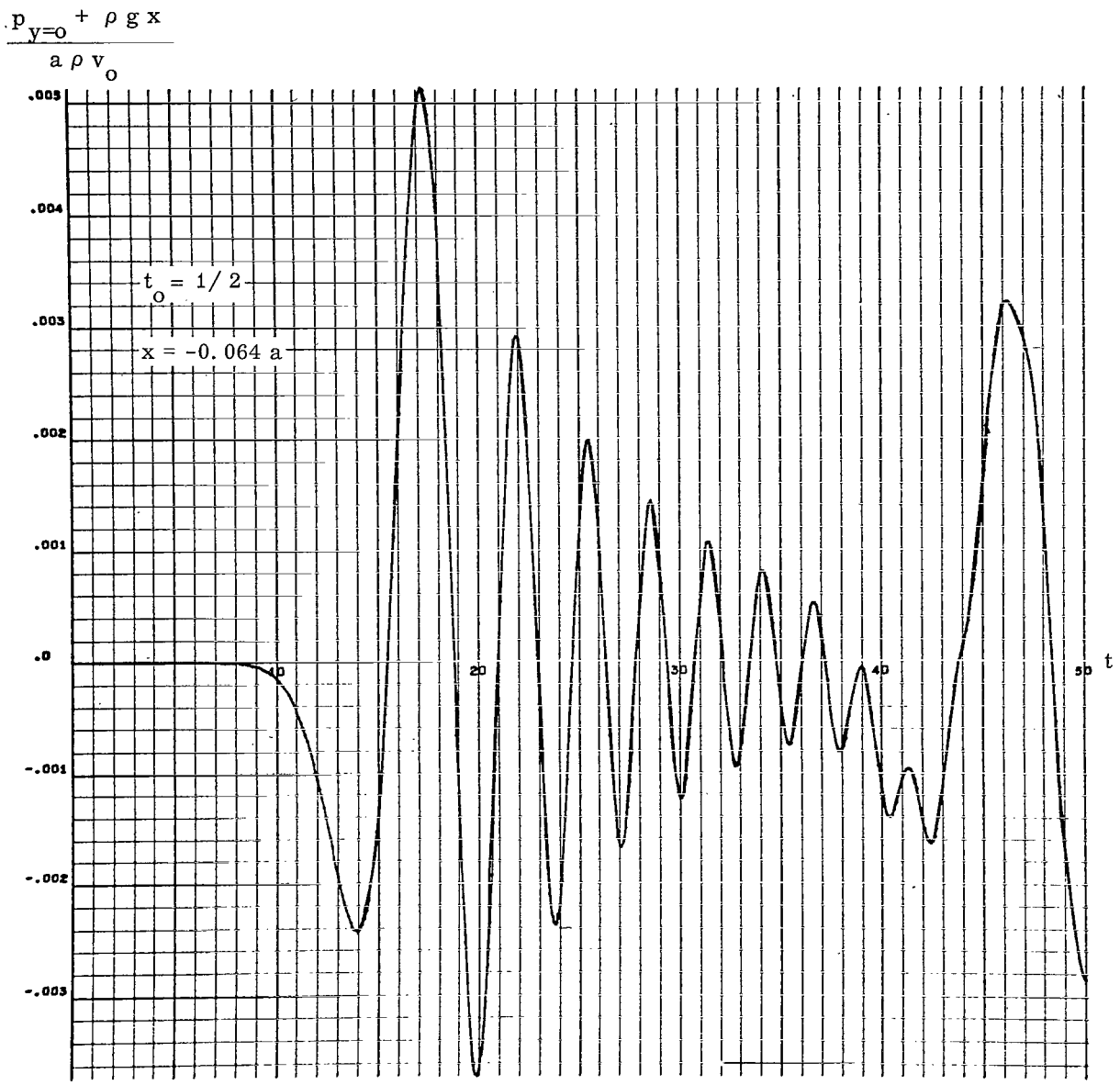

FIGURE 37. PRESSURE DISTRIBUTION AT THE LEFT CONTAINER WALL FOR RECTANGULAR DOUBLE PULSE FOR VARIOUS PULSE DURATIONS

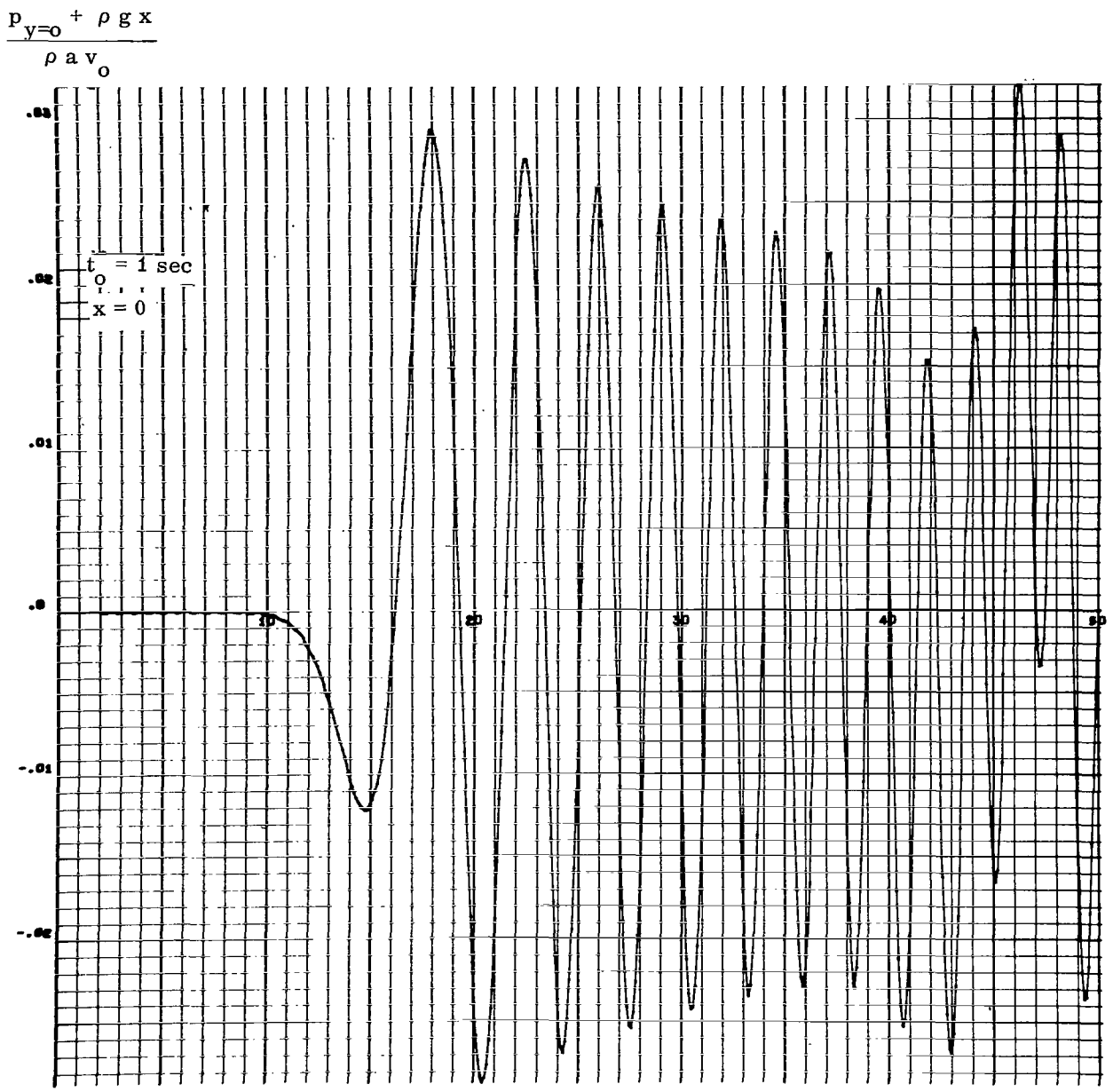

FIGURE 38. PRESSURE DISTRIBUTION AT THE LEFT CONTAINER WALL FOR RECTANGULAR DOUBLE PULSE FOR VARIOUS PULSE DURATIONS

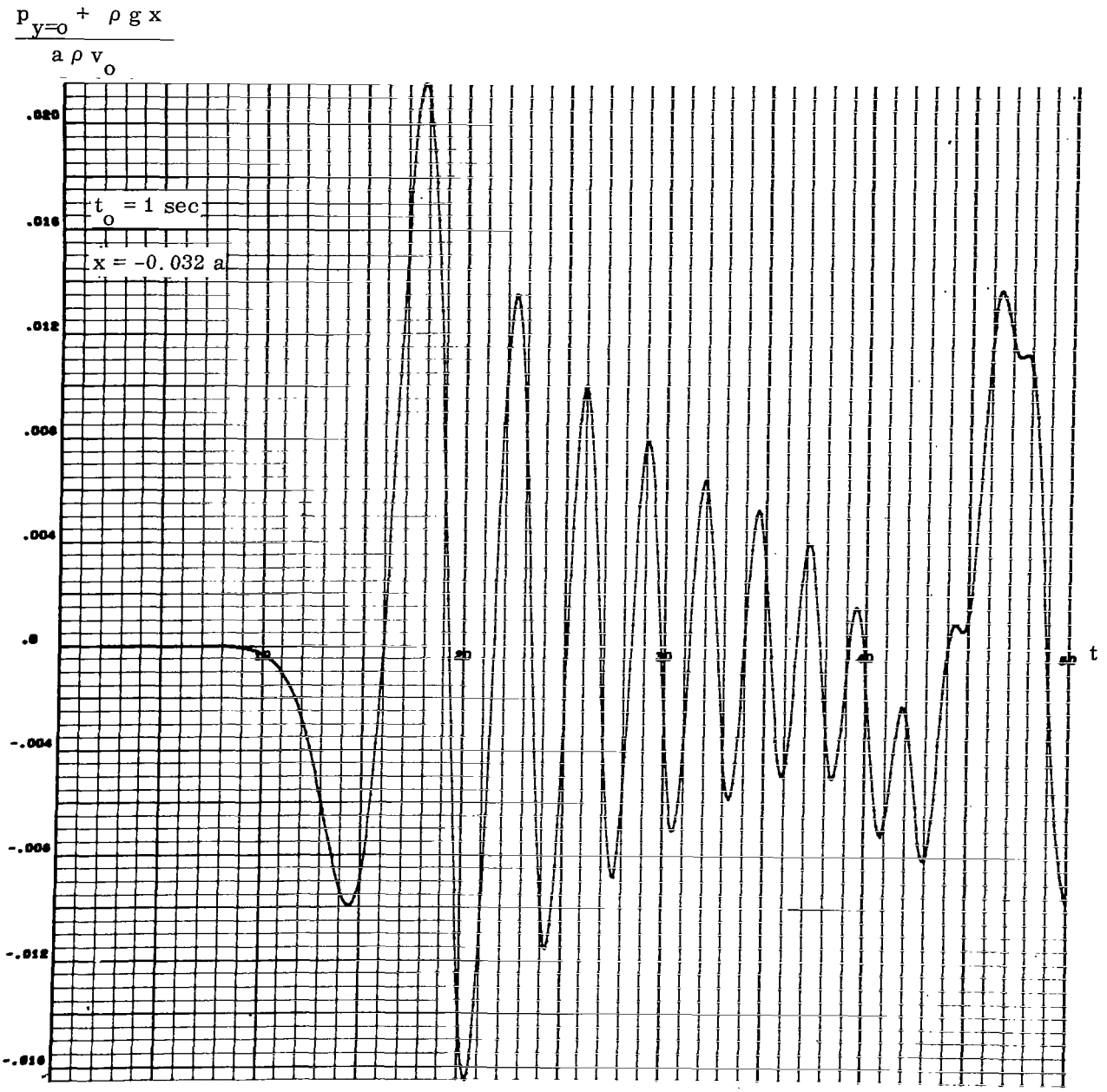

FIGURE 39. PRESSURE DISTRIBUTION AT THE LEFT CONTAINER WALL FOR RECTANGULAR DOUBLE PULSE FOR VARIOUS PULSE DURATIONS

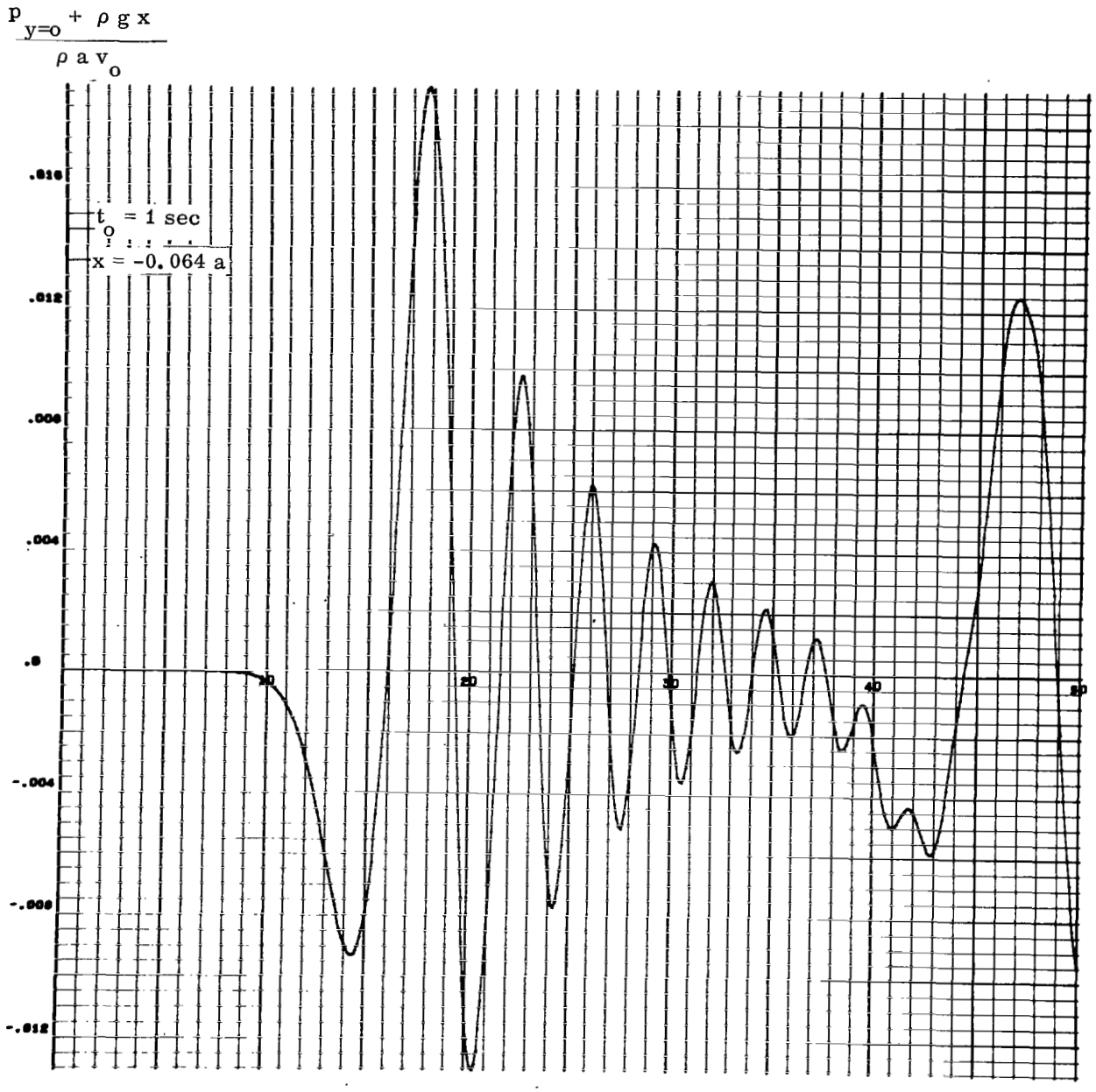

FIGURE 40. PRESSURE DISTRIBUTION AT THE LEFT CONTAINER WALL FOR RECTANGULAR DOUBLE PULSE FOR VARIOUS PULSE DURATIONS

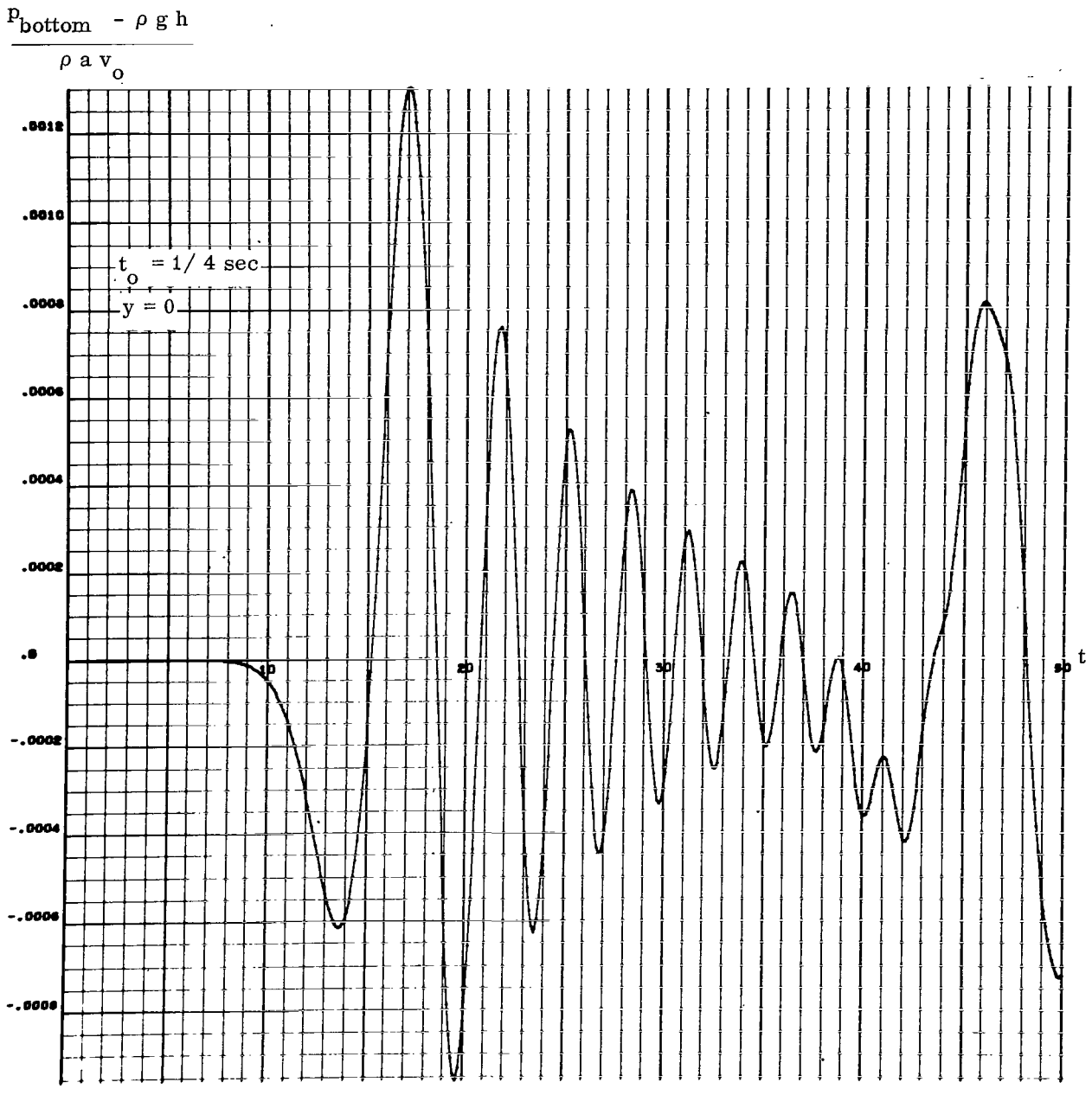

FIGURE 41. PRESSURE DISTRIBUTION AT THE CONTAINER BOTTOM FOR RECTANGULAR DOUBLE PULSE

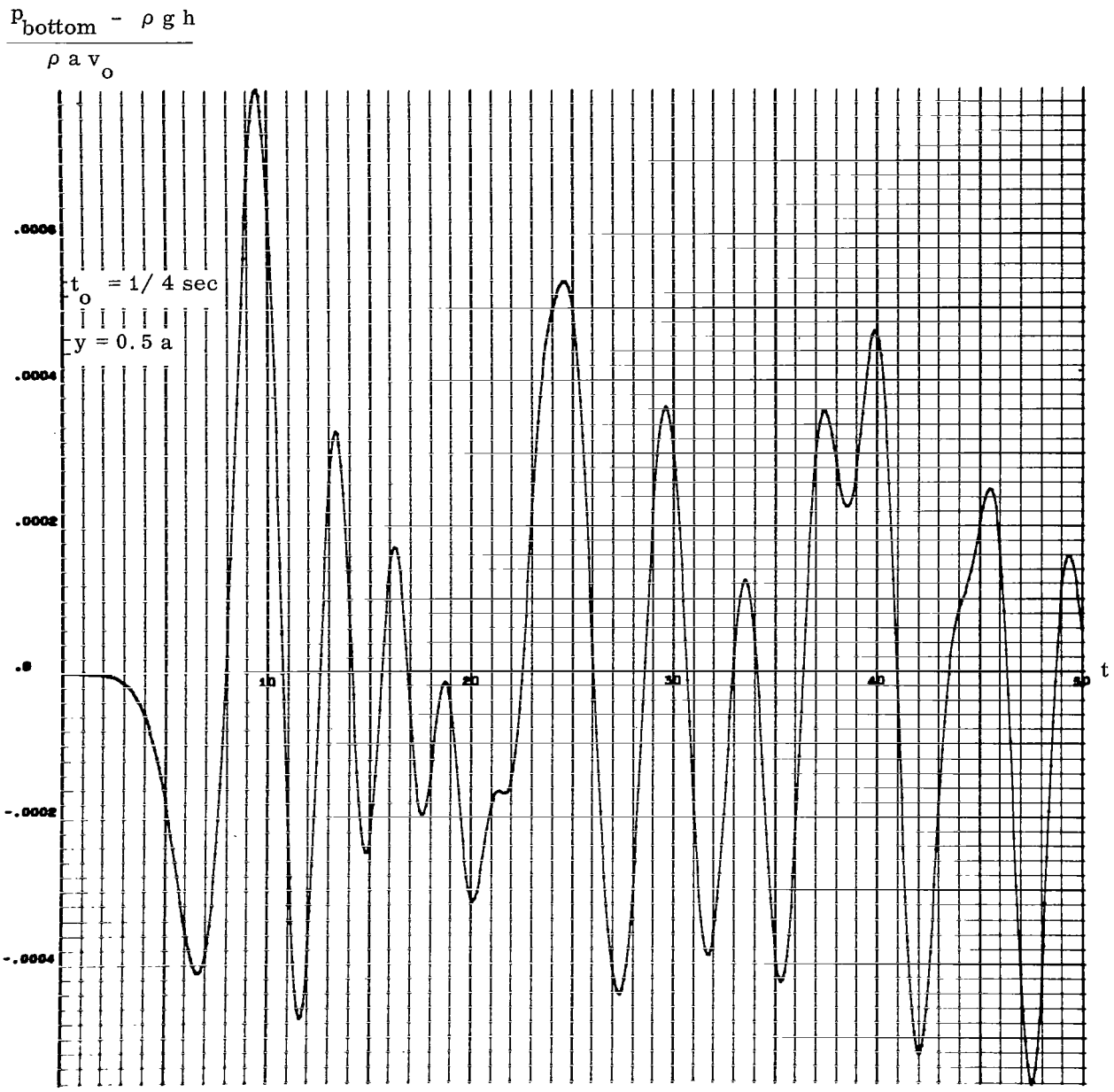

FIGURE 42. PRESSURE DISTRIBUTION AT THE CONTAINER BOTTOM FOR RECTANGULAR DOUBLE PULSE

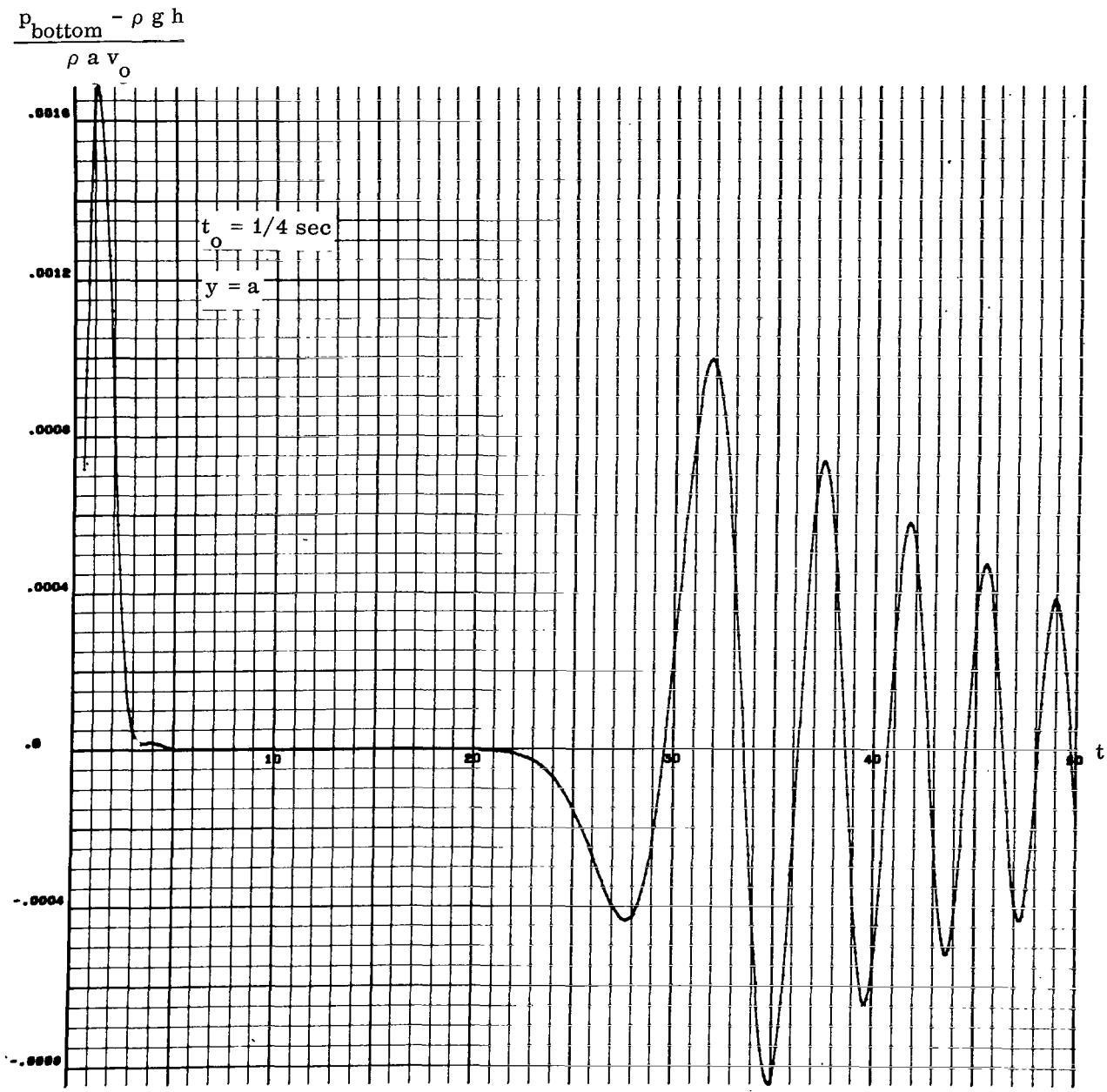

FIGURE 43. PRESSURE DISTRIBUTION AT THE CONTAINER BOTTOM FOR RECTANGULAR DOUBLE PULSE

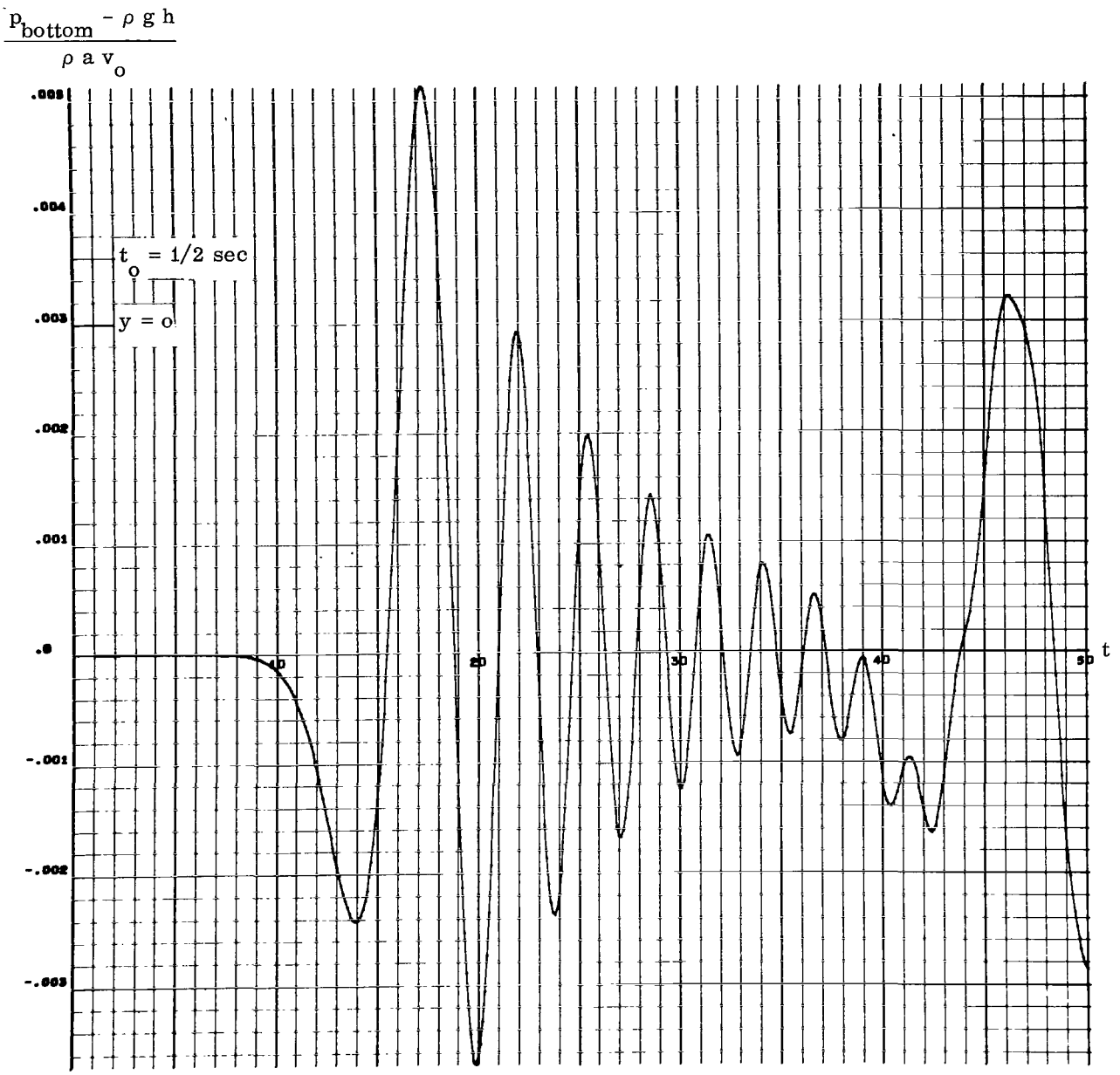

FIGURE 44. PRESSURE DISTRIBUTION AT THE CONTAINER BOTTOM FOR RECTANGULAR DOUBLE PULSE

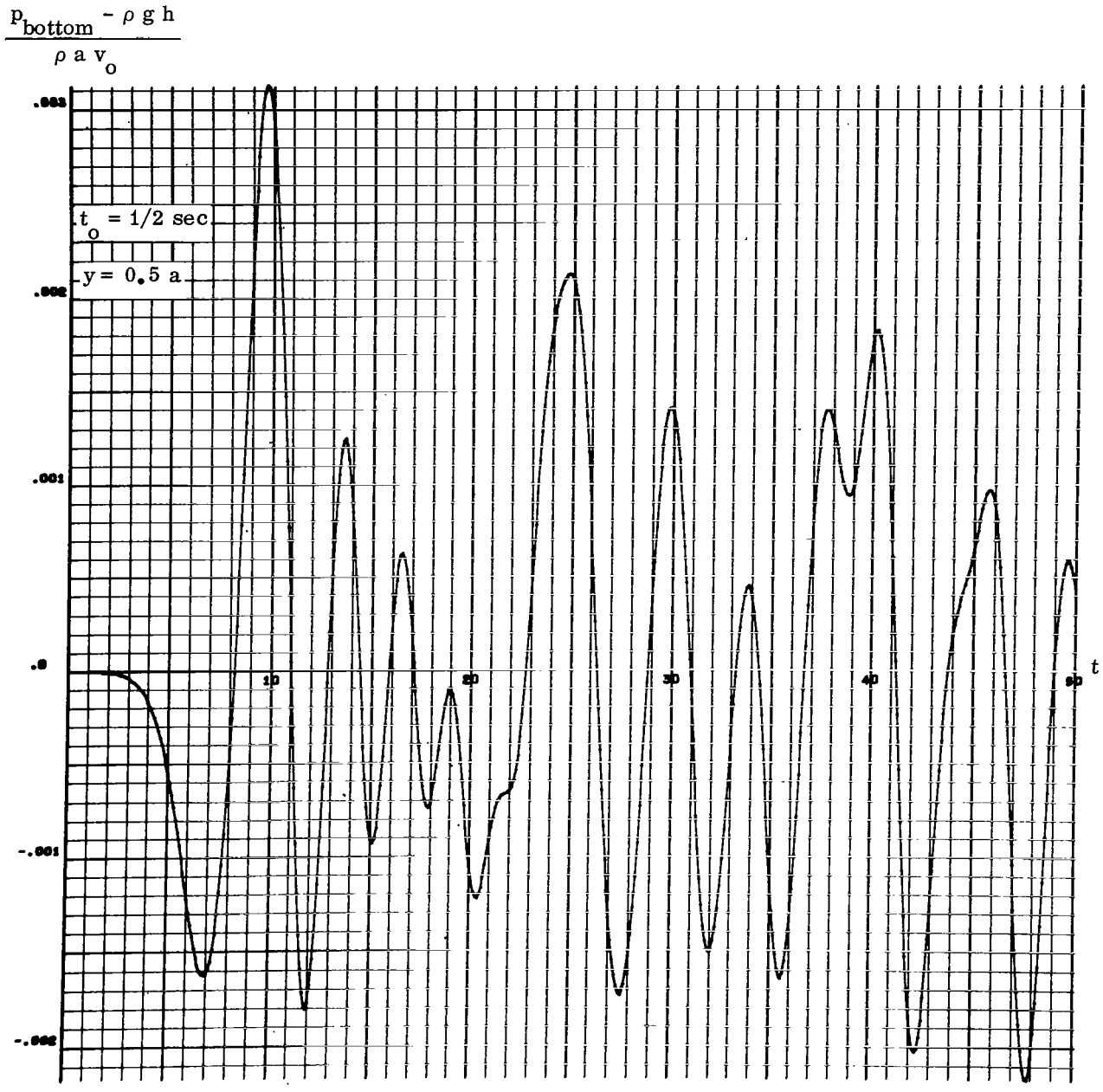

FIGURE 45. PRESSURE DISTRIBUTION AT THE CONTAINER BOTTOM FOR RECTANGULAR DOUBLE PULSE

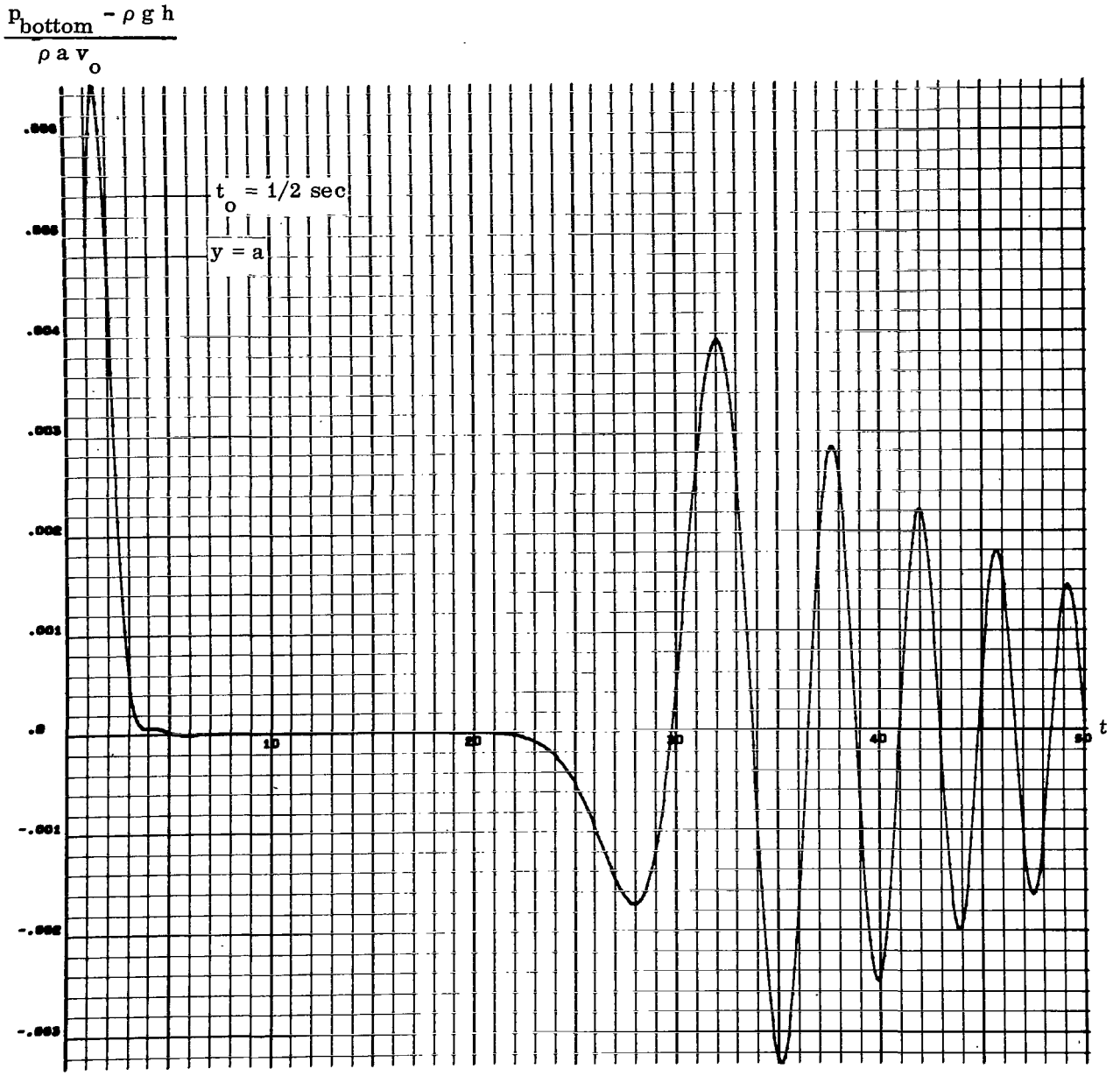

FIGURE 46. PRESSURE DISTRIBUTION AT THE CONTAINER BOTTOM FOR RECTANGULAR DOUBLE PULSE

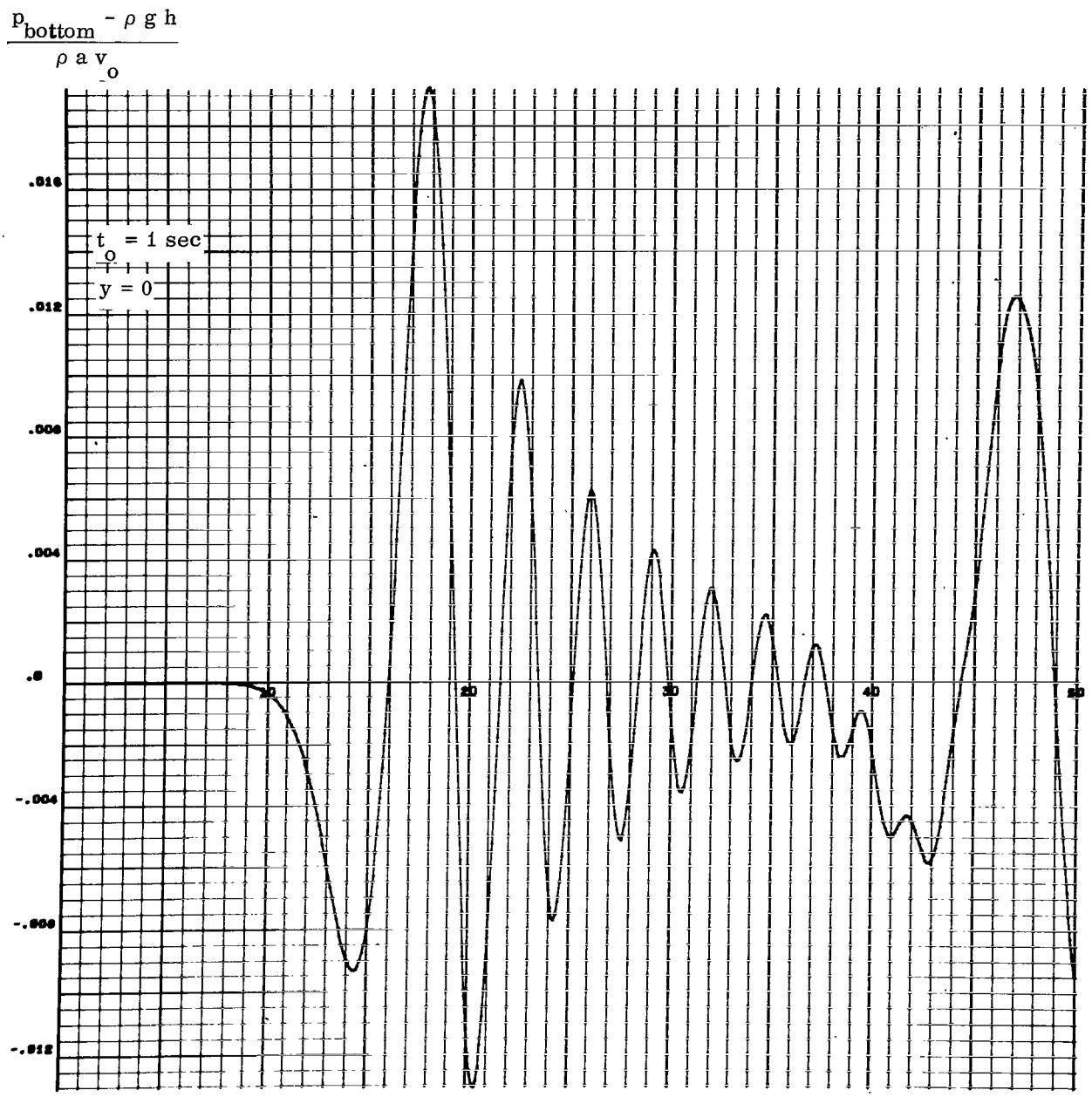

FIGURE 47. PRESSURE DISTRIBUTION AT THE CONTAINER BOTTOM FOR RECTANGULAR DOUBLE PULSE

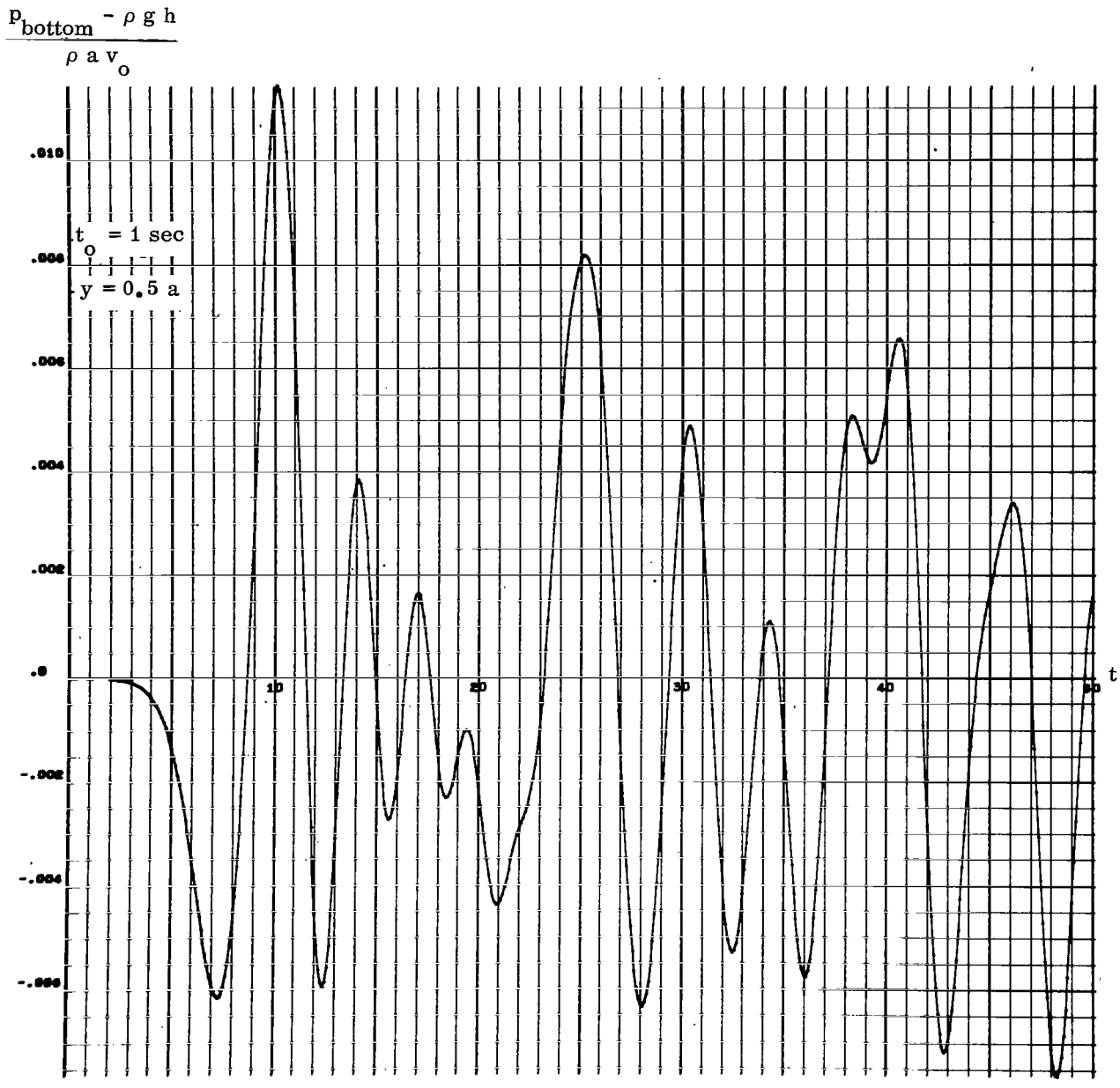

FIGURE 48. PRESSURE DISTRIBUTION AT THE CONTAINER BOTTOM FOR RECTANGULAR DOUBLE PULSE

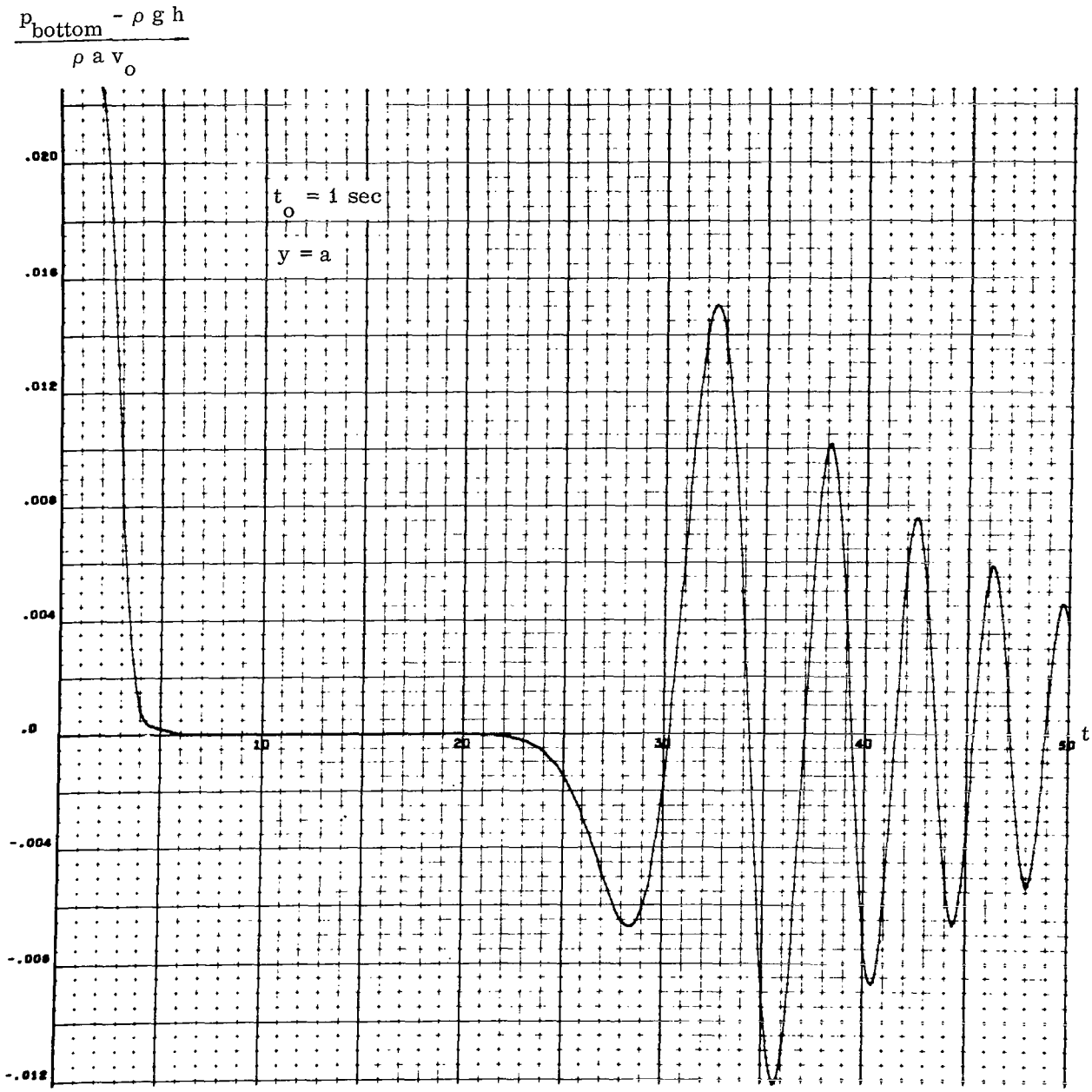

FIGURE 49. PRESSURE DISTRIBUTION AT THE CONTAINER BOTTOM FOR RECTANGULAR DOUBLE PULSE

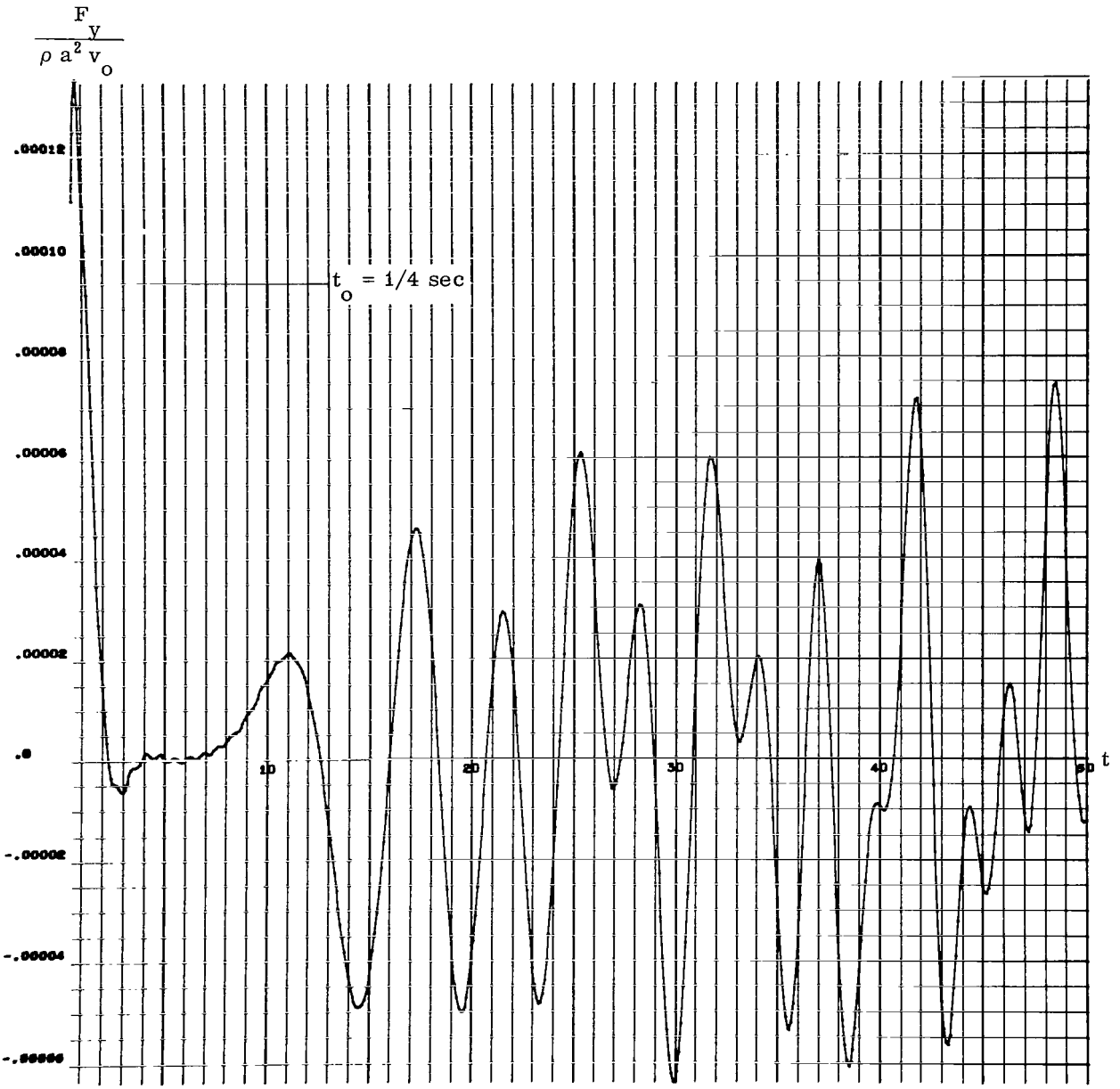

FIGURE 50. LIQUID FORCE FOR RECTANGULAR DOUBLE PULSE FOR VARIOUS PULSE DURATIONS

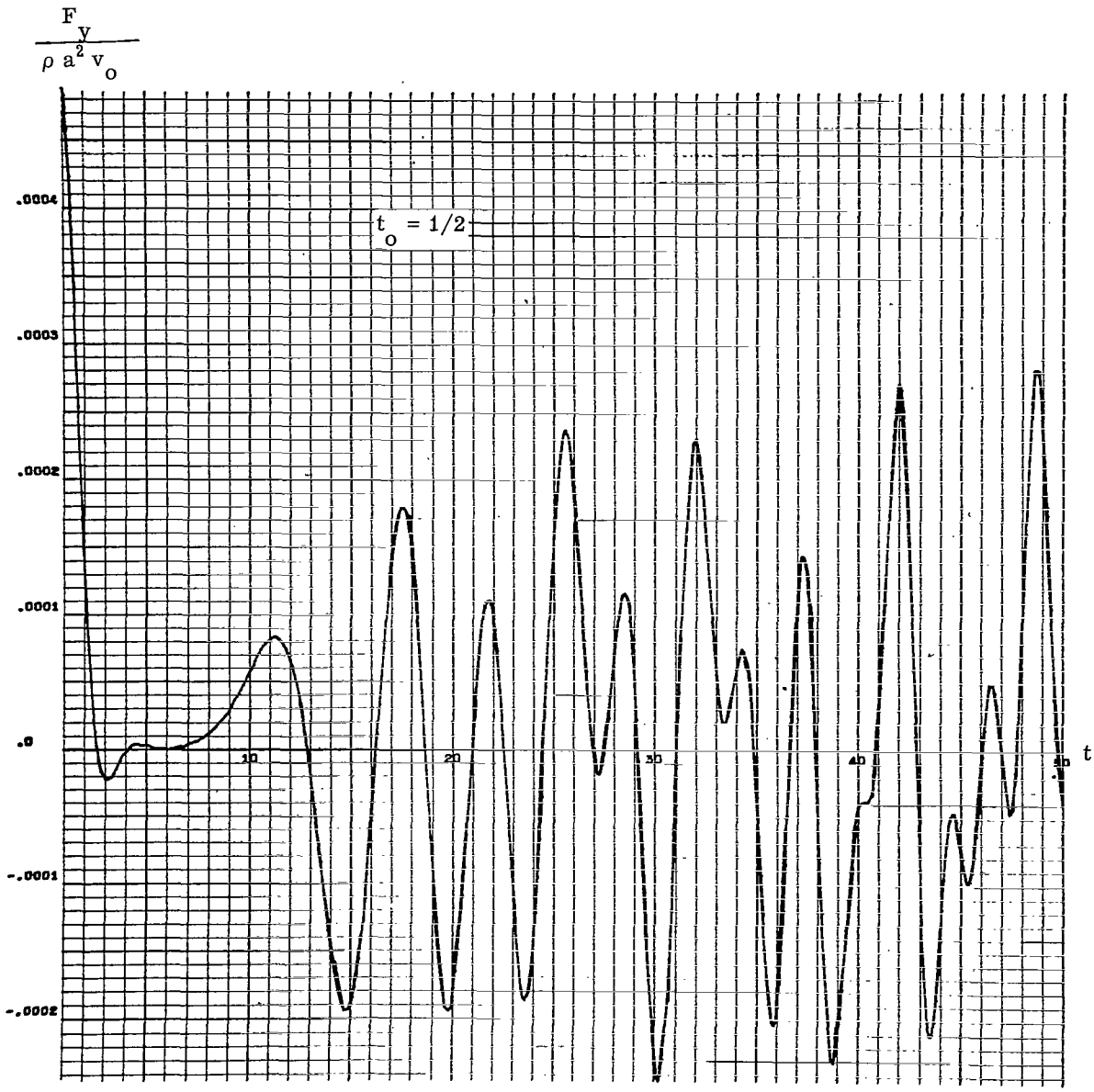

FIGURE 51. LIQUID FORCE FOR RECTANGULAR DOUBLE PULSE FOR VARIOUS PULSE DURATIONS

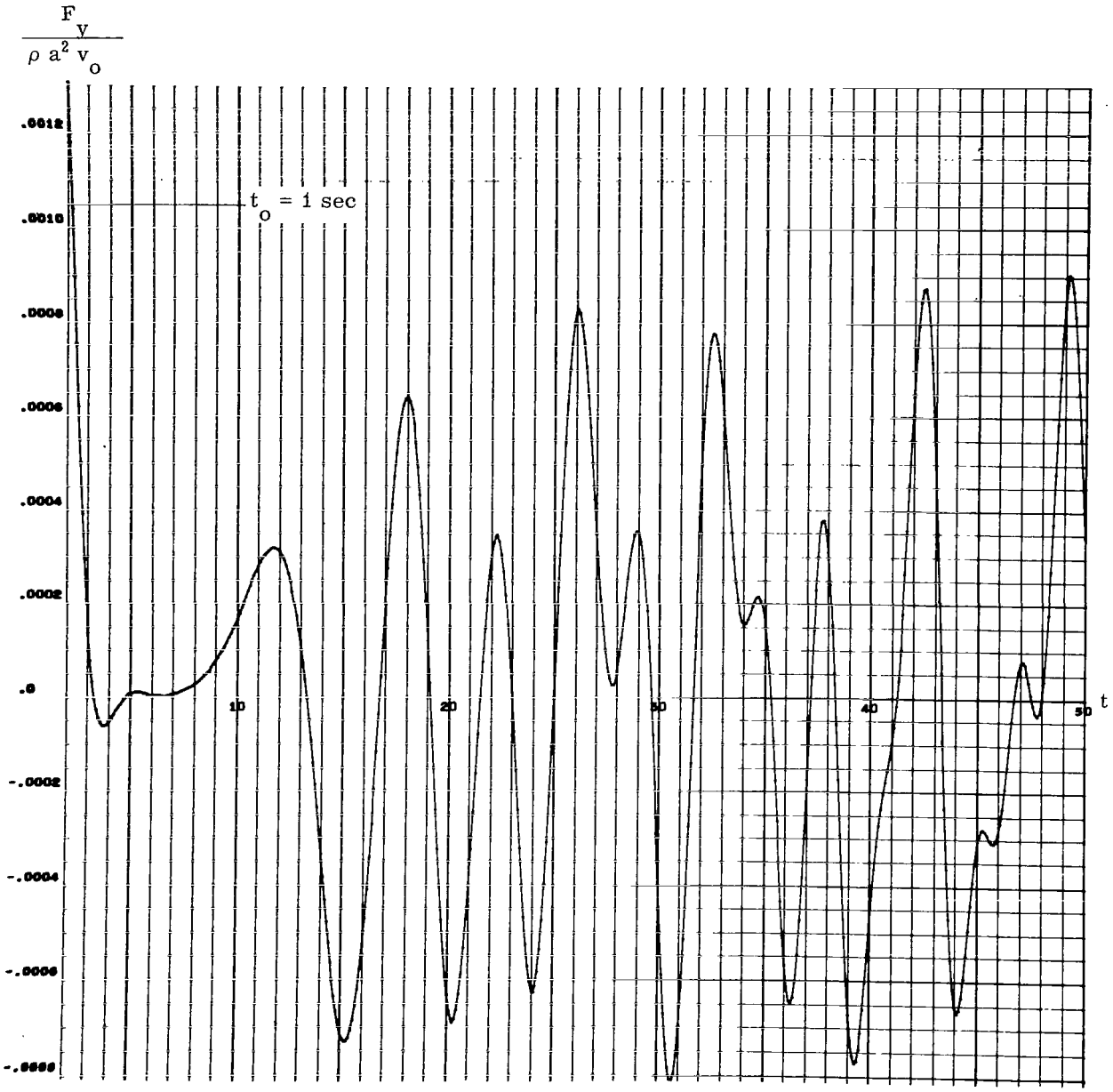

FIGURE 52. LIQUID FORCE FOR RECTANGULAR DOUBLE PULSE FOR VARIOUS PULSE DURATIONS

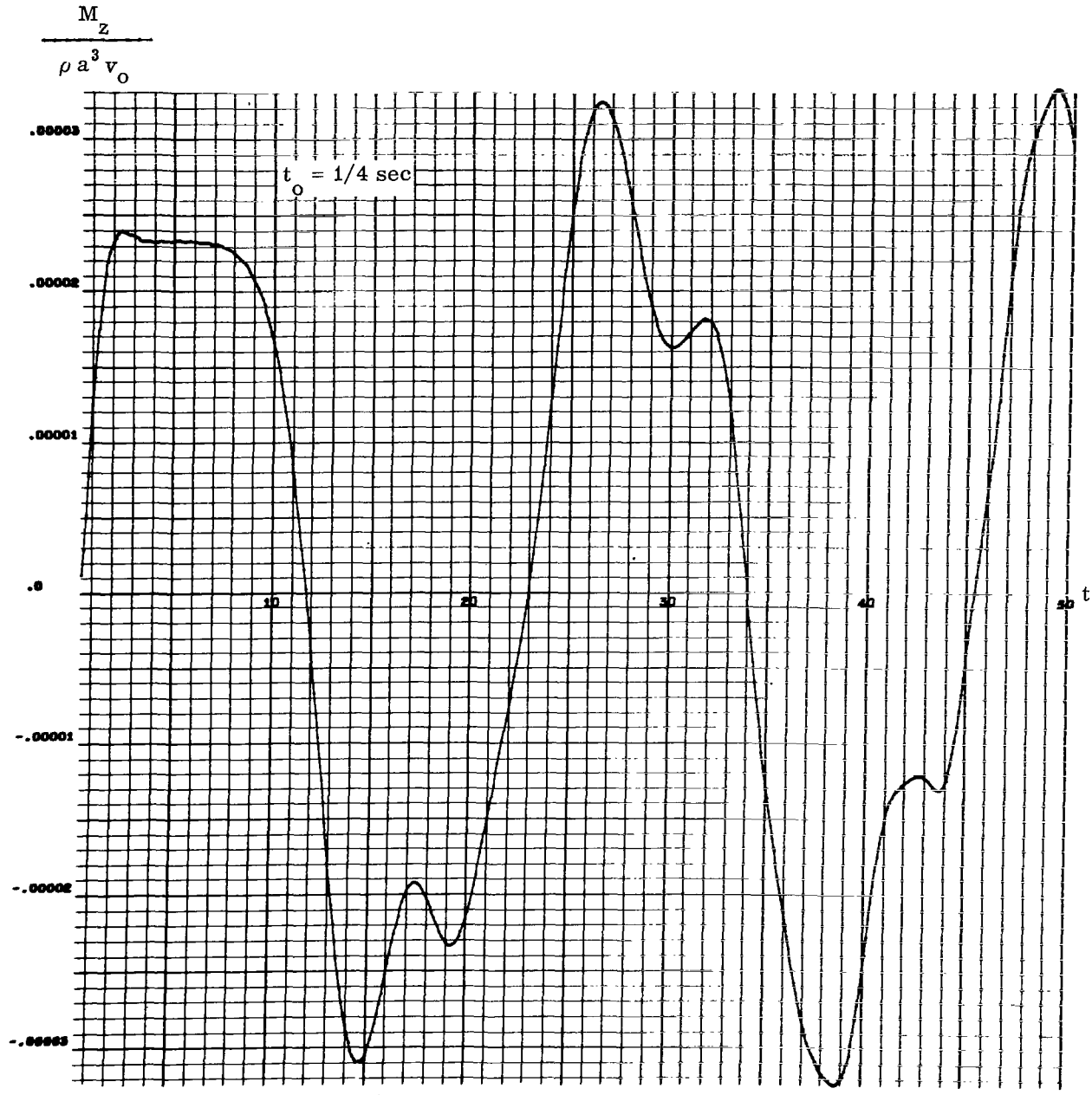

FIGURE 53. LIQUID MOMENT FOR RECTANGULAR DOUBLE PULSE FOR VARIOUS PULSE DURATIONS

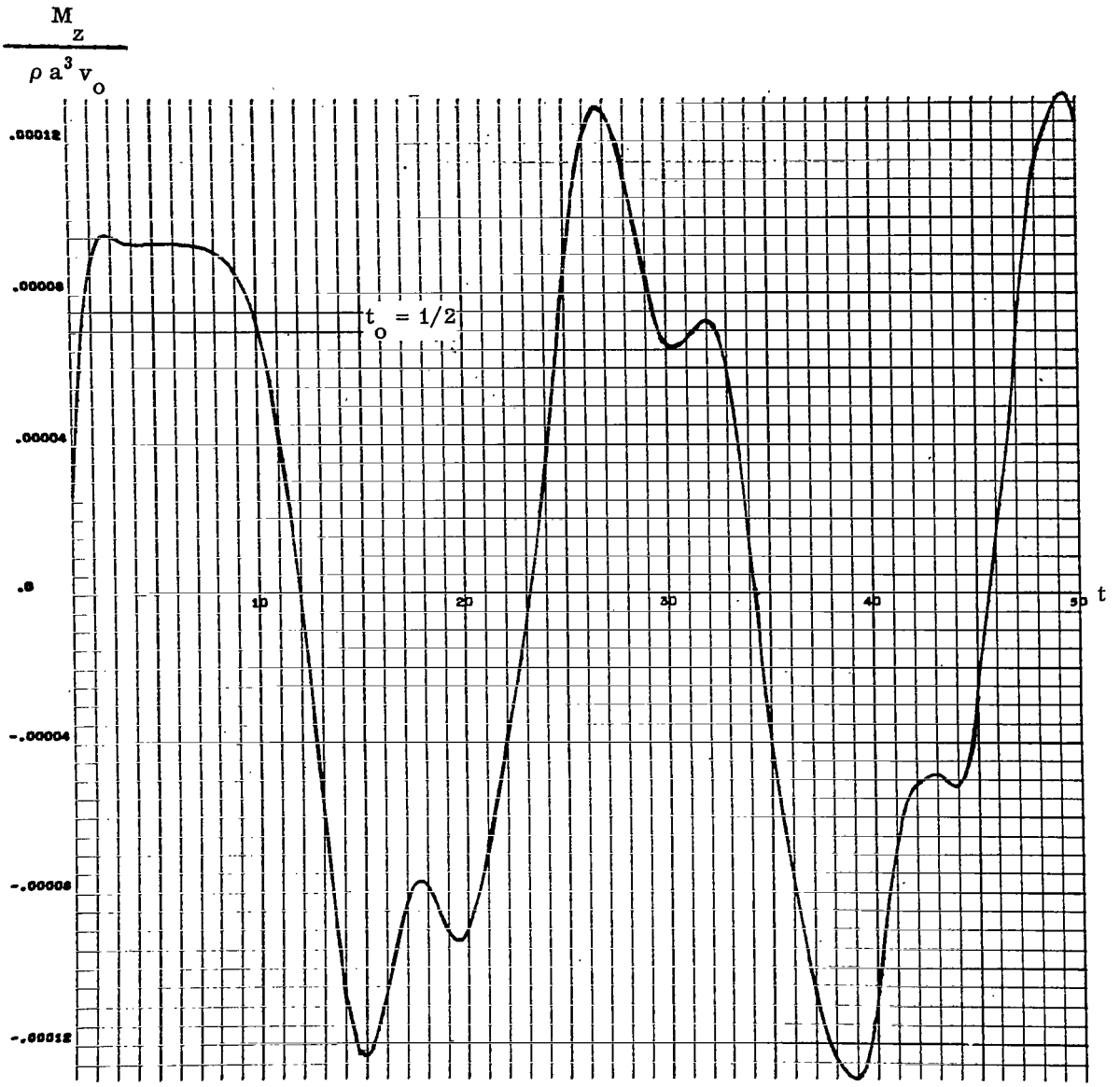

FIGURE 54. LIQUID MOMENT FOR RECTANGULAR DOUBLE PULSE FOR VARIOUS PULSE DURATIONS

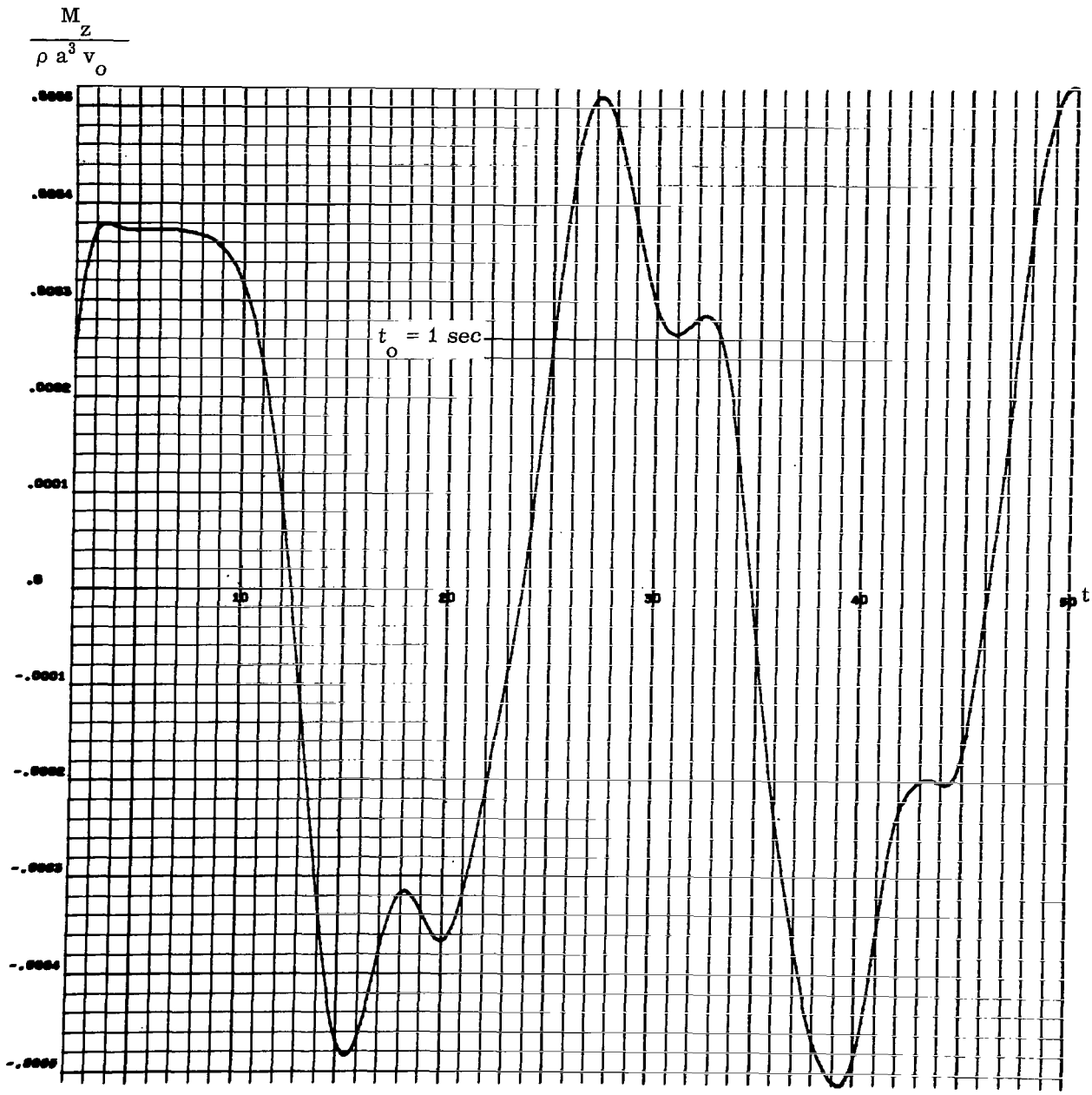

FIGURE 55. LIQUID MOMENT FOR RECTANGULAR DOUBLE PULSE FOR VARIOUS PULSE DURATIONS

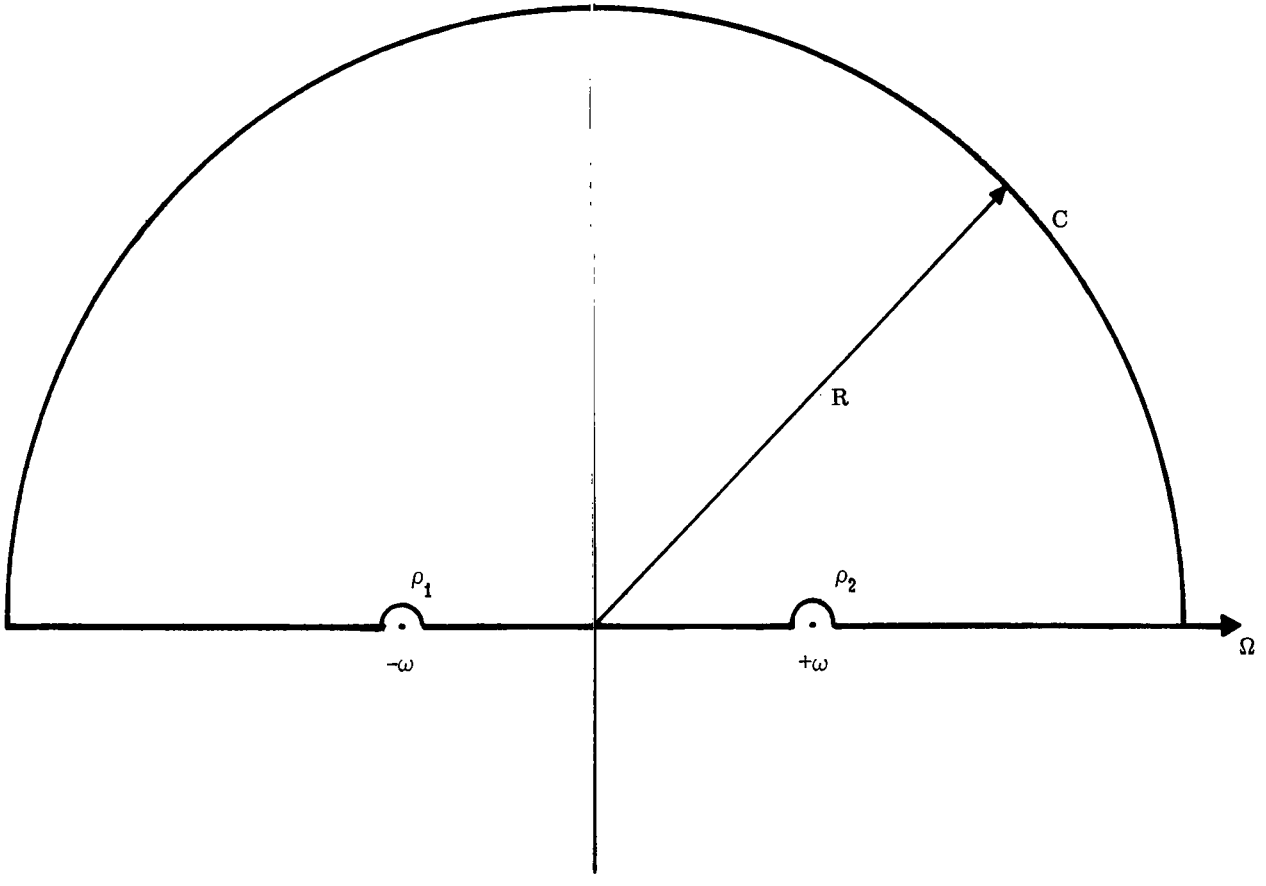

FIGURE 56. PATH OF INTEGRATION FOR IMPROPER INTEGRALS

APPENDIX

EVALUATION OF IMPROPER INTEGRALS

The integrals in the text are improper integrals and require the evaluation of

$$\oint_C f(\Omega)\ e^{ia\Omega}\, d\Omega \qquad \text{with } a > 0.$$

The path C of integration is the real axis and the semicircle around the origin in the upper half plane (Fig. 56).

Evaluation is restricted to two of these integrals. The others are very similar and do not require additional techniques.

The integral

$$\int_0^\infty \frac{\cos \Omega t \sin \Omega t}{\Omega}\, d\Omega = \tfrac{1}{2} \int_0^\infty \frac{\sin \Omega\ (t+T)}{\Omega}\, d\Omega + \tfrac{1}{2} \int_0^\infty \frac{\sin \Omega\ (T-t)}{\Omega}\, d\Omega$$

because $\sin \Omega T \cos \Omega t = 1/2 \sin \Omega (t + T) + 1/2 \sin \Omega (T - t)$. Essentially, it is necessary to determine the value of the integral

$$\int_0^\infty \frac{\sin a \Omega}{\Omega}\, d\Omega$$

since a can be taken to be either T+t or T-t. It is

$$\int_0^\infty \frac{\sin a\ \Omega}{\Omega}\, d\Omega = \frac{1}{4i} \int_{-\infty}^{+\infty} \frac{e^{ia\Omega}}{\Omega}\, d\Omega - \frac{1}{4i} \int_{\infty}^{+\infty} \frac{e^{-ia\Omega}}{\Omega}\, d\Omega .$$

The integral

$$\int_0^\infty \frac{\Omega \cos \Omega t \sin \Omega T}{\omega^2 - \Omega} d\Omega = \tfrac{1}{2} \int_0^\infty \frac{\Omega \sin \Omega (t+T)}{\omega^2 - \Omega^2} d\Omega + \tfrac{1}{2} \int_0^\infty \frac{\Omega \sin \Omega (T-t)}{\omega^2 - \Omega^2} d\Omega$$

yields essentially integrals of the form

$$\int_{-\infty}^{+\infty} \frac{\Omega e^{ia\Omega}}{\omega^2 - \Omega^2} d\Omega .$$

These integrals exhibit singularities on the integration path but their principal value can be found by complex evaluation methods. The integration path is taken along the real axis and a semicircle in the complex Ω-plane. If it can be shown that the integral along the semicircle vanishes with increasing radius of the circle, the value of the integral along the closed path is the same as that of the integral along the real axis from $-\infty$ to $+\infty$. If the integral

$$\oint_{C_1} f(\Omega)\, e^{i\Omega a} d\Omega$$

is considered with $a > 0$ and C_1 a semicircle around the origin in the upper half plane, then $f(\Omega)$ may satisfy the following conditions:

1. $f(\Omega)$ be analytic for $\mathrm{Im}(\Omega) > 0$ except for a finite number of poles.

2. The absolute value of the function $f(\Omega)$ on the curve approaches zero as the radius of the circle C_1 approaches infinity.

$$\lim_{|\Omega| \to \infty} |f(\Omega)| = 0 \qquad \text{for} \qquad 0 \leq \arg \Omega \leq \pi.$$

Then

$$\lim_{|\Omega| \to \infty} \oint_{C_1} f(\Omega)\, e^{i\Omega a} d\Omega = 0, \quad \text{if} \quad a > 0.$$

Proof: With the second condition, it can be concluded with sufficiently large $|\Omega|$, that $|f(\Omega)| < \epsilon$ for all Ω on C_1 and $\epsilon > 0$.

With $\Omega = Re^{i\varphi}$ it is

$$\left|e^{i\Omega a}\right| = \left|e^{ia\,R(\cos\varphi + i\sin\varphi)}\right| = e^{-aR\sin\varphi} \leq e^{-2a\,R\,\varphi/\pi}$$

because of

$$2/\pi \leq \frac{\sin\varphi}{\varphi} \leq 1 \qquad \text{for} \qquad 0 < \varphi \leq \pi/2.$$

Therefore, it is

$$\left|\oint_{C_1} f(\Omega)\, e^{i\Omega a}\, d\Omega\right| = \left|\int_0^{\pi} f(Re^{i\varphi})\, e^{ia\,R\cos\varphi}\,.\,e^{-4\,R\sin\varphi}\,.\,R\Omega e^{i\varphi}\, d\varphi\right|$$

$$< \epsilon R \int_0^{\pi} e^{-a\,R\sin\varphi}\, d\varphi = 2\,\epsilon R \int_0^{\pi/2} e^{-a\,R\sin\varphi}\, d\varphi$$

$$\leq 2\,\epsilon\,R \int_0^{\pi/2} e^{-2a\,R\varphi/\pi}\, d\varphi = \frac{\pi\epsilon}{a}\left[1 - e^{-a\,R}\right].$$

The limit value for $R \to \infty$ $(\epsilon \to 0)$ yields

$$\lim_{R \to \infty} \left|\oint_{C_1} f(\Omega)\, e^{ia\Omega}\, d\Omega\right| = 0.$$

For the type of integrals appearing in the text the function $f(\Omega)$ is a rational function, consisting of two polynomials $h(\Omega)$ and $g(\Omega)$. It is

$$f(\Omega) = \frac{h(\Omega)}{g(\Omega)}$$

with at least the order of $g(\Omega)$ being larger by one than that of $h(\Omega)$, i.e.,

$$0\left(g(\Omega)\right) \geq 0\left(h(\Omega)\right) + 1.$$

Therefore,

$$\lim_{|\Omega| \to \infty} |f(\Omega)| = 0.$$

If the function $f(\Omega)\, e^{i\Omega a}$ satisfies the following conditions:

1. $f(\Omega)\, e^{ia\Omega}$ is analytic in the upper half plane for $\mathrm{Im}\Omega \geq 0$ except for a finite number of poles.
2. $f(\Omega)\, e^{i\Omega a}$ has only simple poles on the real axis.
3. $\lim_{\Omega \to \infty} |\Omega\, f(\Omega)\, e^{ia\Omega}| = 0$ for $0 \leq \arg \Omega \leq \pi$

then

$$\int_{-\infty}^{+\infty} f(\Omega)\, e^{ia\Omega}\, d\Omega = 2\pi i \sum_{\lambda=1}^{n} \text{Res.}\,(a_\lambda) + i\pi \sum_{\lambda=1}^{m} \text{Res.}\,(b_\lambda)$$

where the a_λ's are n poles in the upper half plane $\mathrm{Im}\Omega > 0$ and the b_λ's are m simple poles on the real axis for the function $f(\Omega)\, e^{i\Omega a}$.

Proof: The first part of this statement follows from Cauchy's Theorem and the fact that the integral along the semicircle vanishes. Let us proof the second part of the formula. At $\Omega = \pm\omega$ are simple poles on the real axis. A semicircle of radius ρ is taken around $\Omega = \pm\omega$ in the upper half plane. The contour C consists of the real axis from -R to +R (excluding the segments $\pm\omega - \rho$ to $\pm\omega + \rho$), the semicircles ρ and the semicircle C_1 in the upper half plane having the radius R and the center at the origin. With Cauchy's Theorem,

$$\oint_C f(\Omega)\, e^{ia\Omega}\, d\Omega = \int_{C_1} f(\Omega)\, e^{ia\Omega}\, d\Omega + \int_{(\rho_1)} f(\Omega)\, e^{ia\Omega}\, d\Omega + I_n$$

$$+ \int_{(\rho_2)} f(\Omega)\, e^{i\Omega a}\, d\Omega$$

$$= 2\pi i \sum_{\lambda=1}^{n} \text{Res}\ (a_\lambda)$$

where a_λ are the poles inside the integration path C.

The integral I_n is

$$I_n = \int_{-R}^{-\omega-\rho_1} f(\Omega)\, e^{ia\Omega}\, d\Omega + \int_{-\omega-\rho_1}^{\omega-\rho_2} f(\Omega)\, e^{ia\Omega}\, d\Omega + \int_{\omega+\rho_2}^{R} f(\Omega)\, e^{ia\Omega}\, d\Omega .$$

Where P denotes the prinicpal value,

$$\lim_{\substack{R \to \infty \\ \rho_2 \to 0}} I_n = P \int_{-\infty}^{+\infty} f(\Omega)\, e^{ia\Omega}\, d\Omega$$

In considering the integral

$$\int_{(\rho_2)} f(\Omega)\, e^{ia\Omega}\, d\Omega$$

where, on the semicircle, Ω can be written as

$$+\Omega = \omega + \rho_2 e^{i\varphi} \qquad (0 \le \varphi \le \pi).$$

Since $f(\Omega)\, e^{ia\Omega}$ has at $\Omega = \omega$ a simple pole, the Laurent expansion of the function can be written as

$$f(\Omega)\, e^{ia\Omega} = \frac{b_2}{\Omega - \omega} + \sum_{\mu=0}^{\infty} \alpha_\mu\, (\Omega - \omega)^\mu .$$

The residue at $\Omega = \omega$ is b_2. Therefore,

$$\oint_{(\rho_2)} f(\Omega)\, e^{ia\Omega}\, d\Omega = \int_{\pi}^{0} b_2\, i\, d\varphi + \sum_{\mu=0}^{\infty} \int_{\pi}^{0} \alpha_\mu\, i\, \rho_2^{\mu+1}\, e^{i(\mu+1)\varphi}\, d\varphi$$

which yields with $\rho_2 \to 0$

$$\lim_{\rho_2 \to 0} \left\{ \oint_{(\rho_2)} f(\Omega)\, e^{ia\Omega}\, d\Omega \right\} = -i\pi\, b_2 .$$

The same is valid for other simple poles on the real axis and proves the above statement.

The preceeding integrals satisfy the cited conditions, exhibit only simple singularities on the real axis and are

$$\int_{-\infty}^{+\infty} \frac{e^{ia\Omega}}{\Omega}\, d\Omega = \pi\, i \qquad (a > 0)$$

and

$$\int_{-\infty}^{+\infty} \frac{\Omega\, e^{ia\Omega}}{\omega^2 - \Omega^2}\, d\Omega = \pi\, i \left\{ -\frac{\omega\, e^{ia\omega}}{2\omega} - \frac{\omega\, e^{-ia\omega}}{2\omega} \right\} = -\pi\, i \cos a\omega\, ; \; (a > 0) .$$

For $a < 0$ the integration path C^* has to be taken in the lower half plane ($\pi \leq \arg \Omega \leq 2\pi$). Integration in clockwise direction then yields a negative sign in Cauchy's expression.

Now the first integral

$$\int_0^\infty \frac{\cos \Omega\, t \sin \Omega\, T}{d\Omega}\, d\Omega = \frac{1}{8i} \int_\infty^{+\infty} \frac{e^{i(t+T)\,\Omega}}{\Omega}\, d\Omega - \frac{1}{8i} \int_{-\infty}^{+\infty} \frac{e^{-i(t+T)\,\Omega}}{\Omega}\, d\Omega$$

$$+ \frac{1}{8i} \int_{-\infty}^{+\infty} \frac{e^{i(T-t)\,\Omega}}{\Omega}\, d\Omega - \frac{1}{8i} \int_{-\infty}^{+\infty} \frac{e^{-i(T-t)\,\Omega}}{\Omega}\, d\Omega$$

which yields for $t < T$

$$\int_0^\infty \frac{\cos \Omega\, t \sin \Omega\, T}{\Omega}\, d\Omega = \frac{\pi}{2} \quad .$$

For $t = T$ the third and fourth integral vanish together and the value of the integral is $\pi/4$. For $t > T$ the integrals cancel each other. It is, therefore,

$$\int_0^\infty \frac{\cos \Omega t \sin \Omega t}{\Omega}\, d\Omega = \left\{ \begin{array}{lll} \frac{\pi}{2} & \text{for} & t < T \\ \frac{\pi}{4} & \text{for} & t = T \\ 0 & \text{for} & t > T \end{array} \right\} .$$

The second integral to be evaluated yields

$$\int_0^\infty \frac{\Omega \cos \Omega\, t \sin \Omega\, T}{\omega^2 - \Omega^2}\, d\Omega = \frac{1}{8i} \int_{-\infty}^{+\infty} \frac{\Omega\, e^{i(t+T)\,\Omega}}{\omega^2 - \Omega^2}\, d\Omega -$$

$$- \frac{1}{8i} \int_{-\infty}^{+\infty} \frac{\Omega\, e^{-i(t+T)\,\Omega}}{\omega^2 - \Omega^2}\, d\Omega + \frac{1}{8i} \int_{-\infty}^{+\infty} \frac{\Omega\, e^{i(T-t)\,\Omega}}{\omega^2 - \Omega^2}\, \Omega$$

$$- \frac{1}{8i} \int_{-\infty}^{+\infty} \frac{\Omega\, e^{-i\,(T-t)\,\Omega}}{\omega^2 - \Omega^2}\, d\Omega .$$

This is for $t < T$

$$\int_0^\infty \frac{\Omega \cos \Omega t \sin \Omega T}{\omega^2 - \Omega^2} d\Omega = -\frac{\pi}{8} \cos \omega(t+T) - \frac{\pi}{8} \cos \omega (t+T) - \frac{\pi}{8} \cos \omega (t-T)$$

$$-\frac{\pi}{8} \cos \omega (t-T) = -\frac{\pi}{2} \cos \omega t \cos \omega T.$$

For $t = T$ the third and fourth integral vanish together and the value of the integral is $-\pi/4 \cos 2\omega t$, while for $t > T$ the exponential function exhibits in the third and fourth integral a negative value for $(T-t)$ in the exponent, which results in a change of the integral path from the upper to the lower half plane and vise versa for the fourth integral. It is, therefore,

$$\int_0^\infty \frac{\Omega \cos \Omega t \sin \Omega T}{\omega^2 - \Omega^2} d\Omega = -\frac{\pi}{8} \cos \omega(t+T) - \frac{\pi}{8} \cos \omega (t+T) + \frac{\pi}{8} \cos \omega (t-T)$$

$$+\frac{\pi}{8} \cos \omega (t-T) = \frac{\pi}{2} \sin \omega t \sin \omega T \quad \text{for } t > T$$

It is, therefore,

$$\int_0^\infty \frac{\cos \Omega t \sin \Omega T}{\Omega} d\Omega = \begin{cases} \frac{\pi}{2} & \text{for} \quad t < T \\ \frac{\pi}{4} & \text{for} \quad t = T \\ 0 & \text{for} \quad t > T \end{cases}$$

$$\int_0^\infty \frac{\Omega \cos \Omega t \sin \Omega T}{\omega^2 - \Omega^2} d\Omega = \begin{cases} -\frac{\pi}{2} \cos \omega t \cos \omega T & \text{for} \quad t < T \\ -\frac{\pi}{4} \cos 2\omega t & \text{for} \quad t = T \\ \frac{\pi}{2} \sin \omega t \sin \omega T & \text{for} \quad t > T \end{cases}$$

The other integral expression can be evaluated in a very similar way (see also Ref. 6).

REFERENCES

1. Rayleigh, Lord: On Waves. Philosophical Magazine, series 5.1, 1876, pp. 257-259.

2. Cooper R. M.: Dynamics of Liquids in Moving Containers. American Rocket Society Journal, vol. 30, 1960, pp. 725-729.

3. Abramson, H. N.: Dynamic Behavior of Liquids in Moving Containers. Applied Mechanics Reviews, vol. 16, no. 7, July 1963, pp. 501-506.

4. Bauer, H. F.: Fluid Oscillations in the Containers of a Space Vehicle and Their Influence Upon Stability. NASA TR R-187, 1964.

5. Lorell, T.. Forces Produced by Fuel Oscillations. Jet Propulsion Laboratory: Progress Report 20-149, 1951.

6. DeHaan, D. B.: Nouvelles Tables d'Integrals Definies. 1939. (Available from G. E. Stechert Co., New York.)

"The aeronautical and space activities of the United States shall be conducted so as to contribute . . . to the expansion of human knowledge of phenomena in the atmosphere and space. The Administration shall provide for the widest practicable and appropriate dissemination of information concerning its activities and the results thereof."

—NATIONAL AERONAUTICS AND SPACE ACT OF 1958

NASA SCIENTIFIC AND TECHNICAL PUBLICATIONS

TECHNICAL REPORTS: Scientific and technical information considered important, complete, and a lasting contribution to existing knowledge.

TECHNICAL NOTES: Information less broad in scope but nevertheless of importance as a contribution to existing knowledge.

TECHNICAL MEMORANDUMS: Information receiving limited distribution because of preliminary data, security classification, or other reasons.

CONTRACTOR REPORTS: Technical information generated in connection with a NASA contract or grant and released under NASA auspices.

TECHNICAL TRANSLATIONS: Information published in a foreign language considered to merit NASA distribution in English.

TECHNICAL REPRINTS: Information derived from NASA activities and initially published in the form of journal articles.

SPECIAL PUBLICATIONS: Information derived from or of value to NASA activities but not necessarily reporting the results of individual NASA-programmed scientific efforts. Publications include conference proceedings, monographs, data compilations, handbooks, sourcebooks, and special bibliographies.

Details on the availability of these publications may be obtained from:

SCIENTIFIC AND TECHNICAL INFORMATION DIVISION

NATIONAL AERONAUTICS AND SPACE ADMINISTRATION

Washington, D.C. 20546